Universität für Bodenkultur Wien
University of Natural Resources
and Life Sciences, Vienna

Master Thesis

A functional study of ion-conducting polymer interaction with bilirubin oxidase

Submitted by

Camilla Sophie Artner, BSc

in the framework of the Master programme

Biotechnology UH 066 418

in partial fulfilment of the requirements for the academic degree

Diplom-Ingenieur

Vienna, January 2022

Supervisor:

Assoc.Prof. Dr. Roland Ludwig
Institute of Food Science
Department of Food Science and Technology

AFFIDAVITS

I hereby declare that I am the sole author of this work; no assistance other than that permitted has been used and all quotes and concepts taken from unpublished sources, published literature or the internet in wording or in basic content have been identified by footnotes or with precise source citations.

Vienna, 2022

Camilla Sophie Artner

Acknowledgments

Foremost, I'd like to express my deepest thanks to Elisabeth Lojou and the whole BIP8 (CNRS Marseille) for giving me the opportunity to conduct my thesis. I especially want to thank Elisabeth for her continuous support, her patience explaining the basics and her motivation and immense knowledge. I really enjoyed the atmosphere in the lab and my time working with you!

Further I am extremely grateful to Roland Ludwig for supporting me from Vienna and enabling me to conduct my research in France.

A special thanks also to Klaudia Hradil and the whole XRC for providing me with excellent opportunities and support during my studies. I always felt welcome, it was a pleasure working with you!

I cannot express enough thanks to my loving family, without whom my studies would not have been such an enjoyable pursuit of knowledge. Thank you, Mom, Dad and Larissa and Dominik for always having my back and supporting and encouraging me throughout everything! A special thanks also to my grandparents, their continuous support, Eleonore and Hans, always providing me with home-cooked food, as well as Erwin and Jutta.

Last but not least, I want to mention my friends without whom my studies would never have been the same, having someone to share the stressful times as well as the accomplishments which was a great comfort!

Abstract

The oxygen reduction reaction (ORR) is one of the most important chemical processes in energy converting systems and living organisms. To circumvent the use of expensive and unsustainable metal catalysts like Pt for ORR, redox enzymes have been envisioned. Redox enzymes are attractive for many bioelectrochemical devices such as biosensors, bioreactors or biofuel cells. The oxidoreductase bilirubin oxidase (BOD) belongs to the multi-copper oxidase (MCO) family and efficiently reduces O_2 to water at neutral pH and physiological conditions without creating any toxic byproducts, making it a promising candidate as catalyst for ORR. Despite great advances in electrical wiring, the poor stability of the enzyme and/or the enzyme-based electrode limits any large-scale development. Nevertheless, the usage of enzymes in H_2-based fuel cells is worth investigated since it promises sustainable applications for low energy device powering. In order to realize this, major challenges have to be faced. One challenge poses the selection of the conducting ionomers used as the separator membrane and proton diffusion enhancer as well as a binder for stabilization of the biocatalyst. Depending on the ionomer, the enzyme activity can be strongly influenced. Nowadays Nafion is the main ionomer used as a membrane in industrial processes. It is also widely used in bio-electrochemical studies to protect the electrode from protein leaching. However, not only is Nafion a highly acidic ionomer, but it also possesses environmentally problematic perfluorinated groups. Therefore, it would be beneficial to exchange this ionomer for a better alternative. Non-fluorinated organic polymers such as sulfonated polyether ether ketone (SPEEK), have many advantages such as selectivity to ions, high ionic conductivity, good stability, long life and low production cost. However, they have never been considered as membranes in biofuel cells.

In this study, first basic parameters such as pH are evaluated in regard to enzymatic activity as well as for the individual ionomers. Furthermore, the influence of the presence of ionomers on BOD enzymatic activity and stability are examined both in solution and after enzyme immobilization on pyrolytic graphite electrodes. Different immobilization protocols are realized and evaluated. To study the interactions between ionomers, either SPEEK or Nafion, and the BOD in more detail, sodium dodecyl sulfate polyacrylamide gel electrophoresis and Dynamic Light Scattering were performed. Additionally, parameters that control the decrease in enzyme electroactivity, such as oxygen availability, influence of alcohol, electrical connection and enzyme release were investigated to obtain a better understanding of the effects limiting enzymatic activity and stability.

Kurzfassung

Die Reduktion von molekularem Sauerstoff (ORR) ist eine der wichtigsten elektrokatalytischen Reaktionen in Energieumwandlungssystemen und lebenden Organismen. Um die Verwendung teurer und nicht nachhaltiger Metallkatalysatoren, hauptsächlich Pt, zu vermeiden wurden in den letzten Jahren Oxidoreduktasen als Alternative vorgestellt, da diese eine attraktive Möglichkeit für viele bio-elektrochemische Systeme wie für Biosensoren, Bioreaktoren und Biobrennstoffzellen bieten. Das Redoxenzym Bilirubinoxidase (BOD), welches zu der Familie der Kupferoxidasen (MCO) gehört ist in der Lage unter physiologischen Bedingungen und neutralem pH effizient O_2 zu Wasser zu reduzieren, ohne dass toxische Nebenprodukte in der Reaktion erzeugt werden. Obwohl es in den letzten Jahren zu großen Durchbrüchen in der Wissenschaft gekommen ist, ist der Einsatz im großen Maßstab noch in weiter Ferne. Dies liegt einerseits an dem schlechten Stromfluss und der geringen Stabilität der Enzyme, andererseits an der starken Limitierung des Enzym-Elektroden Systems. Dennoch ist die weitere Forschung für die Verwendung von Enzymen für H_2-Biobrennstoffzellen sinnvoll, da sie eine nachhaltige Anwendung für die Energieversorgung verspricht. Um dies zu realisieren, sind große Herausforderungen zu bewältigen. Eine ist die Auswahl und Verwendung leitender Ionomere, die in den Brennstoffzellen sowohl als Separator-Membranen und Protonendiffusionsverstärker sowie als Bindemittel zur Stabilisierung des Biokatalysators verwendet werden. Heutzutage ist das meist verwendete Ionomer, das als Membran in industriellen Prozessen oder als Schutz vor Auswaschen des Enzymes von der Elektrode in bioelektrochemischen Studien verwendet wird, Nafion. Nafion ist jedoch nicht nur ein stark saures Ionomer, sondern besitzt auch umweltschädliche perfluorierte Gruppen, deshalb wäre eine umweltfreundlichere Alternative wünschenswert. Nicht-fluorierte organische Ionomere, wie das sulfonierte Polyetheretherketon (SPEEK), bieten viele Vorteile wie eine hohe Selektivität für Ionen, gute Ionenleitfähigkeit, hohe Stabilität, eine lange Lebensdauer und geringe Produktionskosten, jedoch wurden sie lange nicht als Membranen für Biobrennstoffzellen in Betracht gezogen. In dieser Studie werden zuerst grundlegende Parameter sowie deren Einfluss auf die Enzymaktivität evaluiert. Zusätzlich wurde der Einfluss der einzelnen Ionomere auf die Enzymaktivität und die Stabilität von BOD sowohl in Lösung als auch im immobilisierten Zustand auf pyrolytischen Graphitelektroden untersucht. Um die Wechselwirkungen zwischen den Ionomeren, SPEEK oder Nafion und der Kupferoxidase BOD genauer zu untersuchen wurden außerdem biophysikalische Analysemethoden durchgeführt sowie verschiedene Immobilisierungsprotokolle verglichen. Außerdem wurden zusätzliche Parameter, die eine negative Auswirkung auf die enzymatische Elektroaktivität haben könnten untersucht, z.B. die Verfügbarkeit von Sauerstoff, der Einfluss von Alkohol und die Ablösung des Enzymes von der Oberfläche, um ein besseres und umfangreicheres Verständnis über die Faktoren, die die Aktivität und Stabilität von Enzymen beeinflussen, zu bekommen.

List of Abbreviations

Abbreviations	Explanations
A	Ampere
ABTS	2,2'-azino-bis(3-ethylbenzothiazoline-6-sulphonique) diammonium salt
BOD	Bilirubin oxidase
CcO	Cytochrome *c* oxidase
Cdl	Double layer capacitance
CE	Counter electrode
CNTs	Carboxylic carbon nanotubes
Cu	Copper
CV	Cyclic voltammetry
Cys	Cysteine
DET	Direct electron transfer
DLS	Dynamic light scattering
EFC	Enzymatic fuel cell
ET	Electron transfer
EtOH	Ethanol
F	Faraday
FAD	Flavin adenine dinucleotide
FC	Fuel cell
His	Histidine
H_2O_2	Hydrogen peroxide
IPA	Isopropanol
kDa	Kilo Dalton
KH_2PO_4	Potassium phosphate monobasic
K_2HPO_4	Potassium phosphate dibasic
L	Liter
LAC	Laccase
M	Molar (mol L^{-1})
MCO	Multicopper oxidase
MET	Mediated electron transfer
mL	Milliliter
mm	Millimeter
mM	Millimolar (mmol L^{-1})

Mv	*Myrothecium verrucaria*
MW	Multi-walled
NaOH	Sodium hydroxide
ORR	Oxygen reduction reaction
PGE	Pyrolytic graphite electrode
PPB	Potassium phosphate buffer
Pt	Platinum
RE	Reference electrode
REA	Real electroactive surface
RI	Refractive index
rpm	Revolutions per minute
RT	Room temperature (~ 20-25°C)
SDS-PAGE	Sodium dodecyl sulfate polyacrylamide gel electrophoresis
SPEEK	Sulfonated polyether-etherketon
SW	Single-walled
TNC	Trinuclear center
UV-Vis	Ultraviolet-visible
µL	Microliter
µM	Micromolar (µmol L^{-1})
WE	Working electrode

Contents

1 Introduction

Over the last years green and renewable energy production and environmental issues have become a major focus in research. Renewable energy sources play a significant role in reaching a green energy production and over the last decades the idea of substituting limited resources needed for energy production with enzymes has surfaced. Enzymes efficiently catalyze millions of energy production reactions in nature each day without producing any toxic waste. Especially in the field of fuel cells (FC) enzymes pose a promising alternative to conventional materials used nowadays, resulting in devices called Enzymatic Fuel Cells (EFC) [1].

1.1 Oxygen reduction reaction (ORR)

Oxygen reduction reaction (ORR) is a key component for energy conversion in biological processes as well as in the field of electrocatalysis concerning FC [2].

In the ORR, oxygen is either fully reduced to water by the four-electron oxygen reduction pathway or only by a two-electron partial reduction of oxygen to hydrogen peroxide (H_2O_2) [3]. The two-electron pathway is only considered a partial reduction since it would be possible to obtain another molecule of water when H_2O_2 dissociates any further [2].

The ORR pathways are considered as follows:

Direct four-electron reduction:

$$4H^+ + O_2 + 4e^- \rightarrow 2\,H_2O$$

Partial two-electron reduction:

$$2H^+ + O_2 + 2e^- \rightarrow H_2O_2$$

$$H_2O_2 + 2H^+ + 2e^- \rightarrow 2H_2O$$

Full oxygen reduction is a key issue since a high energy efficiency is desired when creating a fuel cell. Firstly, H_2O_2, created as an intermediate in the partial reduction, has a deactivating effect on the ORR catalyst which decreases the efficiency. Secondly, with the four- electron reduction the ORR starts at a more positive potential thus reducing the difference between the resulting potential and the potential at equilibrium – called overpotential - which is desirable in order for the reaction to occur faster [2,4].

These different mechanisms occur depending on the catalyst involved in the ORR.

1.2 Catalyst for ORR

As stated above the chosen catalyst performing the ORR is responsible for the reaction mechanism and thus influences the efficiency of the ORR catalytic process. Those catalysts can be split into two main groups: inorganic catalysts and biocatalysts [2].

1.2.1 Inorganic catalysts

Inorganic catalysts are also often referred to as either metal-based or metal-free catalysts. Some examples of the first group are Pt, Pt-alloyed, metal supported by carbon nanomaterials or metal-nitrogen-carbon (M-N-C) and nonprecious metal catalysts. Till today Pt remains the most widely used electrocatalyst [5]. It is the most prevalent catalyst used in fuel cells due to its high efficiency, excellent surface properties and inertness. Nevertheless, there are many limitations arising from Pt as its limited availability while high loading is required, lack of specificity and a high overpotential [2]. To develop an alternative to Pt, further advances in improved catalytic performance have been achieved through graphene sheets and carbon nanotubes (CNTs), with the goal to replace Pt-based electrodes to overcome the problems encountered with Pt [5]. Nevertheless, these advances have not yielded satisfactory results and investigations into more natural ORR processes and their catalyst have been made [2].

1.2.2 Biocatalysts

Living organisms are able to fully convert substrates via natural pathways with a high specificity, selectivity and efficiency though electron transfer by using enzymes more specifically oxidoreductases as catalysts [4]. Those enzymes have the advantage of their wide availability as well as their ability to regenerate. Thus, the implementation of enzymes in fuel cells (EFC) as catalysts has been under intensive research as this would accomplish to meet the need for clean and renewable energy, while providing efficient bioelectrocatalysis[1]. Another benefit of biocatalysts is that those enzymatic catalysts are able to provide an efficient full ORR with almost no overpotential [6,7]. First advances to achieve an efficient electron transport between an enzyme and an electrode have already been made in 1977 [8].

Oxidoreductases consist of a redox center which is either metal-based (Fe, iron-sulfur, heme, Cu, Ni, etc…) or organic such as flavin adenine dinucleotide (FAD). In metalloenzymes, this redox active center is formed by a metal ion which is often embedded in the polypeptide structure, thus shielded from hostile influence but also hidden for electric communication. Two enzyme families that are able to perform four-electron ORR are under investigation nowadays: The cytochrome *c* oxidases (CcO) and

the multi-copper oxidases (MCO)[2]. In this thesis MCOs are discussed in more details with a focus on bilirubin oxidase (BOD).

1.3 Multicopper oxidases (MCOs)

MCOs, belonging to the family of oxidoreductases, are copper containing enzymes which are responsible for substrate oxidation while efficiently reducing oxygen directly to water without the formation of toxic byproducts [9]. Members of this family of enzymes, such as bilirubin oxidase, laccase (LAC) [2], polyphenol oxidase (PPO) and ascorbate oxidase (AO), usually contain at least four Cu centers and possess the three types of copper sites: Type 1 (T1), type 2 (T2) and the binuclear type 3 (T3) [6,9]. These Cu sites have been classified into three types based on their spectroscopic properties, which reflect the geometric and electronic structure of the active site [10]. MCOs usually consist of a T1 center and a trinuclear center (TNC), which are 12-13 Å apart [11] (Figure 1B). The T1 has an intense cysteine (Cys) to Cu (II) charge transfer absorption band at around 600 nm [9,11]. This Cu center accepts electrons from the electron donating substrates such as phenols or metal ions (homogenous catalysis) or from an electrode (heterogenous catalysis). These Cu ions in the protein structure allow for an intramolecular electron transfer by switching their oxidation states [2,12]. The substrate binding site is located near the histidine (His) ligands of the Cu T1. Those electrons issued from the substrate oxidation are transferred by a Cys-His pathway to the TNC. The TNC is constituted of a T2 copper ion and a T3 pair of copper ions, which are coupled via a bridging hydroxide with a characteristic absorption at 330 nm. This is the place where the oxygen reduction takes place [9,11].

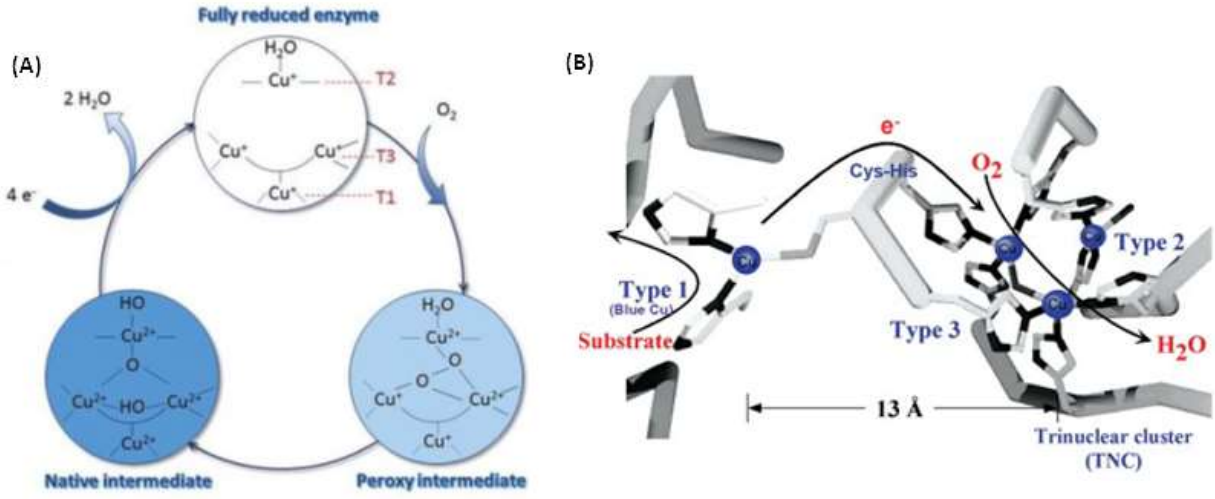

Figure 1: *(**A**) Catalytic cycle for O_2 reduction by BOD with the different redox states of the four Cu atoms [1]. (**B**) Structure of the MCO active site with arrows marking the flow of substrates, electrons (e^-) and O_2 [12].*

The catalytic cycle for O_2 reduction is shown in Figure 1A. Oxygen binds to the fully reduced enzyme and is reduced into water in two successive steps. First, oxidation of T3 Cu atoms leads to the peroxide intermediate state leading to a partial reduction of oxygen. Secondly the native intermediate state is

formed by cleavage of the O-O bond and oxidation of the remaining Cu atoms, concluding the cycle with the release of water and the enzyme returning to its initial fully reduced state [1,2].

1.3.1 Bilirubin oxidase

BOD from *Myrothecium verrucaria* (*Mv*BOD) was first discovered by Tanaka in 1981 [13]. BOD is a monomeric protein with a molecular mass of 60 kDa, with homologous sequences with those of other MCO [14]. The crystal structure of *Mv*BOD (Figure 2) is well known and its mechanism of ORR is described above [2].

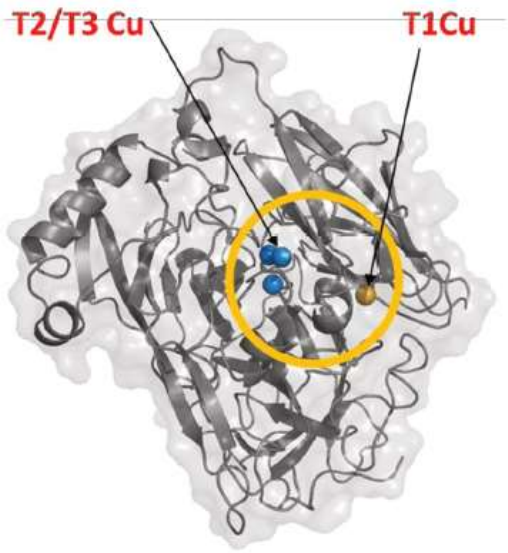

Figure 2: *X-ray crystal structure of MvBOD (PDB ID: 3ABG). Environment of the copper atoms circled in yellow: The copper atom of the T1 in yellow and the coppers T2/T3 of the trinuclear center are shown in blue [2].*

*Mv*BOD is considered a model enzyme for many biochemical and bio-electrochemical investigations since the reaction mechanism, structure as well as the active site are well understood [2]. Furthermore, BOD possesses several advantages over laccase which has been the enzyme of choice for industrial applications over the last decades: BODs have a high activity at neutral pH, high thermal tolerance and a resistance to chloride ions [15], although some research exists that chloride ions have some inhibitory effect on BOD [16]. Thus, they have a better ability to reduce O_2 in physiological conditions, making them excellent candidates for the cathodic reaction in fuel cells [6]. BOD is responsible for the oxidation of bilirubin to biliverdin, water and some purple pigment [14]:

$$bilirubin + {}^{1}/_{2}\, O_2 \rightarrow biliverdin + H_2O$$

In bioelectrocatalytic applications, compared to Pt-based electrodes, BOD is able to achieve a lower overpotential at neutral pH for ORR [2].

1.4 Bio-electrocatalysis and electron transfer (ET)

An important parameter concerning the implementation of bio-catalyst in EFCs is the efficiency of bioelectrocatalysis and thus the electron transfer rate in order to determine the power output such an EFC is able to provide [4]. Electron transfer (ET) is driven by a difference in the redox potential between donor and acceptor sites, moving electrons [2]. This ET rate is depending on the reorganization energy and the distance between the donor and the acceptor sites, thus a distance no greater than 15 Å is essential in order to achieve a direct electron transfer (DET). Therefore, DET is only possible in EFC when the active site of the enzyme is electrically connected with the surface of the electrode [4]. When this is not possible the aid of a redox mediator is required, this process is then called mediated electron transfer (MET) [1]. For DET, the enzyme has to be immobilized directly on the electrode surface in the correct orientation, while for MET the redox mediators achieve the ET between the redox center and the electrode, provided that there exists some affinity between the enzyme and redox mediator (Figure 3) [17].

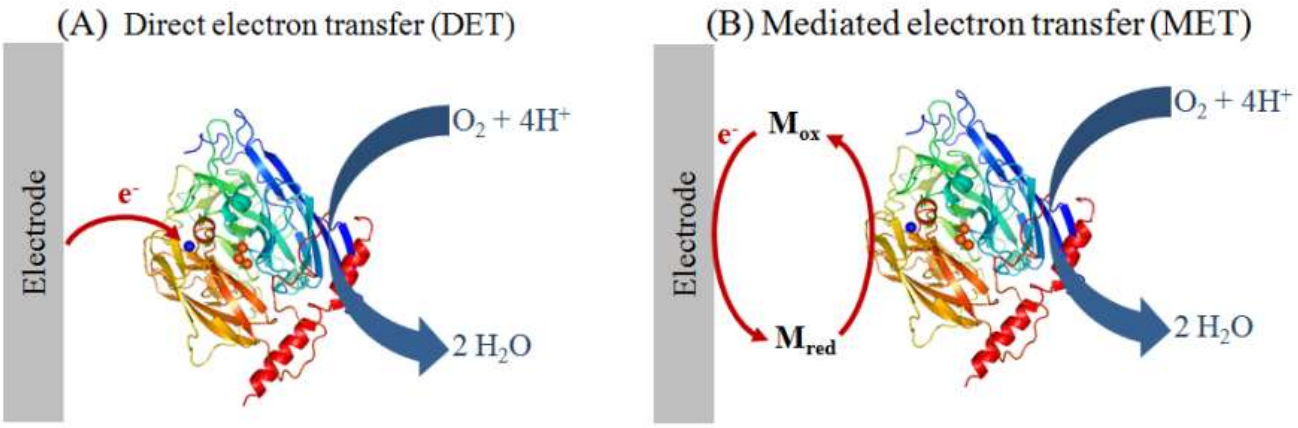

Figure 3: *Schematic drawing of electrocatalysis from BOD to an electrode surface either via (A) DET or (B) MET* [17].

One drawback of DET is the unique orientation of enzyme necessary to allow electrocatalysis while in contrast MET achieves electrocatalysis with enzymes regardless of their orientation [18]. Nevertheless, DET has several advantages over MET in terms of lower thermodynamic losses as well as higher efficiency, since no mediator is necessary which could complicate the reaction and lead to potential obstruction [2]. Additionally, achieving DET is not only favorable due to its simplicity but also because overpotentials that are seen in MET can be decreased when the orientation of the enzyme is accomplished properly so that the redox center – the Cu T1 site in BOD – is located close to the electrode surface, which substitutes the substrate as an electron source [17,18]. Thus, the Cu T1 site is responsible for transferring electrons from the electrode surface to the TNC when BOD is immobilized [18]. This distance between the redox-center and the electrochemical interface should not exceed 1.5 nm to allow for efficient electron tunneling [19]. Additionally, the interaction between the electrode surface and the enzyme should be specific enough to induce and enhance enzyme

attachment on the surface to allow a fast ET and achieve a high catalytic current while preserving its initial conformation in order to maintain a high activity and stability [20]. Therefore, knowledge about the enzyme structure and the interactions, hydrophobic and electrostatic, of the enzyme with the electrode surface will allow for efficient immobilization and electrocatalysis. To ensure efficient DET rates, suitable electron surfaces are essential also considering the distribution of charges present on the surface [4].

In case of BOD carbon nanomaterials, such as carbon nanotubes (CNTs), have been used for modification of the interfaces to enhance the surface-to-volume ratio and provide more favorable surface charges for BOD attachment in order to achieve the correct orientation and increase the DET efficiency [19]. CNTs are rolled layers of sp^2 carbon atoms and either consist of one single graphene layer (single-wall CNTs (SWCNTs)), or multiple layers (multi-wall CNTs (MWCNTs)). They possess a high electronic conductivity and mechanical strength [15]. In previous studies it was established that negatively charged CNTs allow for the optimal orientation of *Mv*BOD [19].

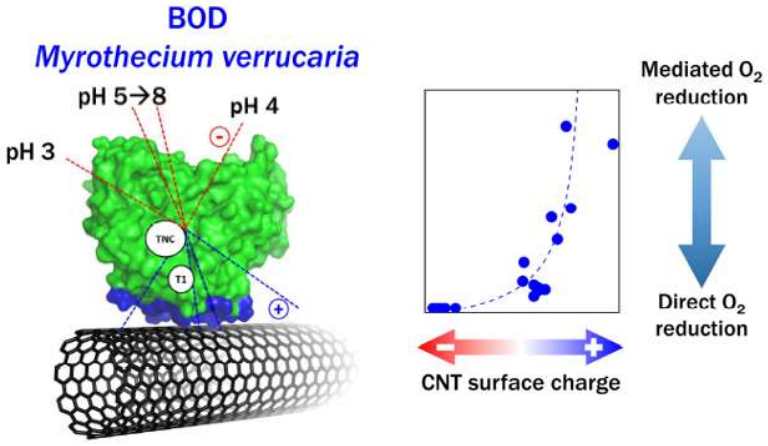

Figure 4: *Electrostatic interaction between MvBOD and CNTs and the influence of the surface charge on DET or MET process for O_2 reduction* [1,19].

In Figure 4 the orientation of BOD depending on various pH values and their influence on the oxygen reduction process is shown. This orientation is not only influenced by the pH but also the electrostatic interactions that occur between the enzyme and the CNT surface. For *Mv*BOD clearly the negatively charged surface of the CNT is advantageous for the proper enzyme orientation to achieve efficient DET[19]. This is explained by the direction of the dipole moment of the protein pointing positive toward the Cu T1.

Experimentally a one-point orientation is difficult to accomplish when performing enzyme immobilization, leading to a distribution of orientations. Through modeling approaches a parameter of orientation can be determined in order to determine the approximately distribution of the enzyme orientations with known variables as the amount of enzyme immobilized and the surface area used for immobilization. This parameter of orientation allows for evaluation of the performed enzyme

immobilization and the comparison of different immobilization techniques: The lower the value obtained the lower the distribution of orientation and the better the DET [21].

1.4.1 Enzyme stabilization

A key parameter restricting the practical application of EFC is the stability of enzymes [1]. Several strategies for the improvement of enzyme stabilization such as protein immobilization, protein cross-linking, protein engineering or evaluation of the medium properties exist. However, achieving a higher enzyme stability should not come at the expense of losing activity during immobilization. Nevertheless, enzyme activity is often reduced due to conformational changes as the enzyme structure is becoming more rigid to increase stability. Decrease in the activity can also arise from leakage of enzyme from the electrode [22]. Enzyme immobilization provides enhanced stability by rigidification of the enzyme structure as well as operational stability to avoid enzyme detachment. This is the case for the immobilization approach: adsorption onto functionalized, charged surfaces with nanostructured materials to enhance the stability by reducing conformational disruption as well as improving the intermolecular interactions [4].

This can also be achieved by the addition of an ionomer, an ion conducting polymer[23], acting as a protective film. The most common ionomer used in bio-electrochemical experiments and industry is Nafion, a perfluorinated sulfonated polymer, which is used as a proton conductive separator membrane in fuel cells, because of its good stability, low operational temperature and high proton conductivity [24,25]. This approach seems promising since a protective layer against enzyme leakage is combined with the possibility for proton diffusion enhancement, which would additionally prevent local pH changed that would be unfavorable for the enzyme. As Nafion contains perfluorinated groups, which is on the one hand expensive and on the other non-sustainable, alternative ionomers free of fluorinated groups are evaluated such as sulfonated polyether ether ketone (SPEEK) [25]. SPEEK possesses some interesting properties, including high thermal and chemical stability, low cost and availability [26]. In Figure 5 the chemical structures of SPEEK (A) and Nafion (B) are compared.

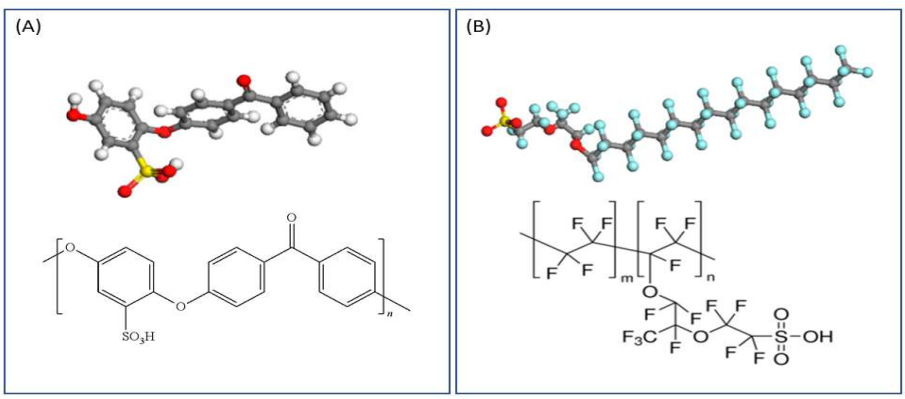

Figure 5: *Comparative chemical structures of (A) SPEEK vs (B) Nafion.*

SPEEK and Nafion possess different microstructures as well as that they differ in the acidity of the sulfonic acid functional groups [25]. Nafion is composed of a hydrophobic backbone and hydrophilic sidechains, which are terminated by sulfonic acid, making it highly hydrophobic, while SPEEK is less hydrophobic [24]. In this thesis the ionomer interaction with BOD is studied to determine the main ionomer parameters that influence both the enzymatic activity and stability. The ionomer SPEEK is compared to Nafion in order to see whether it would function as a sustainable alternative to replace Nafion in EFC in the future.

1.5 Enzymatic fuel cells (EFC)

Fuel cells have been used to generate electricity electrochemically for quite some time [27]. As mentioned above, in the pursuit of green and sustainable energy, fuel cells are considered more and more as electrochemical devices, where the normally employed noble metals for catalysts are exchanged for enzymatic catalysts. EFC are considered a subclass of fuel cells employing redox enzymes as bioelectrocatalyst [4]. A general broad scheme is shown in Figure 6 of how such an EFC, more specifically an H_2O_2 EFC, looks like.

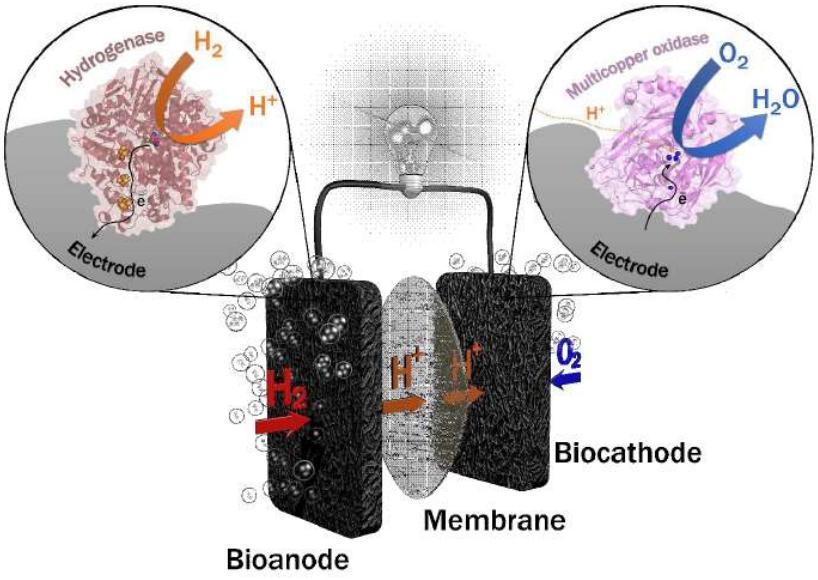

Figure 6: *General scheme of an H_2O_2 EFC. At the anode H_2 oxidation is performed by Hydrogenases, while at the cathode O_2 is reduced into water by MCO such as BOD. Between the two compartments a proton exchange membrane is used as a separator* [1].

H_2/O_2 EFC mostly rely on a hydrogenase at the anode and a MCO, mostly BOD, at the cathode operating under DET conditions [15]. Fuels are oxidized at the bioanode, electrons flow though the external circuit to the biocathode, where the oxidants, mostly O_2, are reduced to water, as can be seen in Figure 6. H_2/O_2 EFC only were developed late in comparison with the glucose/O_2 EFC, with high expectations concerning a massive energy output [28]. Glucose/O_2 EFC have been used and reviewed more extensively

in the beginning of EFC[15], as sugar/O_2 is the most common fuel/oxidant couple to power FC [28]. Further, the implementation of H_2/O_2 EFC is much more complicated, because of the O_2 sensitivity of hydrogenases as well as that mixtures of H_2 and O_2 are explosive under certain concentration conditions. Through extensive research over the last years to gain deeper knowledge in the properties of hydrogenases as well as discovering new hydrogenases with O_2 tolerance and new BODs the development of H_2/O_2 EFC could be realized [1].

H_2/O_2 EFC have many advantages: First, redox enzymes acting as the catalyst are renewable since they can be extracted from living organisms as well as their being biologically degradable. Secondly, the range of usable fuels is diverse as many materials such as sugars, alcohols and hydrogen can be digested by enzymes. Thirdly, redox enzymes exhibit high specificity towards their substrates. Fourth, enzymatic reactions operate mostly at physiological conditions: pH, room temperature and no high pressure, making the operating conditions of the EFC very mild and safe [4]. Nevertheless, many challenges and limitations remain, such as a deeper understanding of the enzymatic properties such as stability as well as the enzymatic behavior once connected to the electrode [4]. Thus, a long way in research remains to increase the stability and improve the electrical connection [1].

2 Aim of the Study

The main objective of this study is to enhance the ability for proton diffusion and the catalytic activity, while achieving a stabilization of the enzyme layer of BOD using the non-fluorinated ion-conducting polymer SPEEK in comparison to Nafion. Since Nafion possesses environmentally harmful perfluorinated groups, it would be beneficial to exchange this ionomer for a better alternative. Non-fluorinated organic polymers have many advantages such as their good combability with enzymes, selectivity to ions, high ionic conductivity, good stability, long life and low production cost. Here SPEEK is examined as such a functionalized non-fluorinated ionomer to consequently be able to replace Nafion in research and industrial processes.

This project should provide a more detailed evaluation of the interaction between the enzyme and the ionomer. To this effect, several objectives are evaluated: Optimization of the immobilization strategy, improvement of the operational stability, investigation of different parameters that influence the activity and stability of BOD and characterization of EBFCs, in order to gain a deeper understanding of the ionomer interaction with BOD.

3 Material and Methods

3.1 Equipment

Table 1: Used equipment and devices in this thesis project

Equipment name	Company	Software
Balance	Mettler AE 240	-
Centrifuge 5417R	Eppendorf	-
Density Meter DMA 4100 M	Anton Paar	-
Heating and Drying oven	Memmert	-
Heat stirrer SB162	Stuart	-
MicroStar 12	VWR	
Microviscometer Lovis 2000 ME	Anton Paar	-
Mini see-saw rocker SSM4	Stuart	-
pH meter	Mettler Toledo	-
Potentiostat	Autolab PGSTAT30	Nova 1.1
PowerPac™ HC	BIO-RAD	-
Refractometer Abbemat 200	Anton Paar	-
Spectrophotometer	Agilent Technologies : Cary Series UV-VIS Spectrophotometer	Cary WinUV Kinetics Application
Thermomixer comfort	Eppendorf	-
Zetasizer Nano series Nano -ZS	Malvern	Zetasizer Software Version 7.12

3.2 Buffers

Buffers are necessary in order to provide a stable environment for proteins by stabilizing the pH and the conductivity of a solution [29].

3.2.1 Potassium phosphate buffer (PPB)

The potassium phosphate buffer (PPB) has a buffer range from 5.8 to 8.0 [30]. PPB was used at the concentration of 50 mM at pH 6.0 and was prepared with potassium phosphate monobasic (KH_2PO_4, 99.0%) and potassium phosphate dibasic (K_2HPO_4, 99.0%), both purchased from Fisher. For the preparation of 50 mM potassium phosphate buffer at pH 6.0, K_2HPO_4 and KH_2PO_4 were mixed in an appropriate ratio, 13.2% and 86.8% respectively, to achieve the desired pH and concentration. All solutions were prepared with Milli-Q water.

3.2.2 Britton-Robinson buffer

The Britton-Robinson buffer, also known as the Universal buffer, has a pH range of 2.0 to 12.0 and is a mixture of 0.1 M phosphoric acid, 0.05 M citric acid and 0.2 M boric acid. The final pH was adjusted with NaOH [31]. All solutions were prepared with Milli-Q water.

3.2.3 HEPES running buffer

SDS-PAGE running buffer 10× was prepared according to Table 2 and the pH was adjusted with NaOH to 8.3.

Table 2: Required components for HEPES running buffer

Components	
Tris	60.57 g
HEPES	119.15 g
SDS	50 mL
EDTA	5.84 g
NaOH	2 g

3.2.4 Loading buffer

The loading buffer for the SDS – PAGE 2× was prepared according to Table 3.

Table 3: Required components for SDS-PAGE loading buffer

Components	
Tris	125 mM
Glycerol	20%
SDS	4%
Comassie Brilliant Blue R250	A few grains
B-mercaptoethanol	10%

3.3 Polymers

Two different polymers were used in order to compare and contrast their influence on the stability and activity of the BOD enzyme: Nafion and sulfonated polyether ether ketone (SPEEK).

The ionomer solutions were diluted in the PPB (pH 6.0) to various ratios ranging from 1:1 (v/v) to 1:500 (v/v) prior usage.

3.3.1 Nafion

Nafion perfluorinated ion-exchange powder (5 wt. %) was obtained from Aldrich Chemical Company Inc.) in solution in a mixture of lower aliphatic alcohols and 10% water.

3.3.2 SPEEK

Sulfonated polyether ether ketone (SPEEK, 5 wt. %) was prepared accordingly in a mixture of 90% 2-Propanol and 10% water, by Dr. Luca Pasquini (Madirel CNRS, Aix-Marseille University), mixing the SPEEK into the solution by gently stirring with a magnetic stirrer for 5 min at 25°C till the polymer was fully dissolved.

3.4 Enzyme

3.4.1 *M. verrucaria* bilirubin oxidase

Bilirubin oxidase from *Myrothecium verrucaria* (*Mv*BOD) was kindly gifted from Amano Enzymes Inc. (Nagoya, Japan). *Mv*BOD has a molecular weight of 60 kDa and is stored at -80°C. Initially, a stock solution of BOD was prepared by diluting BOD in PPB 50 mM, pH 6 to a final concentration of 1 mM. This mixture was divided into 5 µL aliquots and frozen at -20°C. In order to perform the experiments, one aliquot of 1 mM *Mv*BOD was thawed and diluted to a concentration of 10 µM in PPB and kept on ice. Then the *Mv*BOD (10 µM) was mixed with the respective ionomer dilution in a 1:1 (v/v) ratio.

3.5 Electrochemistry

Electrochemistry is a powerful tool to measure thermodynamic potentials and electron transfer rates by relating the flow of electrons to chemical changes. Voltage is applied from an external power source, such as a potentiostat to regulate the electron flow at the electrode. By changing the driving force of such a process, the reaction can be controlled and the necessary parameters to assess related reduction and oxidation processes of molecular species measured [32].

3.5.1 Electrochemical device

Electrochemical experiments were performed in a standard 3-electrode cell using a potentiostat from Autolab PGSTAT30 controlled by Nova software 1.1 (Eco Chemie). For the 3-electrode cell a reference electrode (RE), a counter electrode (CE) and a working electrode (WE) are required. Typical RE are the Ag|AgCl electrode, saturated calomel electrode and $Hg|Hg_2SO_4$ electrode [33], acting as a reference point to measure the potential in the electrochemical cell [32]. Furthermore, the CE, typically a platinum wire or disk, is used to complete the electrical circuit. CE are usually as inert as possible and possess a

large surface area to ensure that the reaction occurring at the CE does not inhibit the one at the WE. The electrochemical reaction is carried out by the WE [32].

A schematic representation of an electrochemical cell is shown in Figure 7.

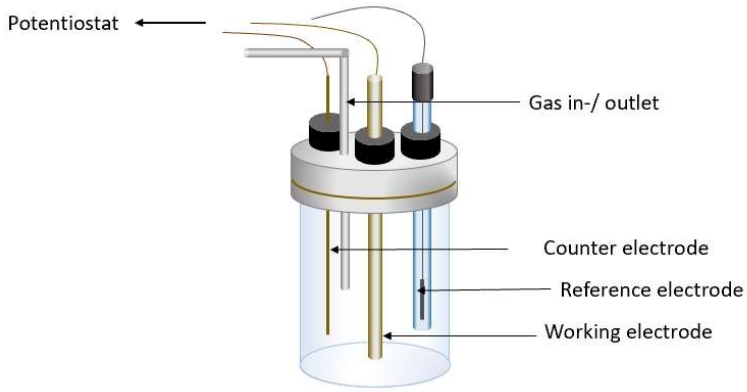

Figure 7: *Schematic representation of a standard 3 - electrode electrochemical cell for CV experiments*

A pyrolytic graphite electrode (PGE, geometric surface = 0.07 cm^2) was used as a working electrode (WE). A $Hg|Hg_2SO_4$ reference electrode (sat. K_2SO_4) and a Pt-wire counter electrode were applied. In the beginning an Ag|AgCl reference electrode was used. An extreme decrease of the enzymatic activity was observed. A detailed study related to chloride inhibition and pH concerning immobilized BOD has been previously conducted, showing that chloride leads to a decrease of catalytic efficiency of BOD [16,34]. Thus, the reference electrode was exchanged to the $Hg|Hg_2SO_4$ reference electrode (sat. K_2SO_4). 50 mM PPB pH 6.0 was used as the electrolyte solution.

Since the reaction happens at the surface of the WE, it is critical that the electrode surface is controlled, which is achieved through polishing [32]. The PGE was polished with a P2400 sandpaper. Polishing was performed to achieve a smooth surface and remove all impurities. Then the electrode was rinsed with MQ-water, sonicated for a few seconds and rinsed again. The PGE was dried before the CNTs were applied.

3.5.2 Carboxylic carbon nanotubes (CNTs)

The CNTs (>95%, (USA)) from NanoLab Inc. and dispersions (1 mg mL^{-1}) were prepared in Milli-Q water by sonicating for 1h. Their characterization, including surface chemistry and charge, was previously made [35]. Five µL of CNTs were drop casted on the surface of the PGE, which was then dried in the oven at 60°C.

3.5.3 Real electroactive area (REA) of the working electrode

In order to assess which is the best protocol for the CNTs application to the PGE, the real electroactive area had to be determined. Thus, first the REA of the PGE was calculated without the application of

any CNTs. Furthermore, different amounts of CNTs were applied to the PGE in order to compare the different REAs created through the process. Cyclic voltammetry at varying scan rates was performed at 200, 100, 20, 10, and 5 mV s^{-1}, which were then plotted against the obtained capacitive current. A linear relationship was obtained, from which the double layer capacitance can be determined:

$$Capacitive\ current = Cdl * \frac{dE}{dt}$$

Capacitive current [A]

Cdl … double layer capacitance [F]

Through this the REA can be calculated:

$$REA = \frac{Cdl}{Cdl^*}$$

REA … Real electroactive surface [cm^2]

Cdl* … specific capacitance of pyrolytic graphite = 10 µF cm^{-2}

3.5.4 Bioelectrode preparation

Primarily enzyme immobilization occurred by a method called drop coating (Protocol A). According to Protocol A, a small aliquot of 2 µL of either the enzyme solution, the ionomer or a mixture of enzyme and ionomer was drop casted on the electrode surface and incubated in the fridge at 4°C for 15 min. Then the bioelectrode was rinsed with Milli-Q water to remove loosely bound enzyme, and transferred to the electrochemical cell for electroenzymatic experiments.

In a second immobilization protocol, Protocol B, the enzyme and ionomer were applied successively to the electrode surface. First, 1 µL of BOD was drop-casted on the PGE and incubated for 15 min at 4°C and then 1 µL of ionomer was immobilized on top and incubated for 15 min at 4°C as well. The PGE was rinsed as well to remove loosely bound materials before measurements.

Another method often used for enzyme immobilization is dip coating. This immobilization protocol, Protocol C, was performed in order to inspect whether the different methods of immobilization lead to contrasting results. Hereby only the process of the enzyme mixture immobilization is different, the rest of the preparation was performed identically. To immobilize the enzyme on the electrode, 40 µL of the enzyme or a mixture of enzyme and ionomer were pipetted into a small cap and the electrode was then dipped into this solution for 15 min at 4°C, while ensuring that the surface of the PGE was submerged fully without any air bubbles. After immobilization the electrode was rinsed to ensure removal of loosely bound enzyme before transferal to the electrochemical cell.

3.5.5 Cyclic Voltammetry (CV)

Cyclic voltammetry is considered to be one of the most popular and powerful tools for studying electrochemical reactions [33]. With this technique it is possible to observe the redox behavior and study the catalysis of a species over a wide range of potential [32,36]. Hence both thermodynamic and kinetic data can be obtained. In CV, voltage is applied to the WE and scanned linearly from an initial value of potential to a point (forward scan) where the direction of the scan is reversed back to the original potential (reverse scan) [32,33]. This point, where the scan direction is reversed, is referred to as the switching point [33,36]. This working electrode potential is further controlled against the RE, possessing a stable equilibrium potential, which is used as a reference point.

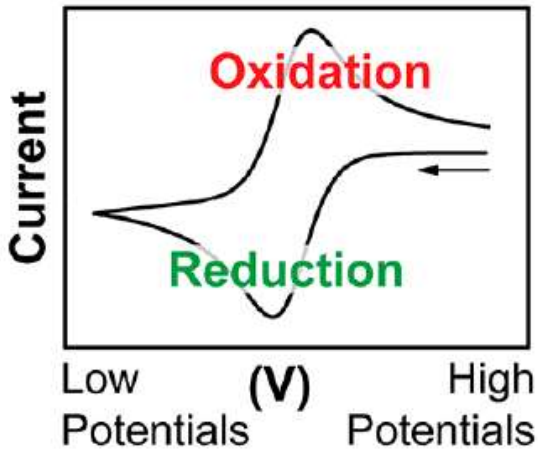

Figure 8: *Example of a cyclic voltammogram showing a reversible reduction/oxidation process* [32].

Consider a reaction at the electrode involving only an electron exchange within a redox couple, freely diffusing to the electrode:

$$Ox + e^{-} \leftrightarrows Red$$

The reduced species (red) in solution are oxidized at the electrode surface and oxidized species (Ox) diffuse back in solution. Thus, by measurement of the current at the WE during the potential scan a voltammogram is obtained. An example of how such a curve looks is shown in Figure 8. On the x-axis the applied potential is plotted, on the y-axis the resulting current at the corresponding potential. During the negative (cathodic) scan direction, the species is reduced as soon as the potential approaches the thermodynamic redox potential of the species. There the current is also called cathodic current.

Another important parameter in CV is the scan rate, controlling the velocity with which the applied potential is scanned [32]. Performing the experiment in an unstirred solution and without a rotating electrode, meaning that the electrode is stationary, the principle underlying the electrochemical reaction bringing the reactant to the electrode surface is diffusion. Diffusion is a relatively slow process limited by mass transport; thus, the reaction cannot proceed in the steady-state. A depletion zone

close to the electrode surface emerges and increases with time [33]. Consequently, mass transport is slowed down, becoming the rate determining step and the current reaches a maximum, referred to either as cathodic peak or anodic peak [33,36]. Through faster scan rates this diffusion layer can be reduced and higher currents can be obtained [32]. A peak shape is observed because the reaction is limited by diffusion of oxygen to the electrode. For the anodic current the scan direction is switched and when the potential is high enough the oxidation process starts [36]. The cathodic and anodic peak currents should be equal, and the average peak potential gives the redox potential of the species.

In the case where a catalytic reaction occurs at the electrode surface, catalysts, either inorganic or organic ones, are involved in product generation. Here a biocatalyst, bilirubin oxidase in this thesis, reduces O_2 to water [35]:

$$2H^+ + {}^1/_2\ O_2 + 2e^- \rightarrow H_2O$$

Figure 9 shows a typical shape for a cathodic catalytic reaction. A sigmoidal curve is obtained, reaching a plateau as the catalytic process occurring at the electrode surface is limited by mass diffusion.

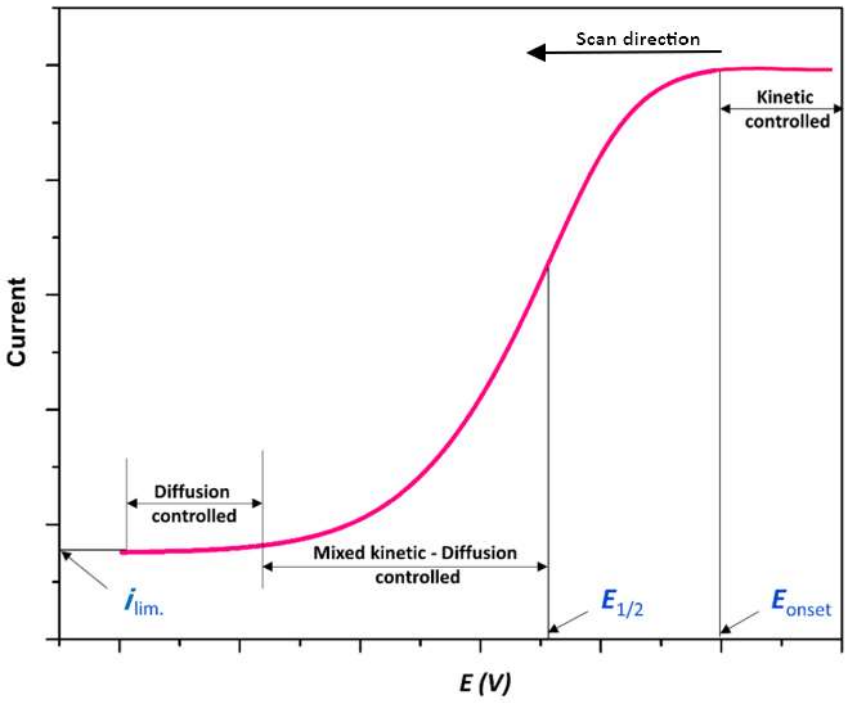

Figure 9: *Typical curve obtained for an electron transfer of a catalytic reaction*[35]

To evaluate the catalytic activity, the onset potential (E_{onset}) and the limiting current (i_{lim}) are important parameters. Often the half-wave potential ($E_{½}$) is used as well. The catalyst is more active, the more positive the E_{onset} is [35]. The E_{onset} is evaluated at the point where the potential is sufficiently negative so that the species available in solution can be reduced by the electrode [36]. From the limiting current values, considering the enzyme coverage is known (which is hard to achieve with enzyme), TN can be calculated.

Typically, CV was performed at a scan rate of 5 mV s^{-1} with a scanning window between 0.23 V to - 0.42 V vs $Hg|Hg_2SO_4$. Oxygen or nitrogen were continuously bubbled throughout the experiments. By bubbling oxygen, the depletion of substrate at the electrode surface was avoided.

All the currents are normalized against the current obtained for 5 µM *Mv*BOD, in order to get rid of any variation in enzyme activity with time. The average activity of BOD was determined at 33.9 µA (± 2.6).

3.5.6 Amperometry

In amperometry, the current is measured as a function of time, where a potential is applied to the WE [37,38]. Initially the potential is applied at a value where no reactions occur before jumping to the recording potential [39]. Depending on the diffusion of analyte to the electrode surface, this measured current fluctuates and is then used to measure the resulting current-time dependence [37,39]. Amperometry was carried out immediately after CV at -0.12 V vs $Hg|Hg_2SO_4$ for an hour, followed by another CV measurement.

3.7 UV-Vis Spectroscopy

Absorption is a commonly used technique when it comes to protein concentration determination. UV-Vis spectroscopy records the absorption of ultraviolet and visible regions of light by a sample [40,41]. The ultraviolet region ranges from 10-400 nm and the visible region extends from 400-800 nm [40]. Absorption spectra are obtained by the excitation of the outer layer of electrons of atoms, which are excited to higher energy levels. Those elevated energy levels are not stable and have to revert back to their initial level, referred to as the "deactivation" process. A relation to correlate the intensity of absorption with the absorbing species was developed by Lambert and Beer [42]. Thus, the kinetic information concerning a protein can be obtained with the UV/Vis spectrum. As the molar absorption coefficient of ABTS is known ($\varepsilon_{420\ nm}$ = 36000 M^{-1} cm^{-1}) [43], the ABTS cation radical concentration can be calculated with the Lambert Beer's law:

$$A = \varepsilon * C * L$$

A …Absorbance at a certain wavelength λ

ε … molar absorption coefficient [M^{-1} cm^{-1}]

C … concentration $ABTS_{ox}$ [mol L^{-1}]

L … pathlength [cm]

The turnover number (TN) can then be determined by:

$$\frac{dA}{dt} = \varepsilon * \mathrm{L} * \frac{dC}{dt}$$

$$\frac{dC}{dt} = \frac{1}{\varepsilon * \mathrm{L}} * \frac{dA}{dt}$$

$$TN = \frac{\frac{dC}{dt}}{c(enzyme)}$$

TN … turnover number [s^{-1}]

Through the turnover number, the number of substrate molecules utilized by an enzyme per second can be illustrated. Thus, the TN can be used to compare different enzymes, different assays, or as done here different conditions.

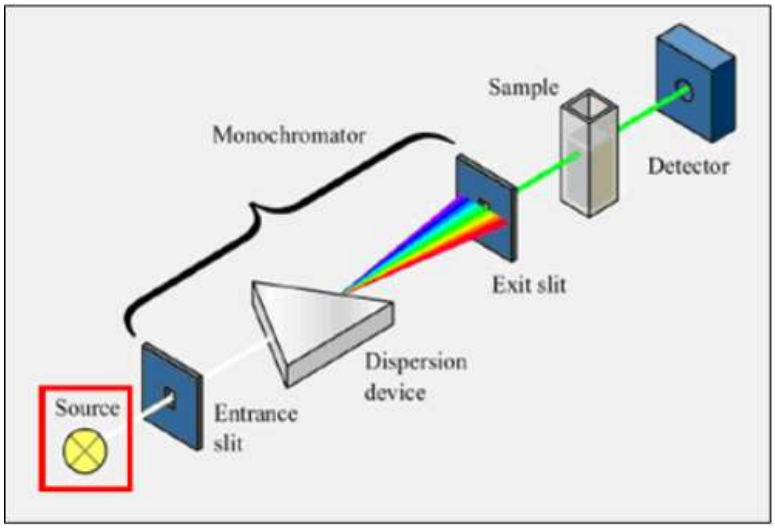

Figure 10: *Schematic representation of a single beam UV -Vis spectrometer. A single beam spectrophotometer consists of a light source, a sample holder, a monochromator in order to split the different wavelengths and a detector* [41].

Enzymatic assays were performed at 25°C by measuring the absorption at 420 nm using an ultraviolet-visible spectrophotometer (Agilent Technologies: Cary Series UV-Vis Spectrophotometer). 2,2'-azino-bis(3-ethylbenzothiazoline-6-sulphonique) diammonium salt (ABTS, ≥98%, Sigma Aldrich) was used as the electron donor. Four replicates were performed for each condition. In the cuvette the *Mv*BOD concentration was 50 nM and ABTS concentration was 1 mM in 50 mM PPB pH 6.0. The respective ionomer dilution was mixed in a 1:1 (v/v) ratio with the enzyme (10 µM) and incubated for 15 min before it was added into the cuvette to measure.

To determine the pH dependency of BOD, PPB was exchanged for the universal buffer. The enzyme was incubated for 15 min at each pH before the measurement. Incubation of the enzyme also lasted

15 min at acidic or alkaline conditions before restoration back to pH 6.0 occurred. Furthermore, the release of the enzyme from the electrode surface was determined via UV-Vis spectroscopy. For this, the electrode was prepared as described above using Protocol A and then incubated in the cuvette in PPB for 10 min at RT before the measurement was performed. Those experiments were performed twice.

3.8 Aggregation experiments

In order to determine whether the ionomers aggregate with the enzyme and to which extent, some aggregation experiments were performed.

3.8.1 Dynamic light scattering (DLS)

Dynamic light scattering is a common measurement technique to analyze particle size. DLS relies on the principle that particles scatter monochromatic light waves in all directions depending on their size and shape [44]. This method is based on the Brownian motion of dispersed particles: solvent molecules and particles collide constantly, inducing particle movement through the generated energy. As smaller particles move at higher speeds than larger particles, the measured movements can be related to size [45]. This occurs through analysis of the scattered light intensity as a function of time to determine the diameter of the particles [46]. Those movements of particles are depended not only on their size, but also on the temperature and the solvent viscosity [45].

3.8.1.1 Refractive index (RI) determination

To measure the refractive index, ionomer dilutions (v/v) were prepared and then dropped on to the refractometer. The temperature was kept constant at 25°C. The RI was determined to measure the density of the solutions.

3.8.1.2 Density measurement

In order to perform the viscosity measurement, the density had to be determined beforehand. This was achieved with a density meter with a constant temperature of 25°C.

3.8.1.3 Viscosity measurement

The viscosity of the various ionomer dilutions (v/v) was measured with a micro-viscometer with a constant temperature of 25°C and the previously determined density with the “Lovis standard” method was used. The ionomer dilution was filled into a capillary with a diameter of 1.59 mm, containing a small steel ball with a diameter of 1.5 mm. Hereby it is important that no air bubbles are

in the capillary in order for the measurement to succeed. The capillary was then closed and put into the micro-viscometer.

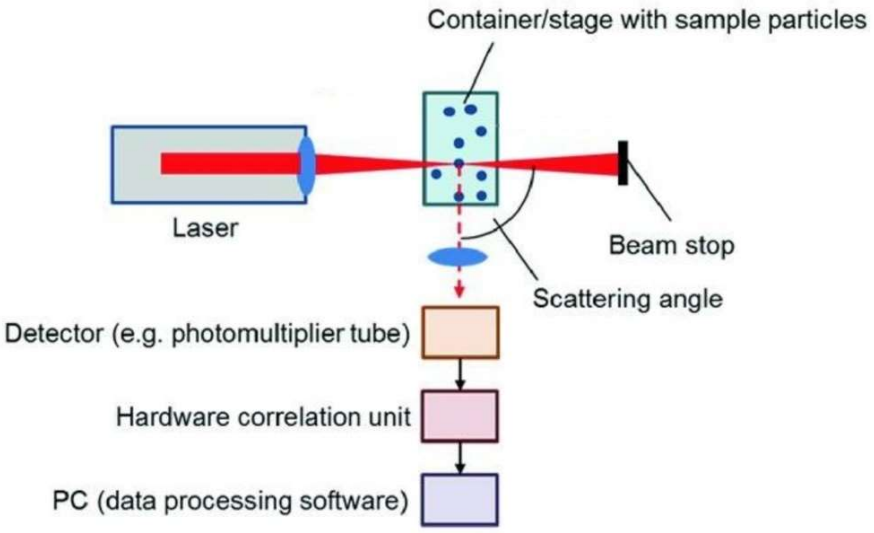

Figure 11: *Schematic diagram of a dynamic light scattering process. Particles scatter the light over time at a scattering angle, directed at a detector*[44].

A schematic diagram of DLS is depicted in Figure 11; a laser is directed at the sample contained in a cuvette. The scattered light is then focused onto a detector at a certain angle over time, which is connected to a downstream data processing setup that is able to translate the obtained particle movements into the corresponding size [44].

Dynamic light scattering was performed with the ionomer dilutions (v/v) alone as well as in combination with *Mv*BOD 10 µM in a Zetasizer machine, the laser having a wavelength of 633 nm. *Mv*BOD was centrifuged at 13500 rpm for 30 min before performing DLS measurements, in order to remove any impurities that could lead to a high background noise and thus disturb the measurement. In order to perform DLS, a ZEN0040 measuring cell was used with a constant temperature at 25°C. The equilibration time was set to 120 s and 3 measurement cycles were performed for each sample. The option 'Protein' was chosen as material with a refractive index of 1.450, while for the dispersant the previously determined data for the refractive index as well as the viscosity was specified in the settings for each individual ionomer dilution. As an analysis model, the 'Protein analysis' was selected for the measurements containing *Mv*BOD and the 'General purpose' method for the ionomer dilutions without enzyme. The ionomer dilution or the ionomer and BOD mixture (v/v) with a total volume of 60 µL was pipetted into the measuring cell and put into the Zetasizer.

3.10.2 Sodium dodecyl sulfate - polyacrylamide gel electrophoresis (SDS-PAGE)

Sodium dodecyl sulfate - polyacrylamide gel electrophoresis (SDS-PAGE) is used to separate and analyze macromolecules such as enzymes based on their molecular weight[47].

Complex formation of the non-polar regions of the enzyme with the SDS occurs due to hydrophobic interactions. The polar head of SDS is responsible for charging the SDS-protein complex with a net negative charge[48]. Larger molecules migrate faster than small ones as molecular weight correlates with the electrophoretic flow speed[49]. Possible aggregation happening between the enzyme and the ionomer can be identified by SDS-PAGE.

For the preparation of the samples 30 µL of each sample was centrifuged for 30 min at 13000 rpm. The supernatant was transferred to a new Eppendorf tube. The pellet was resuspended in 30 µL loading buffer (Table 3) and 30 µL of PPB were added as well. To the supernatant also 30 µL loading buffer were added. Through this separation in the gel, possible aggregation can be identified. To denature the proteins, the mixture was incubated at 95°C for 10 min and then filled into the chambers of the gel (EZBiolab WSHT Precast Gel). A low molecular weight standard from GE Healthcare was applied to the first chamber of each gel to provide a ladder with 10 proteins of known molecular sizes [50]. A voltage of 80–150 Volts for 45–70 min was applied, until the blue marker of the loading buffer reached the very end of the gel. The gel was then removed from the edging and placed in a box with Instant Blue™ on to a see-saw rocker at 40 osc min^{-1} for 1.5 h to stain the gel and visualize the bands. Afterwards the gel was rinsed with deionized water. The bands on the gel were analyzed according to their appearance, referring to the ladder to estimate their molecular size.

4. Results and Discussion

4.1 Determination of the real electroactive surface

In order to determine the increase of the electroactive surface area of the PGE with CNTs and establish the correct amount of CNTs to be immobilized, the REA has to be measured. The capacitive current was plotted against the scan rate velocity to calculate the REA.

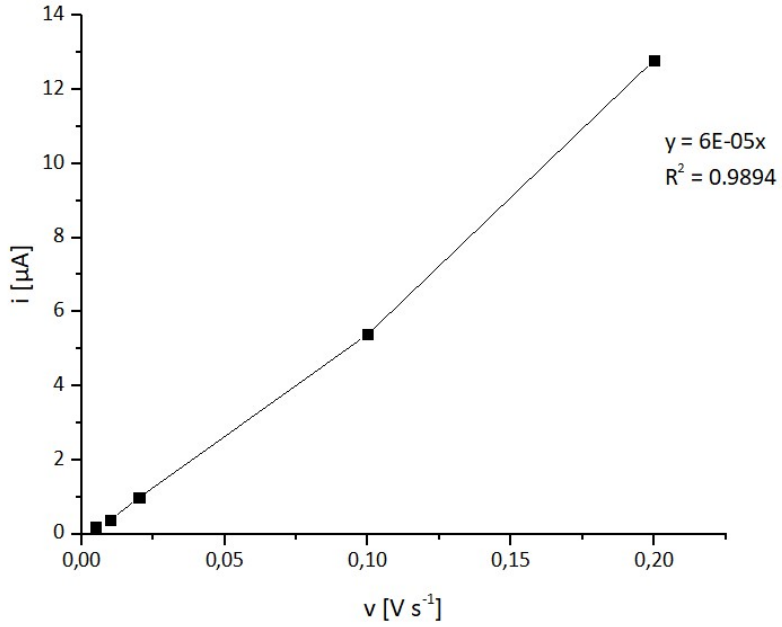

Figure 12: *Real electroactive surface measurements with 5 µL of CNT deposited on PGE at RT.*

Through the obtained linear equation shown in Figure 12, the REA can be calculated. An example calculation for the REA with a 5 µL CNT (1mg mL[1]) layer is shown:

$$Capacitive\ current\ = Cdl\ \frac{dE}{dt}$$

$$Cdl = \ 6 * 10^{-5}\ F\ \triangleq 0{,}00006\ \mathrm{F}\ \triangleq 60\mu\mathrm{F}$$

$$REA\ = \frac{Cdl}{Cdl^*}$$

$$REA\ = \frac{60\mu F}{10\mu F\ cm^{-2}} = 6\ cm^2$$

All other REAs were calculated following the same calculation scheme and the results are shown in Table 4.

Table 4: Calculated real electroactive surface values for different nanotube layers

Nanotube layer [µL]	Real electroactive surface [cm^2]
0	1
2	3
5	6
10	10
5+5	10

It can be clearly observed that with an increase in the amount of CNTs that were applied on the PGE surface, the REA is increasing simultaneously, thus providing a larger surface area for enzyme immobilization. An application of 5 µL CNT was chosen for further experiments for the purpose of combining a large enough electrochemical surface area with a strong mechanical stability of the nanotube layer. The enhancement achieved with CNTs when compared to the geometric surface area (0.07 cm^2) shows an 85-fold increase in the surface area.

4.2 *Mv*BOD activity with pH

Determination of the optimal pH of catalytic activity for BOD is performed to gain some insight into a basic parameter influencing the enzyme. The optimal pH range of *Mv*BOD activity was determined with UV-Vis spectrophotometer with ABTS as the electron donor. The TN was calculated and plotted against the pH, the results are shown in Figure 13.

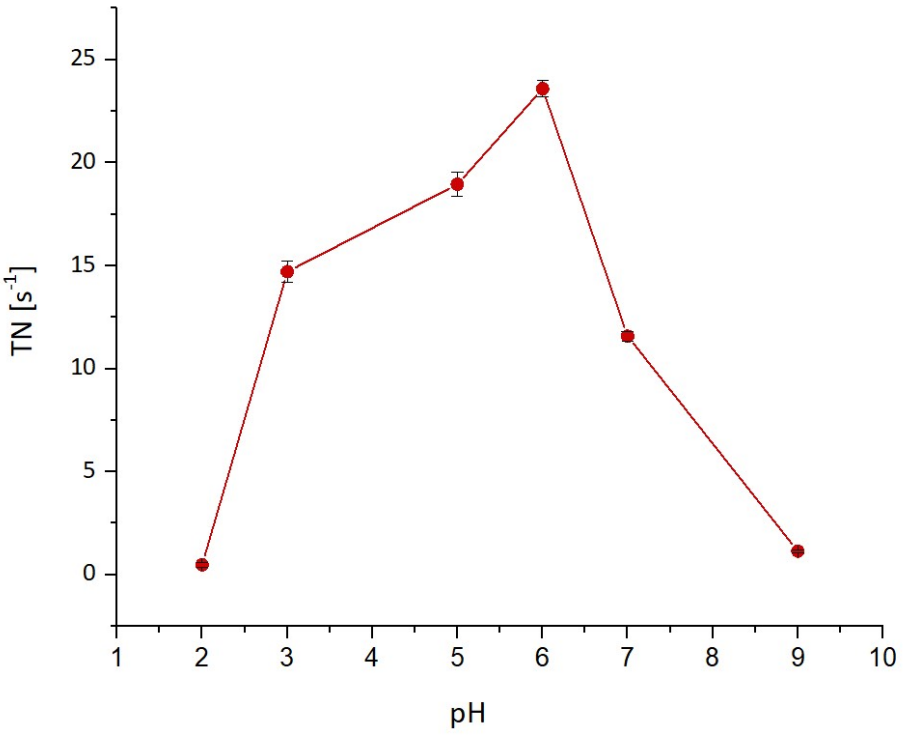

Figure 13: *pH dependency determination of MvBOD activity by UV-Vis SPEC, optimal pH is determined at 6.0.*

A bell-shape evolution is observed. The optimal pH at 6.0 shows a TN of 23.6 s^{-1} (± 0.4). This experiment was performed using the universal buffer instead of the PPB that was usually used to obtain the TN value of *Mv*BOD. For comparison, a TN of 22.6 s^{-1} (± 2.9) was obtained when measuring the activity with the PPB.

Further the regeneration of *Mv*BOD activity dependent on the pH was examined.

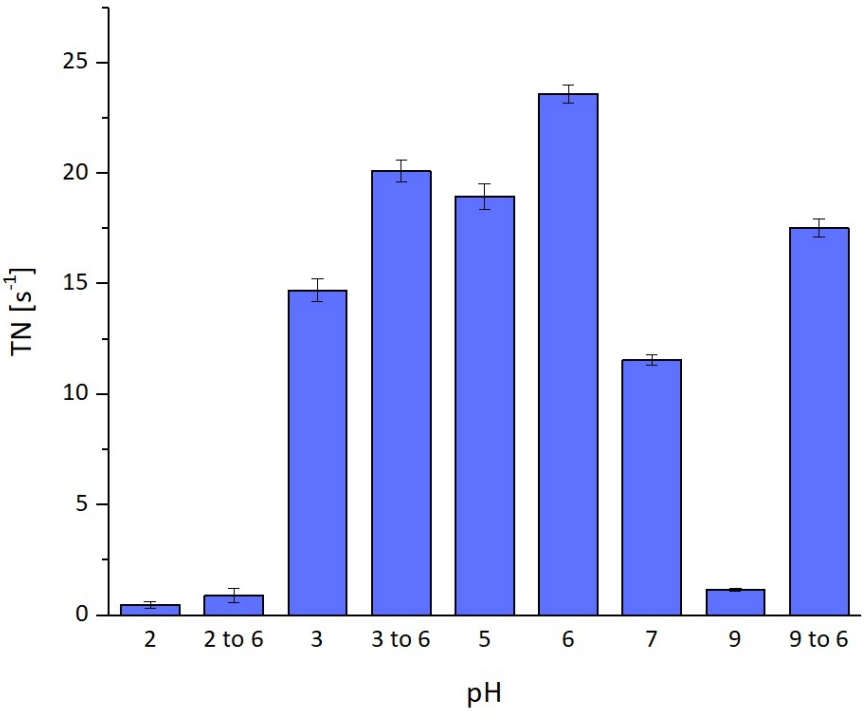

Figure 14: *pH dependency of MvBOD activity by UV-Vis SPEC.*

Figure 14 shows the regeneration of activity of *Mv*BOD after incubation at pH levels that are far from the optimal range. The highest activity is, as expected, obtained at the optimal pH of 6.0 with a TN of 23.6 s^{-1}, as stated above. The TN at pH 5.0 is just below the one of pH 6.0 with an obtained TN of 19 s^{-1} (± 0.6), which is still 84% of the activity at pH 6.0. Whereas the TN obtained at pH 7.0 is already reduced to around 50% with a value of 11 s^{-1} (± 0.2).

Furthermore, it can be clearly seen that at pH 2.0 there is almost no activity remaining with an obtained TN of 0.5 s^{-1} (± 0.1) as well as that the regeneration of the enzyme activity is not possible when the enzyme is transferred back to the optimal pH of 6.0. However, for pH 3.0 where an initial TN of 14.7 s^{-1} (± 0.5) was measured, enzyme activity could be restored to almost 90% of the original activity after the enzyme was returned to pH 6.0. Remarkably, for pH 9.0 where a very low TN of 1.1 s^{-1} (± 0.06) was determined, the activity could be regenerated to 78% of the original activity. Thus, it was established that the activity of *Mv*BOD is affected by pH and that the activity of the enzyme is non-reversibly lost at pH 2.0, probably by loss of the copper atoms and unfolding.

4.3 pH Modulation by ionomers

As SPEEK and Nafion are sulfonated ionomers they are strong acids. SPEEK has a pK_a of -1 and Nafion of -6 [51]. To check whether the pH of the ionomers has an impact on enzymatic activity, the pH of the ionomers as well as the pH of the ionomers in their various dilutions was measured. These results also assist in evaluating and making the differentiation between the effect of pH and other properties.

4.3.1 Nafion

The pH of the individual components as well as the pH of various Nafion dilutions that were used during the experiments were determined and are shown in Tables 5, 6 and 7.

Table 5: pH of individual components.

	pH
PPB 50 mM	6.09
Milli-Q H_2O	6.81
Nafion	1.80

Table 6: Influence of Nafion on the pH with varying dilutions.

	pH	
Nafion dilution (v/v)	+ PPB	+ H_2O
1:1	2.73	2.06
1:10	5.50	2.64
1:50	5.95	2.76
1:100	6.02	3.12

Table 7: Influence of Nafion on the pH with varying dilutions in the presence of 10 µM BOD.

Nafion dilution (v/v) + BOD 10µM	pH
1:1	3.61
1:10	5.15
1:50	6.05

Nafion on its own is very acidic, but already the Nafion 1:1 (v/v) dilution with PPB increases the pH to 2.7 meaning that there is possibility for enzyme activity, since the pH should not fully denature the enzyme. Already at the 1:50 dilution the pH is almost back to the optimal pH for BOD activity.

4.3.1 SPEEK

The pH of the individual components as well as the pH of the various SPEEK dilutions, that were used during the experiments were determined and are shown in Tables 8, 9, and 10.

Table 8: pH of individual components.

	pH
PPB 50 mM	6.09
Milli-Q H_2O	6.81
SPEEK	1.28

Table 9: Influence of SPEEK on the pH with varying dilutions.

	pH	
SPEEK dilution (v/v)	+ PPB	+ H_2O
1:1	1.87	1.48
1:10	3.19	2.10
1:50	5.68	2.72
1:100	5.91	3.02

Table 10: Influence of SPEEK on the pH with varying dilutions in the presence of 10 µM BOD.

SPEEK dilution (v/v) + BOD 10µM	pH
1:1	2.56
1:10	3.96
1:50	5.65
1:100	6.04

SPEEK shows a very high acidity, even more than Nafion, which is linked to the 2.5 times higher content of sulfonate groups present in SPEEK. Even SPEEK that is diluted with PPB in a 1:1 ratio has a pH below 2. Therefore, expectations are that the lowest SPEEK dilution will lead to enzyme denaturation, meaning loss of activity. Only SPEEK in a 1:100 dilution is back at the optimal pH range for BOD. Below that the conditions for the enzymatic activity are not ideal, even though concerning the 1:50 dilution the pH should not immensely influence the enzymatic activity, as the pH value at 5.65 is close to the optimal pH range.

By dilution of the ionomers in PPB pH 6.0 the sulfonate groups were expected to be neutralized. Only higher dilutions allowed for complete neutralization of the pH. Nevertheless, the pH and the ionic strength of the buffer were kept the same during all experiments. Examining the effects of changing

the parameters of the buffer solution will be the next step to evaluate if an improvement of enzyme activity or stability can be achieved.

4.4 *Mv*BOD activity in solution

First the activity of the enzyme in solution with the respective ionomers was studied.

4.4.1 Influence of Nafion

In Figure 15 the TN for BOD with the various Nafion dilutions that were obtained by UV-Vis spectroscopy are compared.

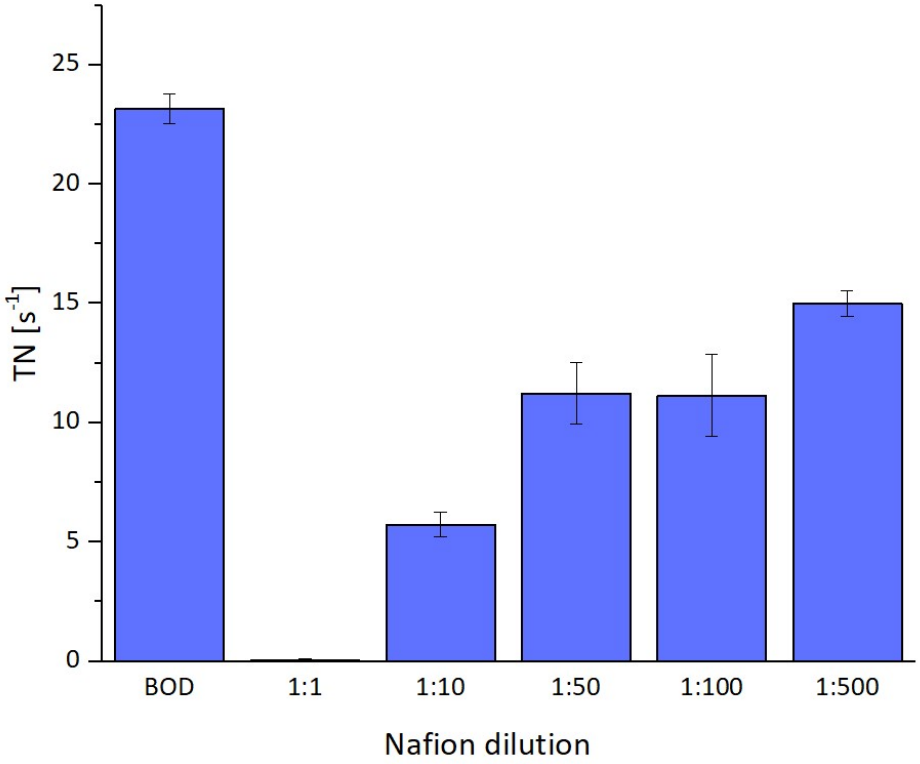

Figure 15: *Comparison of the* TN *obtained by UV-Vis SPEC at 420 nm for various Nafion dilutions in combination with MvBOD 50 nM in a cuvette.*

The activity of the BOD in the presence of Nafion decreases with an increase in the Nafion concentration. Concerning the dilution with the highest amount of Nafion (1:1 dilution), pH could be a factor influencing the enzyme activity, since the measured pH of this Nafion concentration was still below 3. For the dilutions with less amount of Nafion present, especially starting with the 1:50 dilution, the pH returns to the optimal range for BOD activity. Nevertheless, the measured TN shows that the activity in those cases is still more than 50% less than compared to BOD alone. This leads to the conclusion that the pH is not the limiting and most influential factor that decreases the enzyme activity, but that Nafion possesses properties that impact the catalytic efficiency of BOD. Even when only a small amount of Nafion is present, the turnover number is only at 65% of the original value, indicating that the effect of Nafion on the enzyme in solution is very powerful.

Furthermore, the stability of BOD activity in the presence of Nafion over 1 h was examined by UV-Vis spectroscopy.

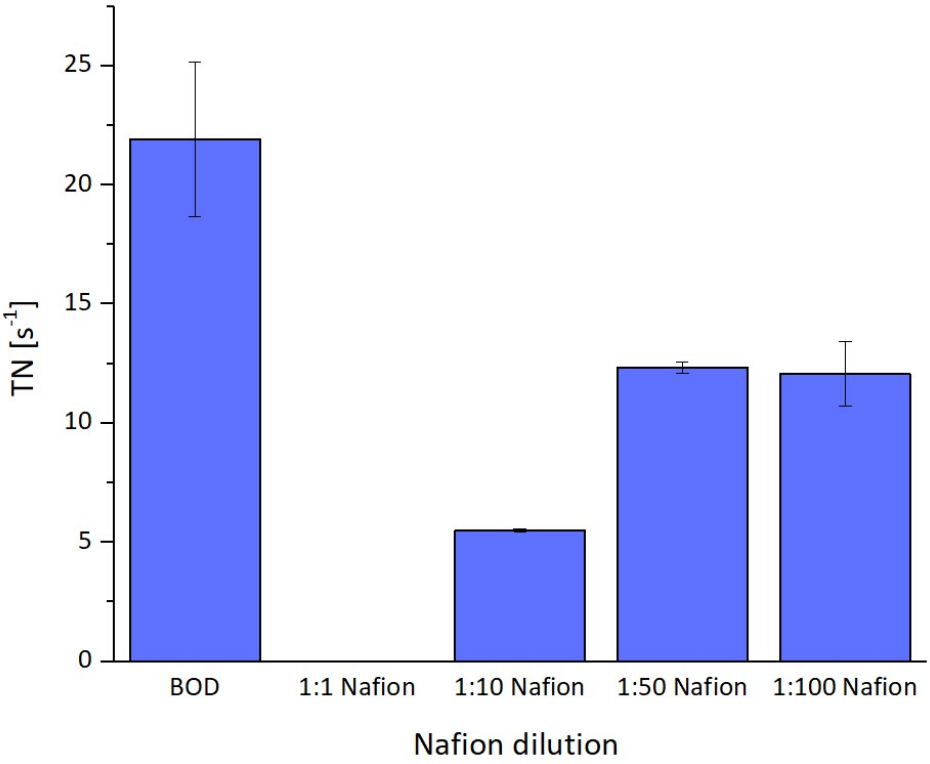

Figure 16: *Comparison of the stability of the TN obtained by UV-Vis SPEC at 420 nm for various Nafion dilutions in combination with BOD 50 nM in a cuvette taken over 1 h.*

The values that were measured during the course of one hour did not vary with any significance. Therefore, the conclusion can be drawn that the enzyme activity remains stable after its initial decline that is created due to the influence of Nafion. If compared to the values of Figure 15, the turnover numbers obtained over 1 h are highly similar whatever the Nafion dilution. One can suggest that the remaining active enzyme in the different ionomer dilution is not affected by the presence of Nafion. In other words, it would suggest that Nafion affects the amount of available enzymes molecules, but only few modification are made after the initial mixing.

4.4.2 Influence of SPEEK

In Figure 17 the turnover numbers that were obtained by UV-Vis spectroscopy for the enzyme with various SPEEK dilutions are compared.

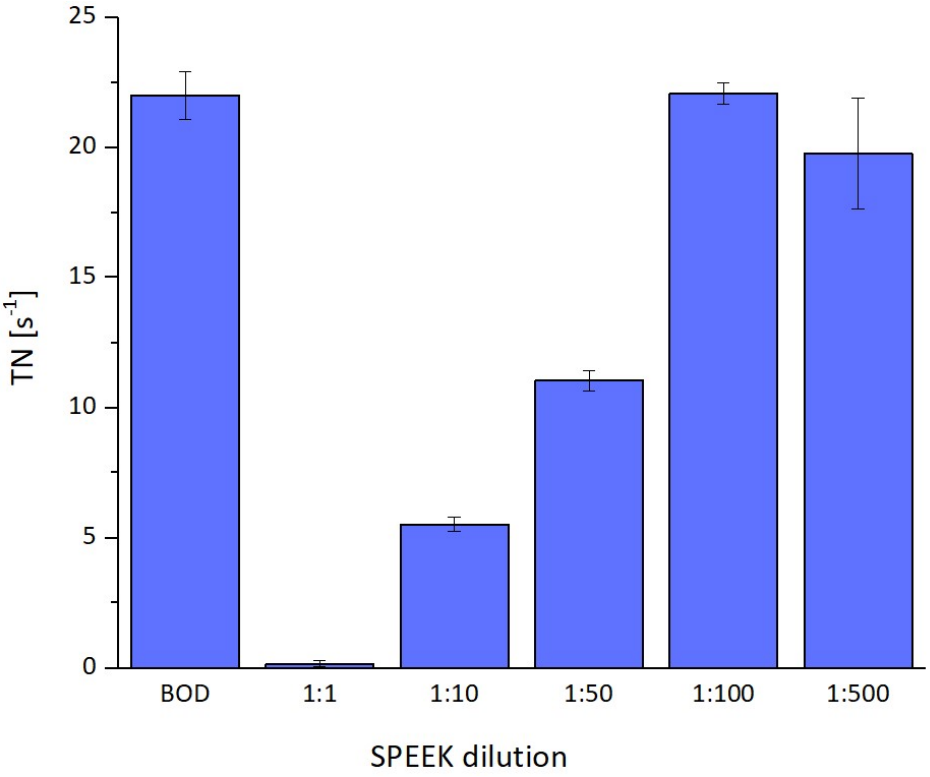

Figure 17: *Comparison of the TN obtained by UV-VIS SPEC at 420 nm for various SPEEK dilutions in combination with BOD 50 nM in a cuvette at 25°C.*

Overall, an increase in the concentration of SPEEK leads to a decrease in enzyme activity. Almost no activity of BOD is obtained with the 1:1 dilution. Here the pH is likely to play an immense role, resulting in the irreversible loss of activity due to its high acidity. Even at the 1:10 dilution the pH is presumably having a significant impact on the enzyme activity, resulting in only 23% of the initial enzyme activity. Concerning the 1:50 dilution, where the activity is still only at half of the activity than for BOD alone, even though the pH is almost back to the optimal range with around 5.6, other properties of SPEEK also seem to have an influence on the catalytic efficiency of the enzyme. When the amount of SPEEK is further reduced the activity is recovered and the turnover number is in the same dimension as when only BOD is measured. This leads to the conclusion that the impact that the properties that SPEEK possess is less severe on BOD in solution than those of Nafion.

4.5 *Mv*BOD activity in the immobilized state

The oxygen reduction by *Mv*BOD in the immobilized state is examined, in order to have a reference.

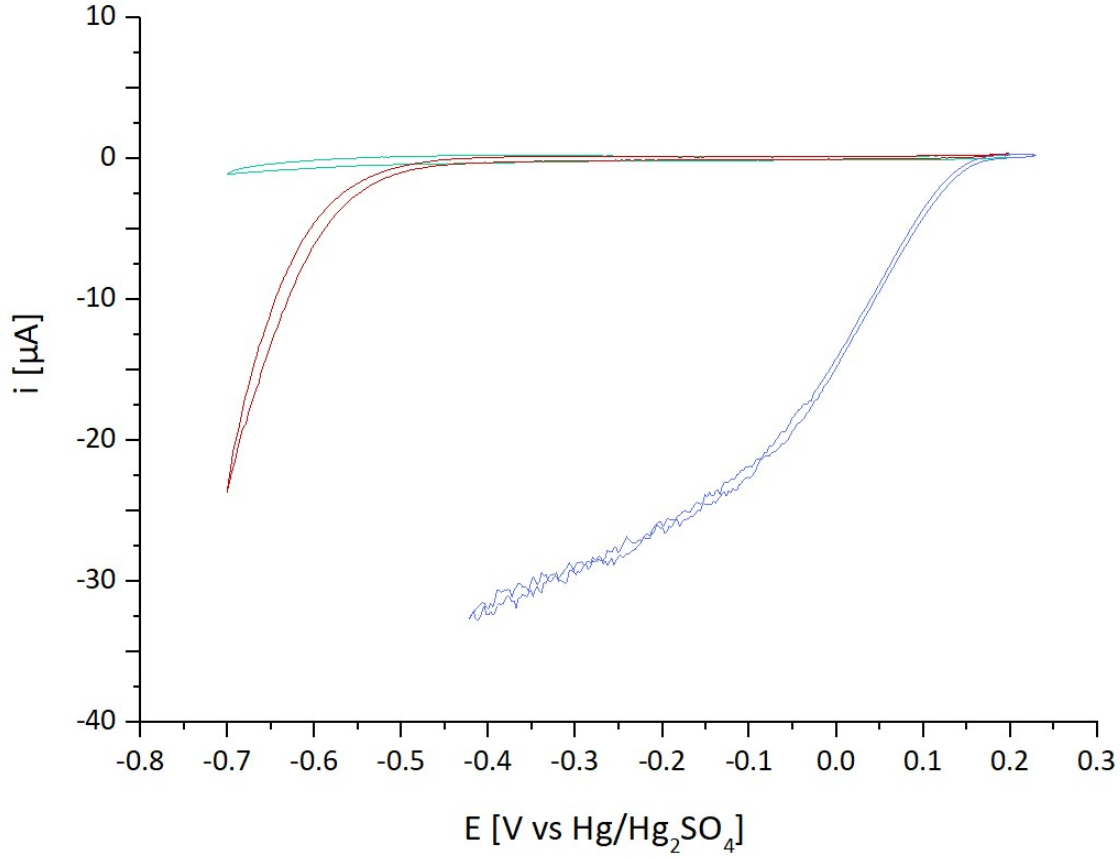

Figure 18: *CVs obtained at 3 different conditions: CNTs under N_2 (green), CNTs under O_2 (red) and CNTs with 5 µM BOD under O_2 (blue) on PGE electrode. 50 mM PPB pH 6. Scan rate: 5 mV s^{-1} at RT.*

The green curve was obtained by measuring the current at the PGE modified with CNTs under N_2. As expected, no faradic current can be observed, as no redox species are present in the electrolyte.
To define the potential window required to measure the enzymatic activity, the oxygen reduction only is measured at the PGE modified with CNTs. The resulting CV curve is depicted in red. Here the oxygen reduction occurring in the absence of the biocatalyst is initiated at a potential of -0.52 V vs $Hg|Hg_2SO_4$. The voltammogram obtained by CV for O_2 reduction by *Mv*BOD shows a well-developed sigmoidal curve. This is characteristic of a direct catalytic oxygen reduction by *Mv*BOD. The Cu T1 site, the first electron acceptor of this enzyme, is responsible for this direct electron transfer. DET is expected since the positive environment of the Cu T1 center of *Mv*BOD interacts with the negative induced charge at the electrode by the CNT layer [52]. The onset potential was determined, according to Figure 9, to be in the range of 0.15 to 0.16 V. The onset potential was looked at for all the measurements performed, and was found to be always in the same range for only *Mv*BOD. This onset potential is markedly different from that obtained in the absence of the enzyme, underlining the efficiency of the catalysis: The enzyme allows O_2 to be reduced at a potential of - 650 mV and higher. The curve

reaches a plateau and the limiting current is determined at - 33,9 µA (± 2,6). This plateau is proportional to the TN and to the enzyme coverage. Unfortunately, the enzyme coverage is a data hardly obtained with enzymes, precluding an easy determination of the TN.

Figure 19 displays a typical curve obtained by chronoamperometry under O_2 of a PGE modified by CNTs and *Mv*BOD.

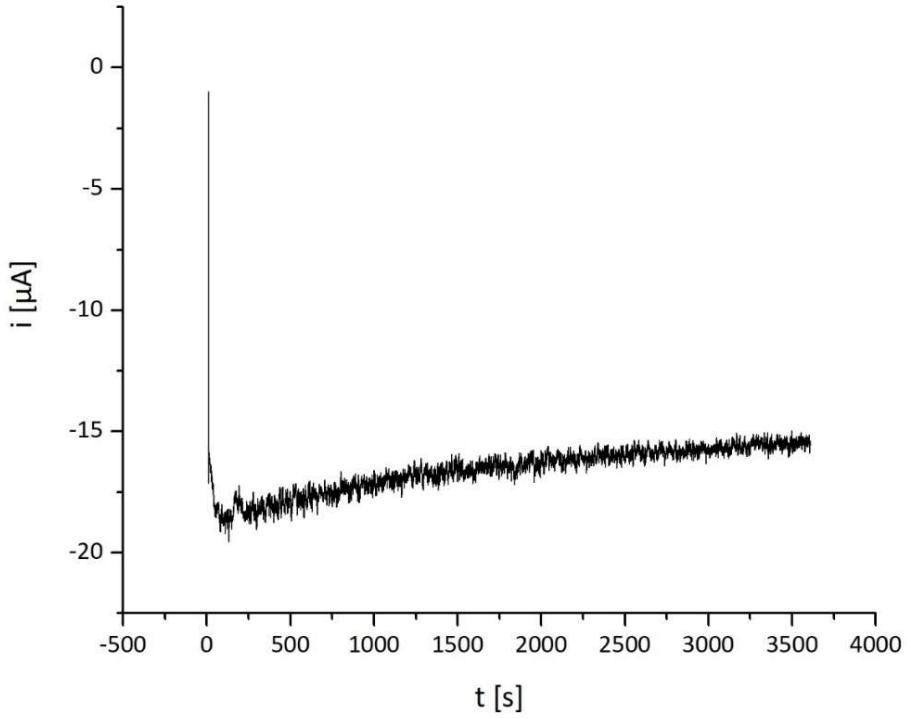

Figure 19: *Stability of the catalytic signal of MvBOD followed by chronoamperometry for 1 h recorded at -0.12 V under O_2 after initial CV at RT.*

The stability of the bioelectrode without any added ionomer was measured by chronoamperometry. As can be seen in this graph the current decreases slowly over 1 h, leaving a remaining 80% of the initial current at the end. In Figure 25 and Figure 30 the stability of the enzyme alone and the enzyme in combination with the ionomers is compared and the standard deviation for the values obtained by CV for only BOD are given as well.

4.6 *Mv*BOD activity in the immobilized state as a function of ionomer concentration

Subsequently the influence of ionomer at the electrode on the enzymatic activity was investigated. A first observation is that in combination with the ionomers, the onset potential for O_2 reduction does not seem to be notable modified.

4.6.1 Nafion

The catalytic process for O_2 reduction by the enzyme immobilized together with Nafion on the PGE modified by CNTs was followed by CV. Figure 20 shows a typical voltammogram for *Mv*BOD mixed with Nafion 1:10.

This curve portrayed here has a similar shape as the CV curves obtained from the enzyme in combination with Nafion 1:1 as well as Nafion 1:50. Only the limiting current obtained for each measurement is different. The individual results are compared against each other in Figure 24.

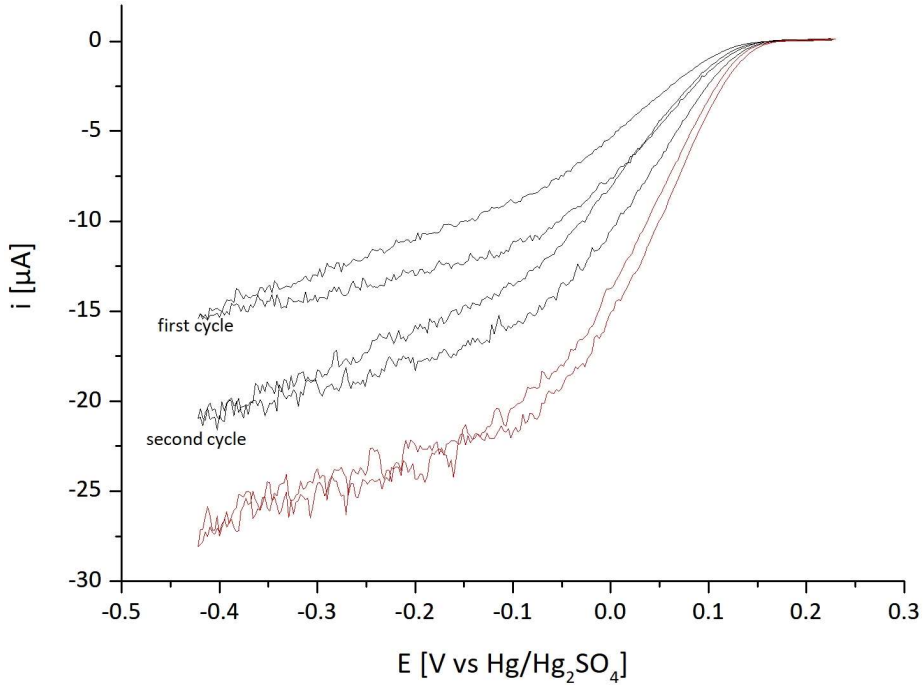

Figure 20: *CVs showing catalytic response obtained under O_2 before (black curve) and after (red curve) the chronoamperometry from BOD + Nafion 1:10 (v/v) mixture after adsorption on a CNTs modified PGE. Scan rate: 5mV s^{-1} at RT under O_2.*

Interestingly, the limiting current is increasing during the second cycle of CV, indicating that the enzyme activity is increasing. Furthermore, the limiting current after the amperometric measurement shows a further increase, although during the measurement the current stays constant during the first and second cycle. This increase in activity over time was only observed when the immobilization technique according to Protocol A was used as well as for the three lowest Nafion dilutions that were examined.

The increase in activity over time might be explained by two different processes. On the one hand, this process might be due to an activation of the enzyme when transferring the bioelectrode to the electrochemical cell at pH 6.0 while the bioelectrode with high Nafion concentration is at a lower pH. On the other hand, a reorganization of the Nafion film could occur that could decrease enzyme

encaging (see below). The limiting current obtained at the end is in the same range than with BOD alone. Thus, Nafion, at least at this dilution, has not much of a negative influence on BOD activity.

Figure 21 shows the catalytic signal obtained by CV for O_2 reduction by BOD with Nafion 1:100. This curve portrayed here is also representing the measurement results obtained from the enzyme in combination with Nafion dilution 1:200 and 1:500. The individual results are plotted against each other in Figure 24 as varying limiting currents are obtained for each measurement.

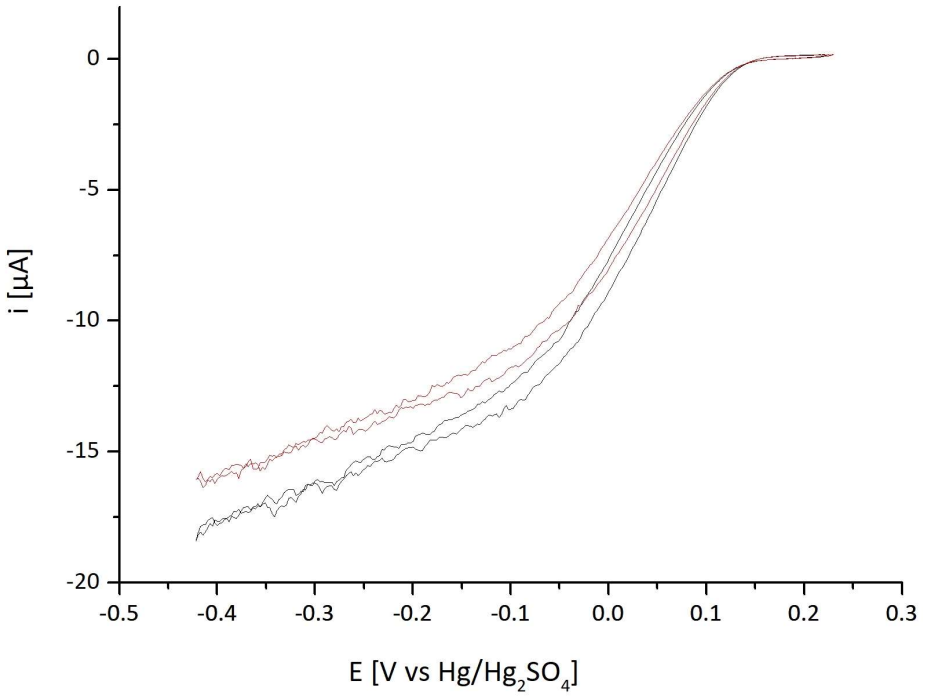

Figure 21: *CVs showing catalytic response obtained under O_2 before (black curve) and after (red curve) the amperometry from BOD + Nafion 1:100 (v/v) mixture after adsorption on a CNTs modified PGE. Scan rate: 5 mV s^{-1} at RT under O_2.*

In Figure 21 the catalytic signal obtained from CV done before chronoamperometry is higher than after the current that is measured after 1 h, establishing that some enzyme activity is lost over time. However, the loss of enzyme activity is not tremendous. The consecutive cycles obtained by CV were the same. The stability of the catalytic current as a function of enzyme and ionomer dilution was tracked with amperometry over the course of 1 h.

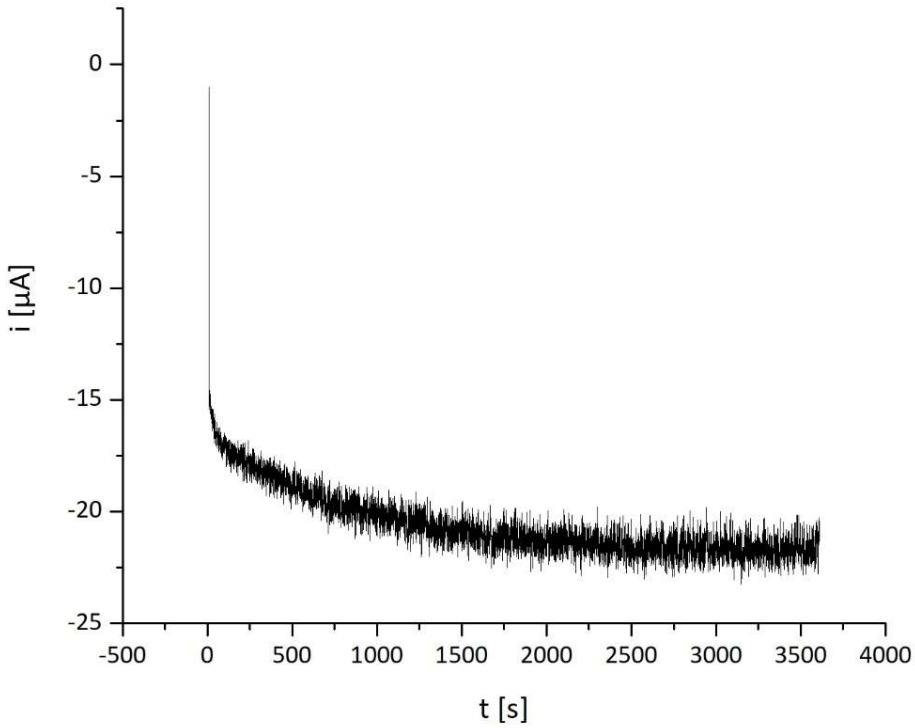

Figure 22: *Stability of the catalytic signal of BOD + Nafion 1:10 (v/v) mixture by chronoamperometry for 1 h recorded at -0.12 V under O_2 after initial CV at RT under O_2.*

Figure 22 is typical for the chronoamperometry data obtained from of the enzyme in combination with Nafion 1:1, Nafion 1:10 as well as Nafion 1:50. It clearly shows that the current is increasing over time, especially during the first 2000 s, and then tends to stabilize. At the end the current obtained is 130% of the initial current. Only the percentage increase over the initial current varies as a function of the Nafion dilution. The individual results are compared against each other in Figure 25.

.

In Figure 23 the amperometric data are shown for Nafion 1:100. This graph is given as an example to illustrate and represent the results obtained for Nafion dilution higher than 1:100.

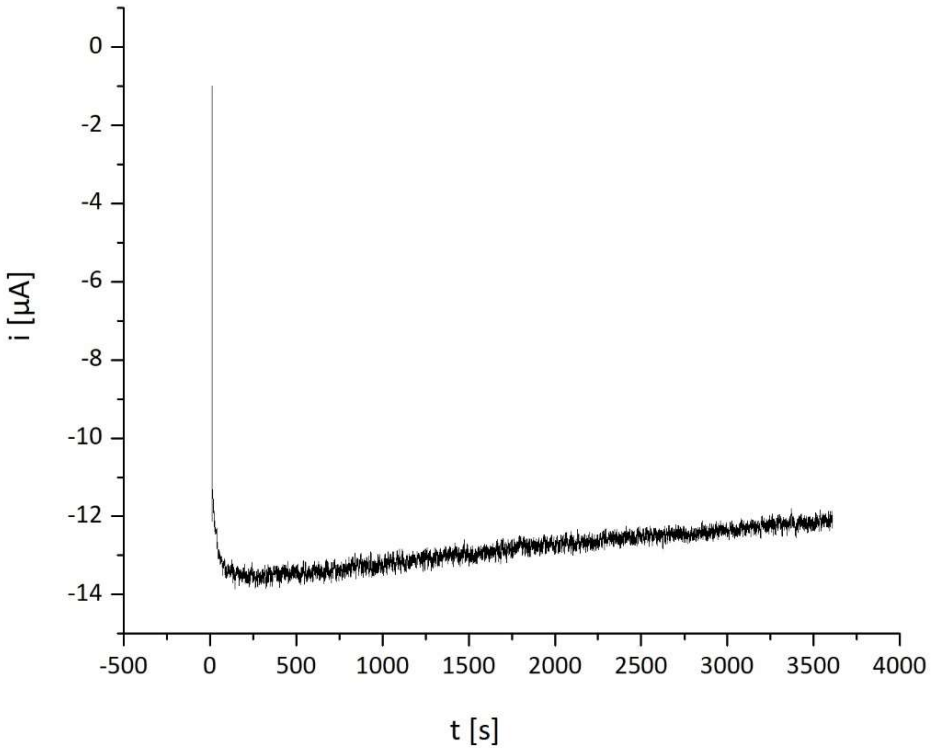

Figure 23: *Stability of the catalytic signal of O2 reduction by MvBOD + Nafion 1:100 (v/v) mixture by chronoamperometry for 1 h recorded at -0.12 V under O_2 after initial CV at RT under O_2.*

In these conditions, the current is decreasing over time.

In order to compare the impact of each Nafion concentration on BOD activity, the normalized limiting currents are plotted in Figure 24.

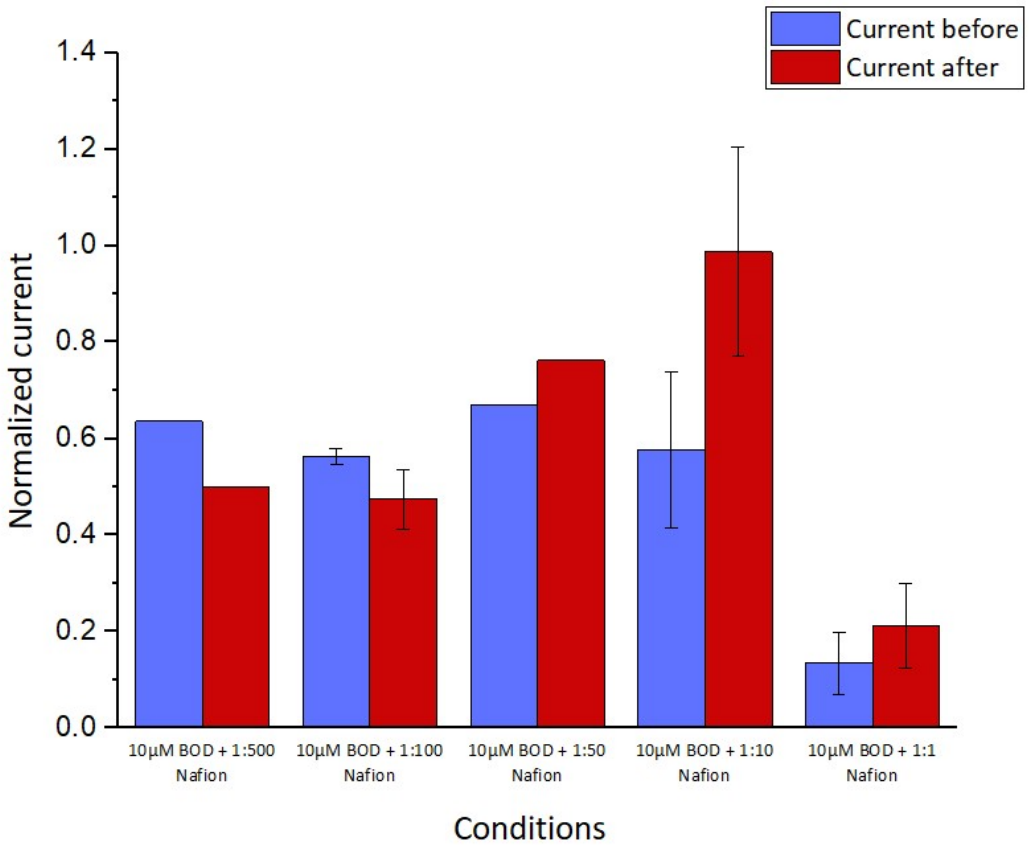

Figure 24: *Comparison of normalized current with the respective standard deviation obtained from CVs showing catalytic response obtained under O_2 before (blue) and after (red) the chronoamperometry from BOD + various Nafion (v/v) mixtures after adsorption on a CNTs modified PGE. Scan rate: 5 mV s^{-1} at RT.*

When a high amount of Nafion is added, as it is the case with the 1:1 dilution, only a low enzymatic activity is obtained, which might be linked to the acidic pH as discussed previously. Concerning all other dilutions, 60–70% of the initial activity is achieved. Thus, a higher activity than recorded by UV-Vis spectroscopy in solution is obtained once the enzyme is immobilized on the electrode in the presence of ionomer. Although not proved at the moment, these differences can be attributed to the organization of Nafion on the electrode surface.

In Figure 25 the different values for bioelectrode stability that were calculated are contrasted to each other.

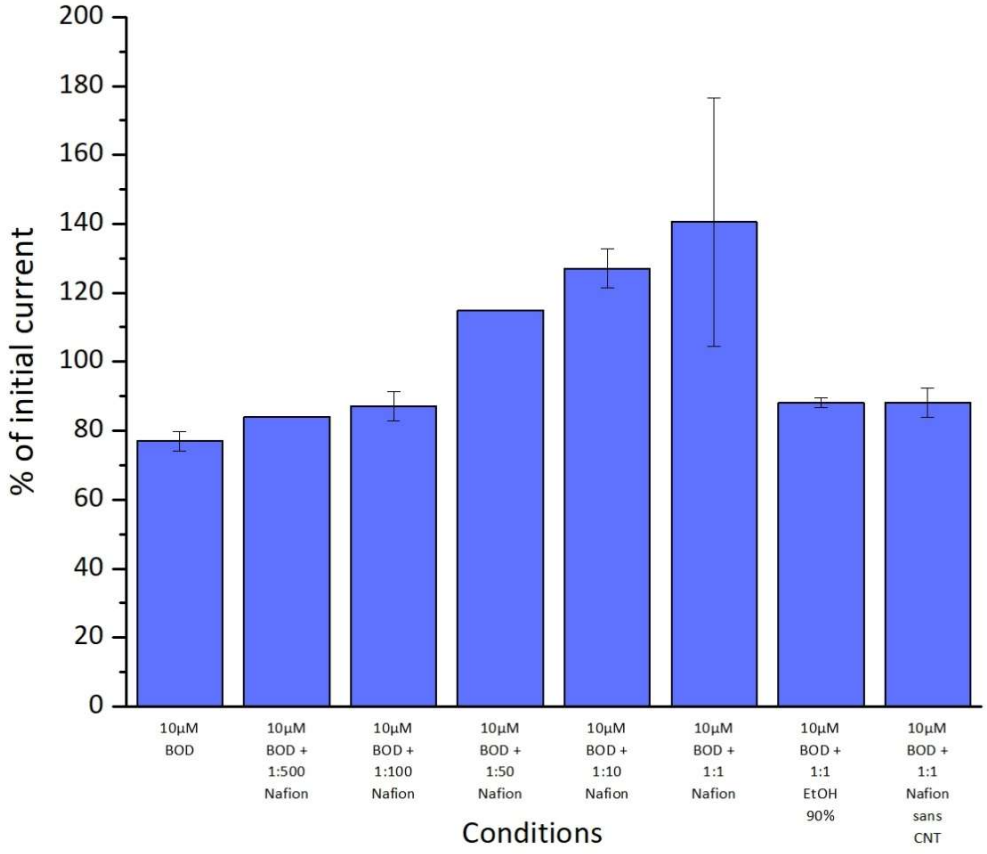

Figure 25: *Comparison of stability of the catalytic signal determined by chronoamperometry for 1 h recorded at -0.12 V under O_2 of BOD + various Nafion (v/v) mixtures after initial CV at RT.*

This shows that the overall stability is around 80% of the initial current for BOD alone. In combination with Nafion the percentage rises to around 90% for most cases. Exceptions are the 1:1, 1:10 and 1:50 Nafion dilutions as in those cases the current increases, surpassing the initial current.

These results suggest that Nafion is responsible for enzyme activity limitation, a process that seems to occur in the beginning of the encounter of Nafion and BOD. Then as the stability remains high, the enzymes that remain active after mixing with Nafion mostly stay active. A possible explanation could be that Nafion encapsulates the enzyme, thus the enzyme is not electrochemically connected to the electrode surface and cannot perform oxygen reduction, explaining the lower limiting current obtained when Nafion is present than compared to only BOD. This encapsulation seems to also appear in solution, thus a lower TN is obtained when Nafion is present.

4.6.2 SPEEK

Figure 26 shows the CV curve obtained for O_2 reduction by the enzyme in combination with SPEEK 1:1.

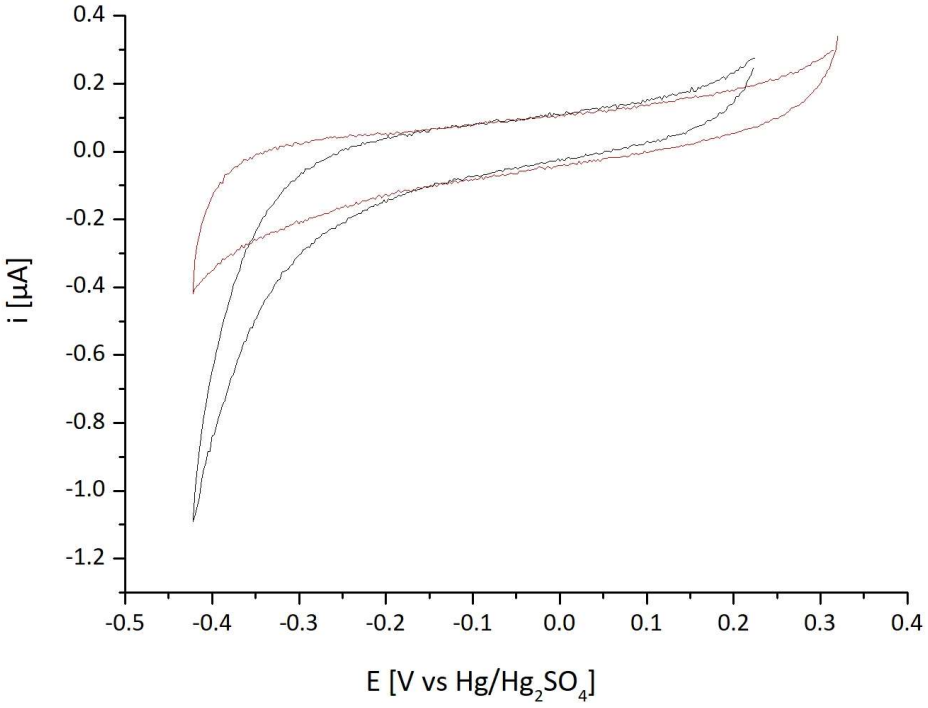

Figure 26: *CVs showing catalytic response obtained under O_2 before (black curve) and after (red curve) the chronoamperometry from BOD + SPEEK 1:1 (v/v) mixture after adsorption on a CNTs modified PGE. Scan rate: 5 mV s^{-1} at RT under O_2.*

No catalytic current is obtained when the enzyme is immobilized on the electrode with SPEEK 1:1. As has been discussed before, the pH of this mixture is extremely acidic, which presumably causes this complete loss of enzyme activity.

In Figure 27 the voltammogram produced from BOD with the SPEEK 1:100 dilution is shown. These curves are given as typical CVs for SPEEK dilution higher than 1:1. For all the measurements different limiting currents were produced, which are compared in Figure 29.

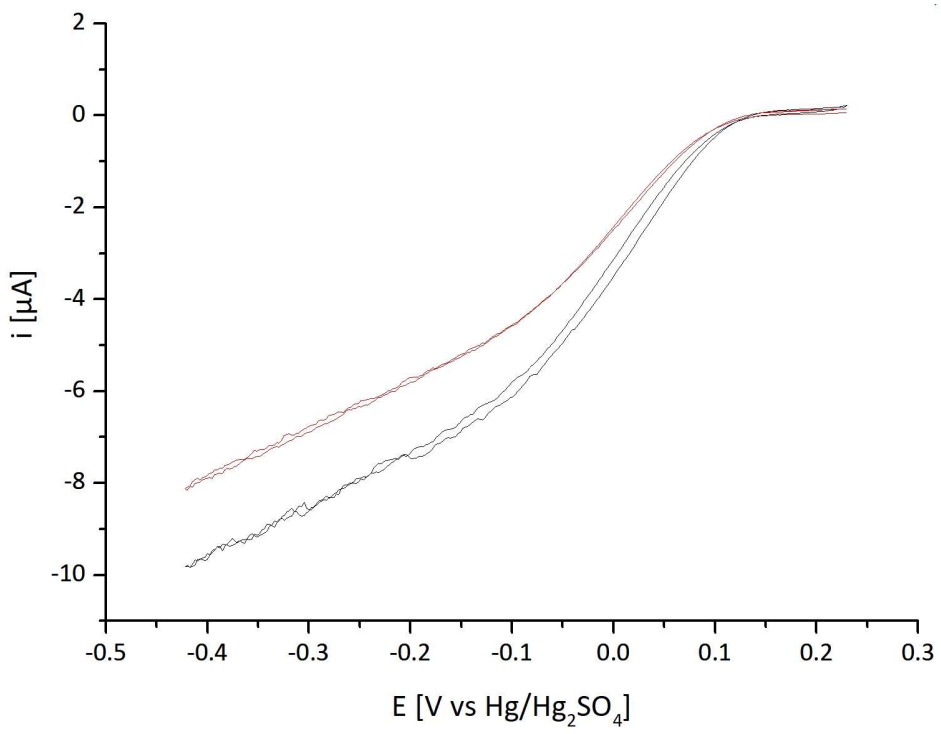

Figure 27: *CVs showing catalytic response obtained under O_2 before (black curve) and after (black curve) the chronoamperometry from BOD + SPEEK 1:100 (v/v) mixture after adsorption on a CNTs modified PGE. Scan rate: 5 mV s^{-1} at RT under O_2.*

A higher dilution of SPEEK allows a catalytic current for O_2 reduction to be observed. The current obtained before chronoamperometry is lower than the current obtained for the enzyme alone and then decreases, although only moderately. The consecutive cycles measured by CV were the same. Several possibilities could be responsible for this behavior. Either some biomaterial is released from the electrode surface, thus reducing the overall current or the polymerization pattern of SPEEK further develops over time, encapsulating more and more enzyme, therefore also reducing the amount of enzyme that is able to perform oxygen reduction. Amperometry was also performed with the SPEEK 1:1 dilution. No current was obtained during this measurement, which is not shown, and in agreement with CV measurements.

Figure 28 shows the chronoamperometry curve obtained for O_2 reduction by *Mv*BOD mixed with the SPEEK 1:100 dilution.

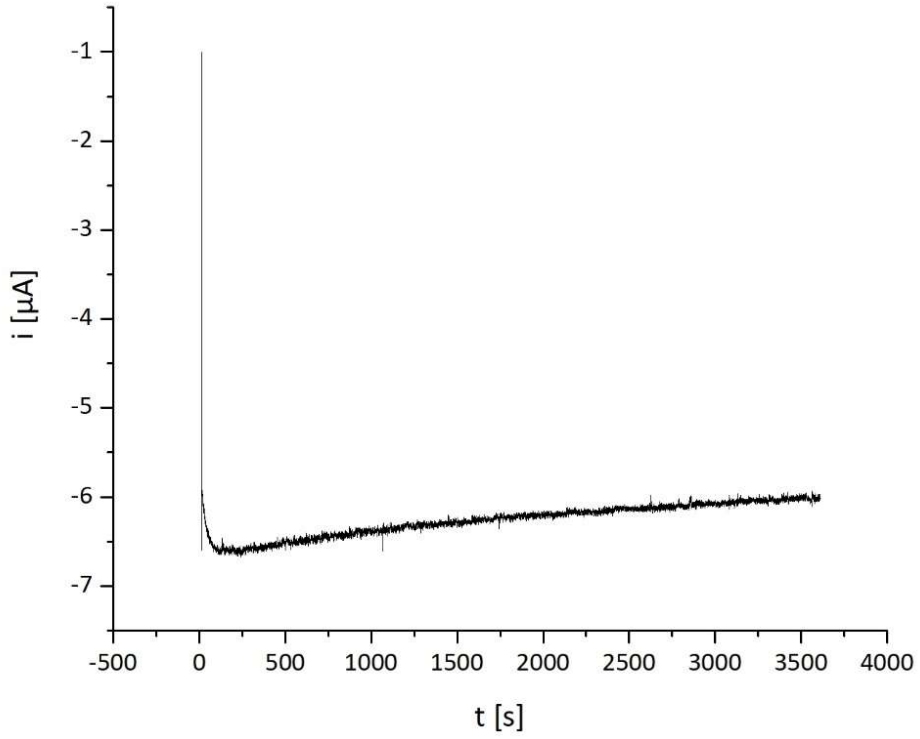

Figure 28: *Stability of the catalytic signal of BOD + SPEEK 1:100 (v/v) mixture by chronoamperometry for 1 h recorded at -0.12 V under O_2 after initial CV at RT.*

The current is progressively decreasing during the hour of recording. This graph is given as an example to illustrate and represent the results obtained for all the other measurements (except with SPEEK 1:1 where no catalytic current could be recorded).

Figure 29 contrasts the normalized currents obtained with different SPEEK dilutions and the enzyme that were immobilized on the PGE.

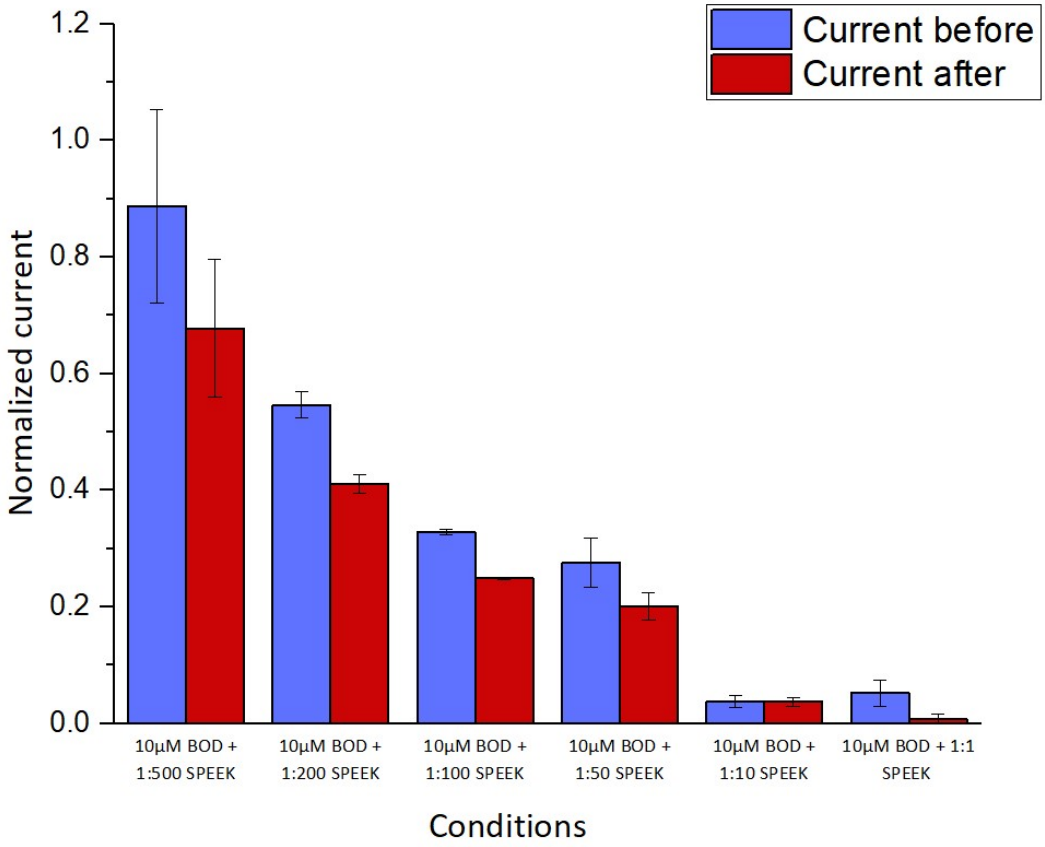

Figure 29: *Comparison of normalized current obtained from CVs showing catalytic response obtained under O_2 before (blue) and after (red) the chronoamperometry from BOD + various SPEEK (v/v) mixtures after adsorption on a CNTs modified PGE. Scan rate: 5 mV s^{-1} at RT.*

The activity obtained with the 1:10 dilution of SPEEK is very low, which might also be due to the acidic pH at this dilution. However even when the pH moves closer to the optimal range for enzyme activity at the 1:50 and 1:100 dilution, the activity of the enzyme is still remarkably reduced: It is close to 60% less. When the amount of SPEEK is further decreased the activity increases, but only at the 1:500 dilution the activity is at 90% of the initial activity. These results are not in accordance with the results obtained by UV-Vis spectroscopy, where the activity of BOD was fully recovered at the 1:100 dilution. The lower electroactivity compared to activity in solution may have different origins. It might be caused by BOD leaching from the electrode surface, the organization of the SPEEK film encapsulating the enzyme when polymerization occurs or by the enzyme not being electrically connected to the electrode because SPEEK might attach to the Cu T1 site. No matter the origin, these results clearly highlight a different behavior of BOD when in contact with either Nafion or SPEEK.

The different remaining currents measured by chronoamperometry are given in Figure 30.

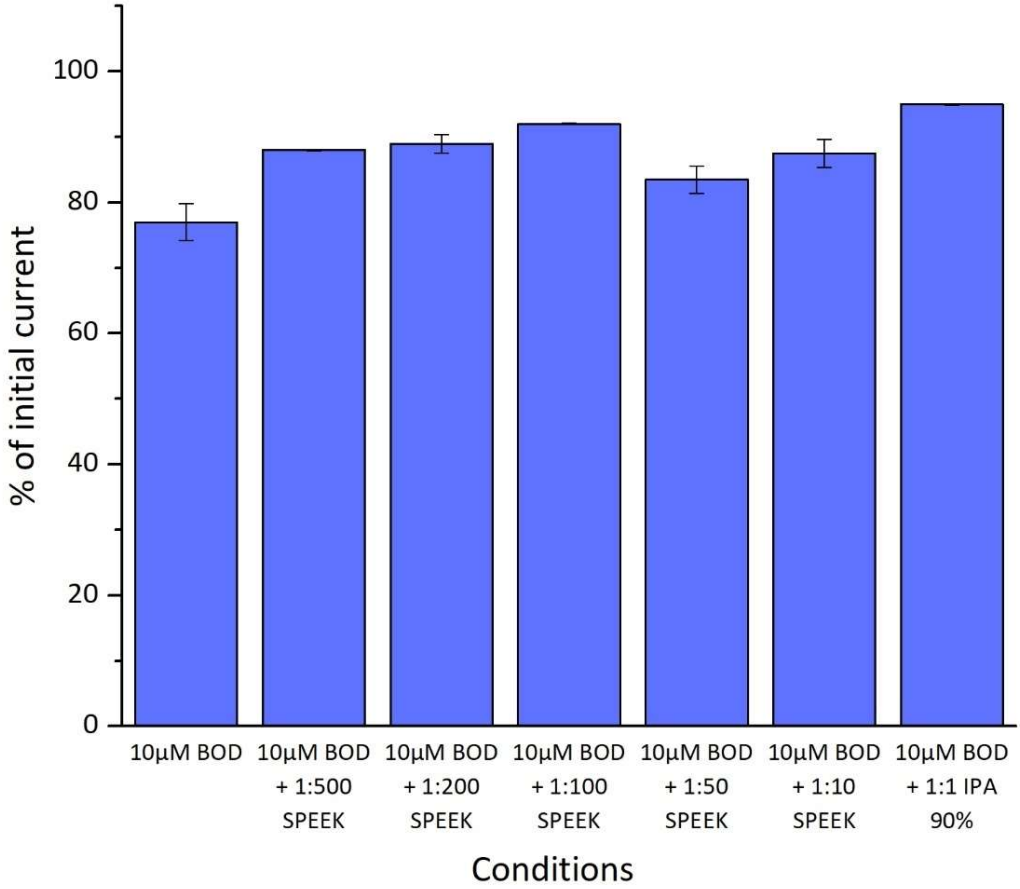

Figure 30: *Comparison of stability of the catalytic signal determined by chronoamperometry for 1 h recorded at -0.12 V under O_2 of BOD + various SPEEK (v/v) mixtures after initial CV at RT.*

The overall stability is around 90%. These results are the same as the ones obtained with Nafion. Therefore, also here the conclusion can be drawn that the majority of the enzyme that is deactivated by SPEEK becomes inactive in the beginning of the mixing of BOD and SPEEK, but that most of the enzyme remaining active after the addition of SPEEK, stays active as the consecutive cycles obtained by CV do not vary and the activity deceases only slowly over time.

4.7 Parameters that can control the decrease in enzyme electroactivity

In order to examine the discrepancies in the results obtained by electrochemical measurements and UV-Vis spectroscopy, additional experiments were performed. Further some parameters that could additionally influence the activity of BOD were examined to eliminate or prove their involvement in the reduction of catalytic efficiency.

4.7.1 Influence of alcohols

We first checked that the decrease in activity was not related to the EtOH and isopropyl alcohol (IPA) content present in Nafion and SPEEK solutions. The enzyme was mixed with the respective alcohol concentration present in the ionomers, and was then immobilized using Protocol A.

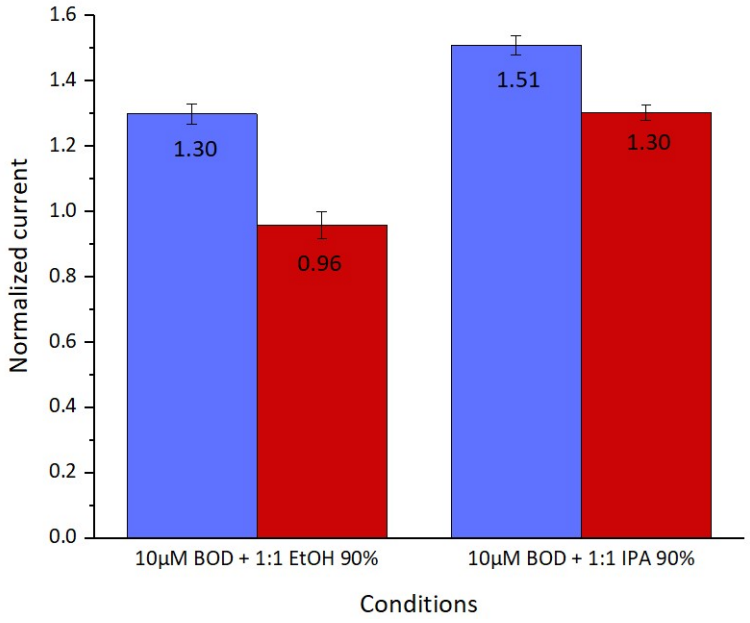

Figure 31: *Comparison of normalized current obtained from CVs showing catalytic response obtained under O_2 before and after the chronoamperometry from BOD + EtOH and BOD + IPA mixtures after adsorption on a CNTs modified PGE. Scan rate: 5 mV s^{-1} at RT.*

As shown in Figure 31 the presence of alcohol in the ionomer mixtures is not affecting the electrocatalytic activity of BOD in the presence of IPA and EtOH. An increase in the activity is even recorded when compared to BOD alone that could be ascribed to better enzyme immobilization. Presence of alcohol therefore cannot explain the decrease of activity recorded in the presence of ionomers.

4.7.2 Oxygen availability

Then the supply of oxygen for enzymatic catalysis was examined, to determine whether substrate diffusion through the ionomer film could limit the catalysis. Indeed, when organized as membranes, Nafion and SPEEK are used in fuel cells because they are impermeable to gases. One may wonder whether the ionomer deposited at the electrode may also play a barrier role to gas diffusion.

4.7.2.1 Nafion

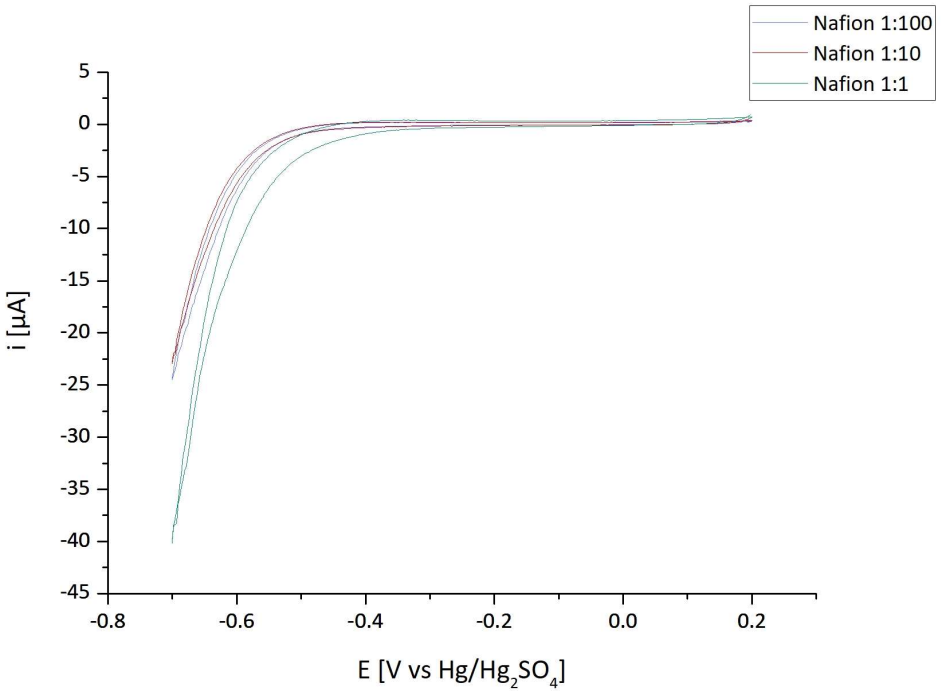

Figure 32: *CV for oxygen reduction as a function of Nafion dilution on PGE, 1:100 (blue), 1:10 (red) and 1:1 (green). CV recorded at a scan rate: 5 mV s^{-1} at RT under O_2.*

Oxygen reduction occurs no matter of the Nafion dilution with similar rates. For the Nafion 1:1 dilution a shift of the potential to a more positive value can be observed, which might be caused by a shift in the pH, which is discussed below.

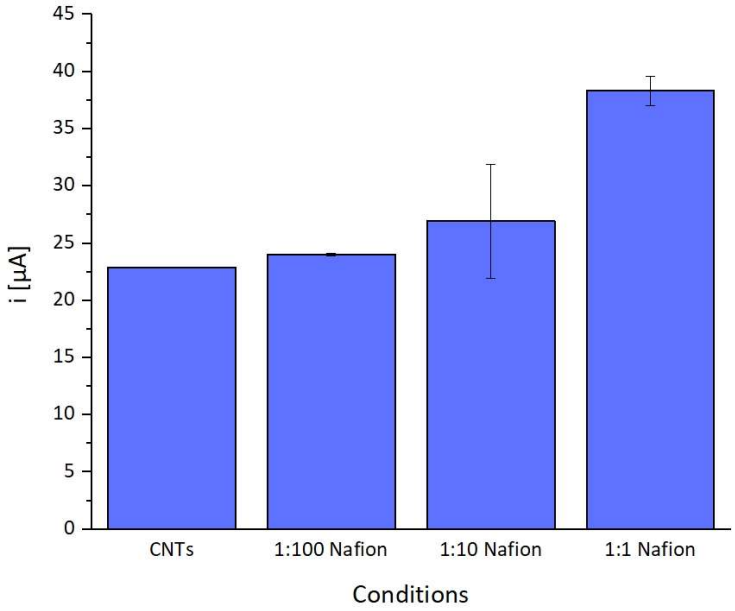

Figure 33: *Comparison of reductive currents obtained at -700 mV for oxygen reduction through Nafion films made from 1:100, 1:10 and 1:1 dilutions.*

These results suggest that oxygen is able to enter through the Nafion film without restrictions. Thus, oxygen limitation is not a restricting factor influencing the enzymatic activity of *Mv*BOD in the presence of Nafion deposited at the electrode with the enzyme. These results were unexpected as one of the main functions of Nafion as a membrane in the fuel cell is its impermeability for gases.

In the presence of Nafion 1:1 a positive shift in potential is visible on the CV curve (Figure 32). This shift can be induced by the more acidic pH of this dilution.

Considering the Nernst equation [39]:

$$\boldsymbol{E = E^{\circ} + \frac{0.059V}{n} * \frac{[Ox]}{[Red]}}$$

E … potential
E° … standard potential of a species
n … number of electrons
Ox … products of the concentration of the oxidized species
Red … products of the concentration of the reduced species

The different potentials for oxygen reduction at pH 6 and at pH 3.61 corresponding to the pH of Nafion 1:1 dilution can be calculated.

$$4H^{+} + O_2 + 4e^{-} \rightarrow 2H_2O$$

$$E = E^{\circ} + \frac{0.059V}{n} * \frac{[H_2O]}{[H^{+}] * [O_2]}$$

$E°_{O2/H2O}$ = 1.23 V
$[H_2O]$ = 1
$[O_2]$ = 1

$$pH = -\log\,[H^+]$$

$$E_{pH6} = 1.23V + \frac{0{,}059V}{4} * \frac{1^2}{(10^{-6})^4}$$

$$E_{pH6} = 0.876\,V$$

$$E_{pH3.6} = 1.0176\,V$$

The potential at the more acidic pH is shifted towards the positive potential, the difference between the two potentials is 0.1416 V. The potential was shifted by subtracting the value 0.039 V from the measured potential, so that the oxygen reduction starts at the same potential for the different Nafion films. The potential shift that is necessary in order to have the same onset potential is smaller than the calculated theoretical difference in potential. One hypothesis might be that the pH displayed by the deposited Nafion is different from that in solution.

The higher current that is observed for the Nafion 1:1 dilution is a result of this shift of the onset potential, which is rectified in Figure 34, in order to compare the current more accurately.

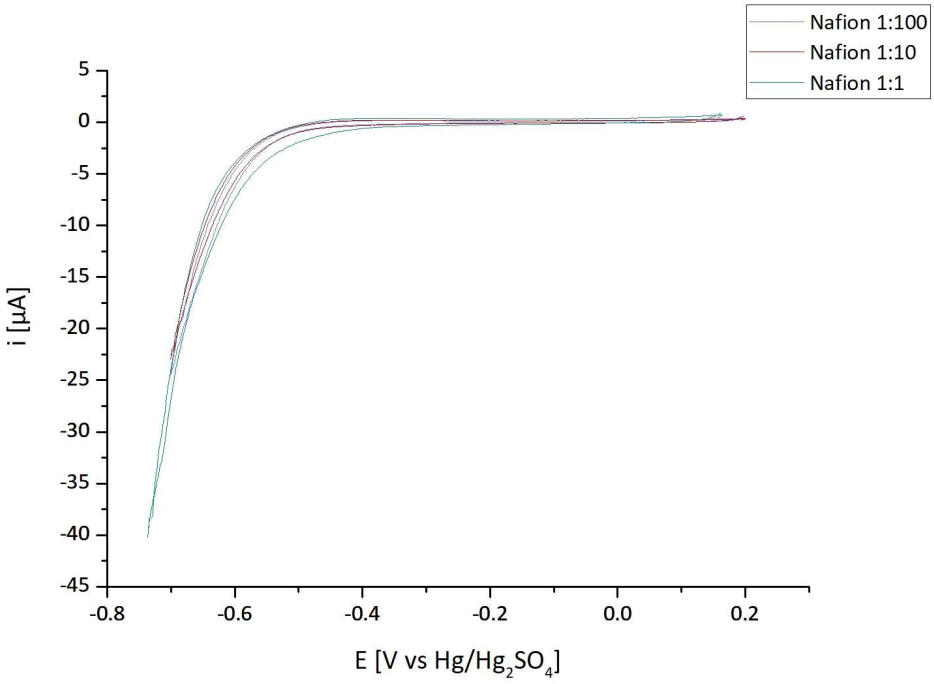

Figure 34: *Oxygen reduction at Nafion deposits from 1:100 (blue), 1:10 (red) and 1:1 (green) Nafion solutions. A numerical shift of potential of 39 mV was applied for Nafion 1:1. CV recorded at a scan rate: 5 mV s^{-1} at RT under O_2.*

The new obtained limiting current is plotted in Figure 35.

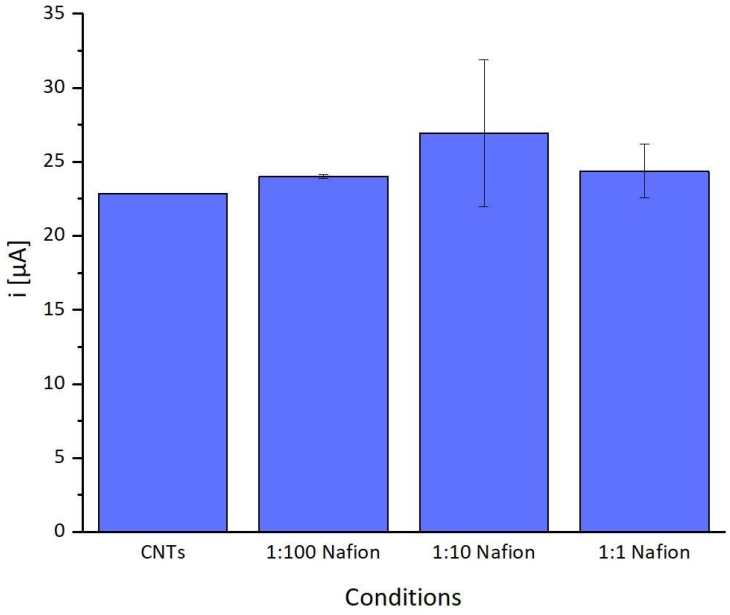

Figure 35: *Comparison of current obtained at -700 mV for oxygen reduction through films Nafion 1:100, 1:10 and 1:1, with numerical shifted potential for Nafion 1:1.*

Through the numerical shift of the CV curve obtained with Nafion 1:1, the current obtained at the potential of -700 mV is very similar for each condition. Thus, no matter the amount of Nafion, even for dilutions with a high Nafion content, oxygen is able to permeate though the Nafion film created on the electrode surface.

4.7.2.2 SPEEK

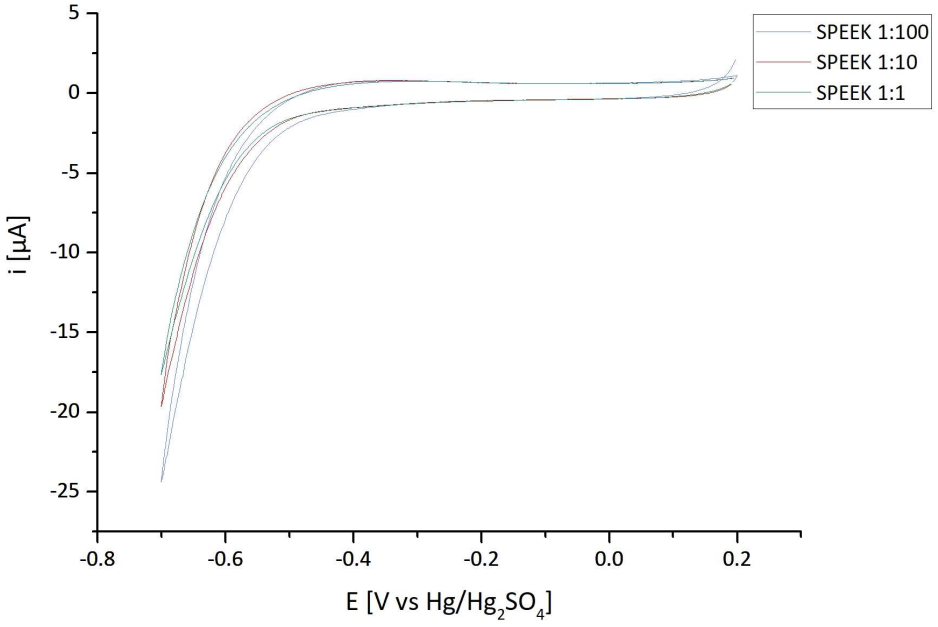

Figure 36: *Determination of oxygen reduction as a function of SPEEK films on PGE, 1:100 (blue), 1:10 (red) and 1:1 (green). CV recorded at a scan rate: 5 mV s^{-1} at RT under O_2.*

The current obtained with SPEEK is around 25% lower compared to Nafion and tends to decrease with the SPEEK concentration. Nevertheless, oxygen is able to pass through the film. No shift in potential is observed here for the acidic SPEEK 1:1 dilution.

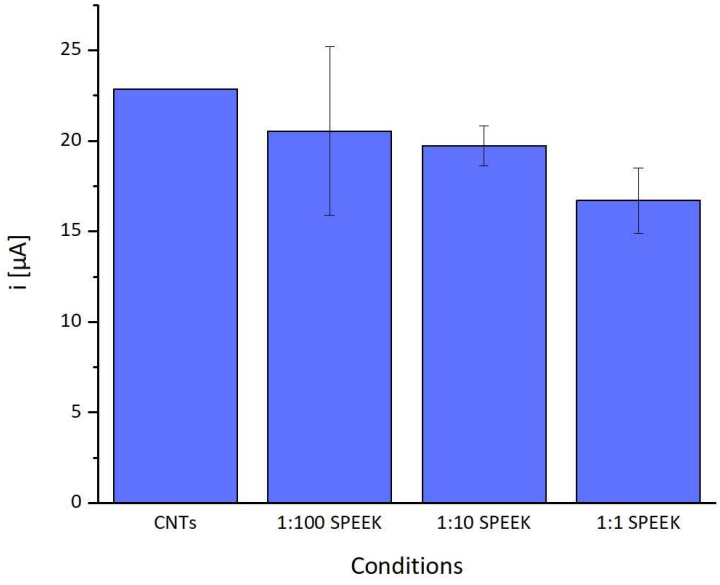

Figure 37: *Comparison of current obtained for oxygen reduction through films of SPEEK 1:100, 1:10 and 1:1.*

Here as well the results indicate that oxygen is able to enter the SPEEK film. Nevertheless, the higher the SPEEK concentration the less the obtained current, suggesting that the organization of the SPEEK film decreases oxygen reduction, thus limiting the activity of *Mv*BOD to some extent.

4.7.3 Electrical connection (ABTS) addition

ABTS is added to the solution in order to check whether BOD is electrically connected to the CNTs on the PGE or if this is impeded by the ionomer. The addition of ABTS will provide unhindered access for electron diffusion through the polymer film to the BOD and electrode and initiate a MET.

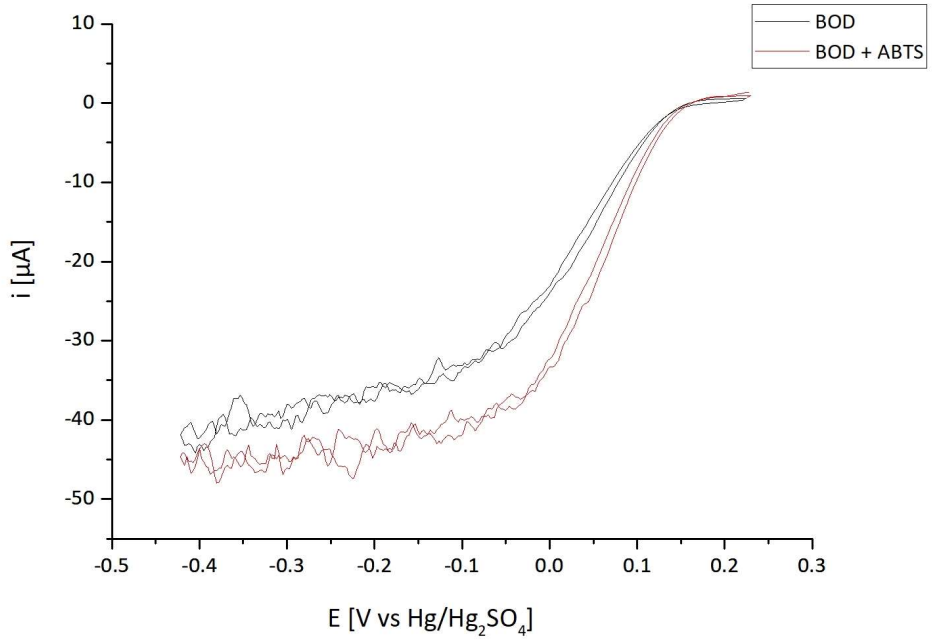

Figure 38: *O_2 reduction by MvBOD 10 µM with (red) and without (black) ABTS (200µM). CV recorded at a scan rate: 5 mV s^{-1} at RT under O_2.*

In Figure 38 only BOD is immobilized on the electrode surface as a control experiment to evaluate how ABTS changes the catalytic current. A small enhancement can be observed, both in terms of half wave potential and limiting current, thus indicating that the orientation of the enzyme leaves some possibility for MET. Nevertheless, DET is the main electron transfer regime that is occurring. In accordance, the parameter of distribution of orientation of BOD was determined by CV fitting. This parameter evaluates the distribution of distances between the Cu T1 and the electrode, which will further induce a distribution of electron transfer rates. The lower it is, the narrower is the distribution of orientation. Values close to 3-4 should be obtained for a narrow enzyme distribution orientation. In our conditions, a value of 6.3 was calculated meaning that despite a negative surface induced by CNTs, a proportion of enzymes are not oriented for DET. This population can however participate to the catalysis through a mediated process.

4.7.3.1 Nafion

Initially the electroactivity of ABTS alone in the presence of Nafion was measured in order to examine if ABTS is able to pass though the film created by Nafion.

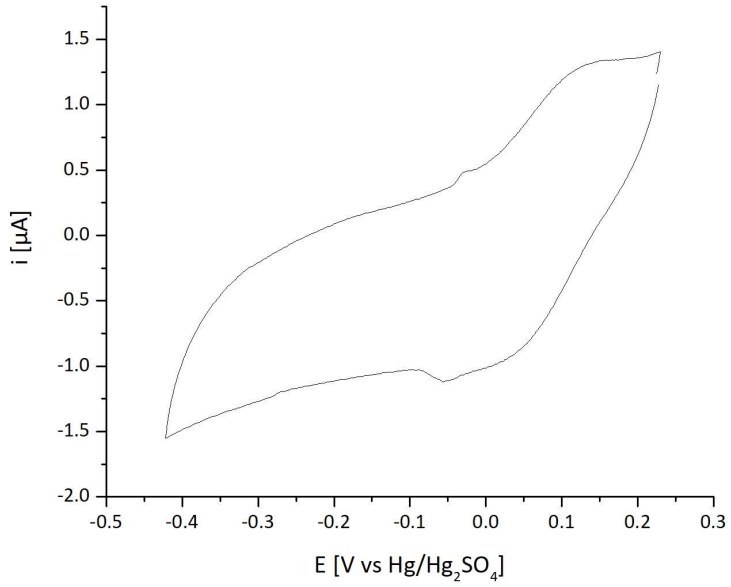

Figure 39: *CV for ABTS at the PGE modified by CNT with Nafion 1:10 (v/v) with ABTS (200µM). CV recorded at a scan rate: 5 mV s^{-1} at RT under O_2.*

Though not very distinguishable, the CV behavior of ABTS in the presence of Nafion, shows both cathodic and anodic peaks at the redox potential of 160 mV, characteristic of the redox potential of the ABTS redox species. This proves that ABTS is able to pass through the Nafion film deposited on the PGE. Under N_2, where no catalytic current is expected, only the redox signal for ABTS can be observed.

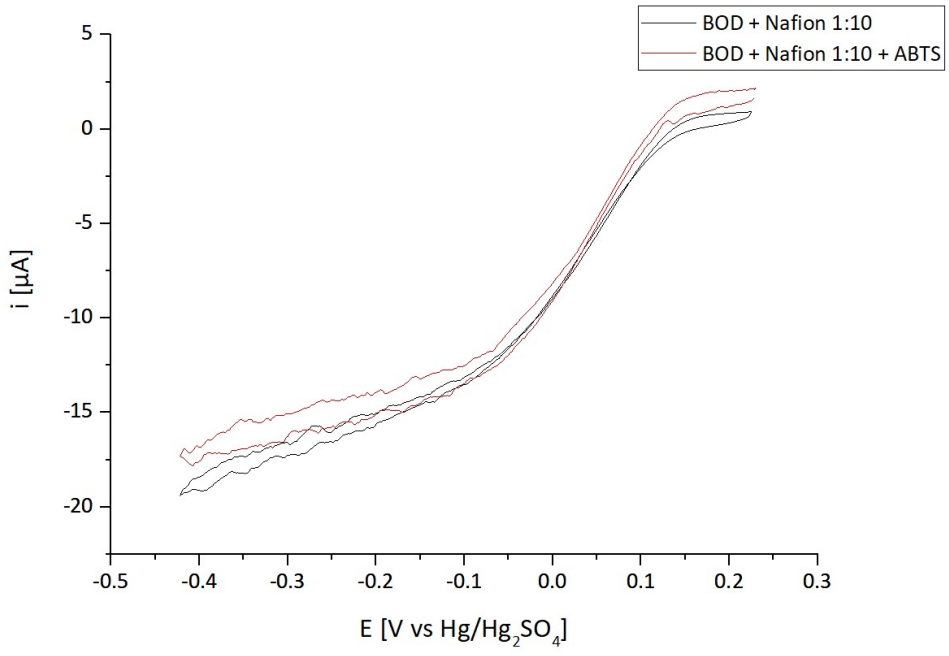

Figure 40: *O_2 reduction by MvBOD in combination with Nafion 1:10 (v/v) with (red) and without (black) ABTS (200µM). CV recorded at a scan rate: 5 mV s^{-1} at RT under O_2.*

The catalytic current shows no modification after the addition of ABTS in the case of Nafion. No MET is observed.

Considering the UV-Vis spectroscopy results, where the activity is never fully recovered even with low amounts of Nafion, a lot of enzyme appears to be unavailable for DET as well as MET. This might be caused by Nafion polymerizing with BOD to large aggregates and encapsulating the enzyme. By this encapsulation the enzyme is not accessible anymore, either to perform DET or MET. Examining the electrode surface by microcopy can provide more detailed information on the processes occurring between BOD and Nafion on the PGE surface.

4.7.3.2 SPEEK

For SPEEK also the ability of ABTS to pass through the film on the PGE to initiate MET was examined.

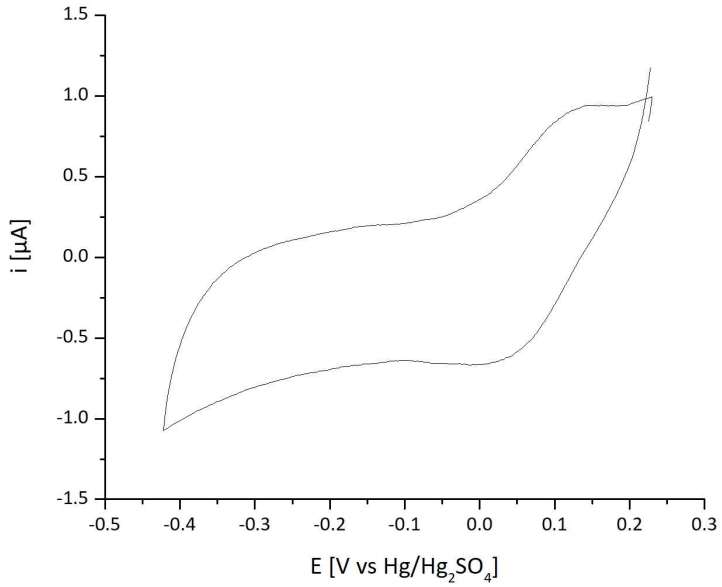

Figure 41: *CV for ABTS at the PGE modified by CNT with SPEEK 1:10 (v/v) with ABTS (200µM). CV recorded at a scan rate: 5 mV s^{-1} at RT under O_2.*

The electroactivity of ABTS is proven by the obtained cathodic and anionic peaks, verifying that ABTS is able to permeate through the SPEEK film. Under N_2, where no catalytic current is expected, only the redox signal for ABTS can be observed.

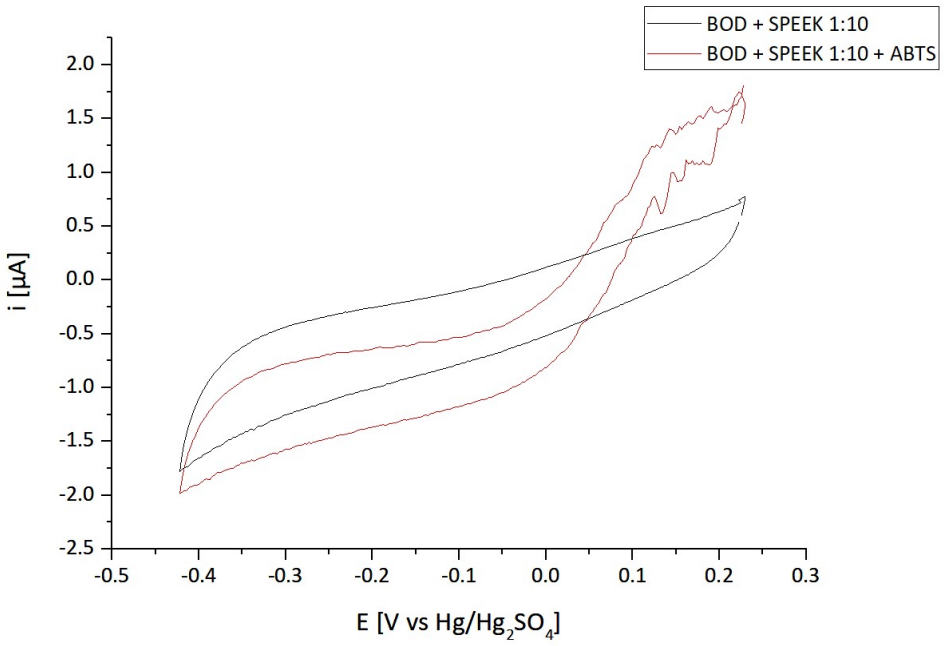

Figure 42: *O_2 reduction by MvBOD in combination with SPEEK 1:10 (v/v) with (red) and without (black) ABTS (200µM). CV recorded at a scan rate: 5 mV s^{-1} at RT under O_2.*

A small increase in the enzymatic activity can be observed with the addition of ABTS in the presence of SPEEK, thus demonstrating that some, but very small MET is taking place. Some increase in the steepness of the catalytic current is observed which could indicate that some BOD is electrically isolated in the SPEEK film, limiting the DET activity of the enzyme. This suggests that SPEEK is encapsulating the enzyme when polymerization occurs.

4.7.4 BOD – release

Another factor contributing to the decrease of the catalytic current could be enzyme leaching from the electrode surface. Therefore, the release of BOD from the PGE was examined via UV-Vis spectroscopy.

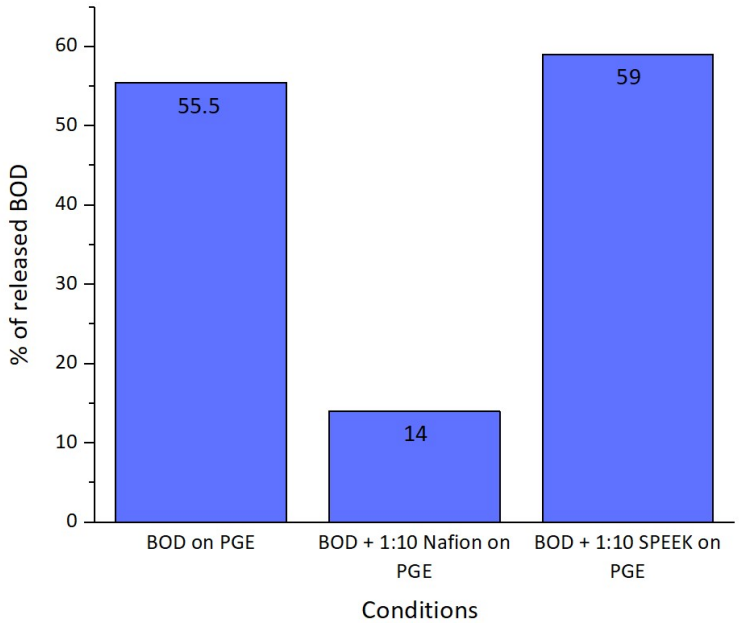

Figure 43: *Release of BOD into solution after immobilization on PGE modified with CNTs obtained by UV-Vis SPEC at 420 nm for Nafion 1:10 and SPEEK 1:10 in combination with BOD 50 nM in cuvette at 25°C.*

The release of BOD from the PGE surface into solution amounts to 55%. The same is observed when the enzyme is immobilized with SPEEK. However, when BOD is immobilized with Nafion a decrease in release occurs: Only around 15% of BOD detach from the electrode surface and are released into solution. This observation leads to the conclusion that while SPEEK provides weak to no protection from BOD release, Nafion shields the enzyme from detachment. This supports the expectation that Nafion encapsulates the enzyme rendering it inactive, while hindering it from leaching. Thus, a different polymerization behavior between the enzyme and the respective ionomer could explain these divergent results. To properly evaluate experimental results and to obtain high quality, sensitivity and reproducibility of the obtained data should always be considered. These parameters are significant since minor changes in the experimental conditions should not affect the results. Here, further experiments are required in order to fully determine and understand the processes that underly and influence this leaching behavior and to achieve reproducibility. In some cases, black streaks could be observed leaving the electrode surface. Nevertheless, the values measured by UV-Vis spectroscopy did not vary whether some black streaks occurred or not, which was very unexpected. These results have to be checked in further experiments conducted on protein release.

The results obtained by studying the influence of various parameters suggest that the film organization that occurs between BOD and the different ionomers controls the enzyme activity. To further examine this, different immobilization protocols were investigated.

4.8. Electroactivity in the presence of ionomers with different immobilization protocols

Additionally, to the Protocol A, two other immobilization methods were considered: Protocol B and Protocol C, to examine their influence on the catalytic current.

4.8.1 Nafion

Additionally, as the protocol for immobilization concerning mixture of ionomer and enzyme as well as deposition were varied, the results are compared and plotted in Figure 44.

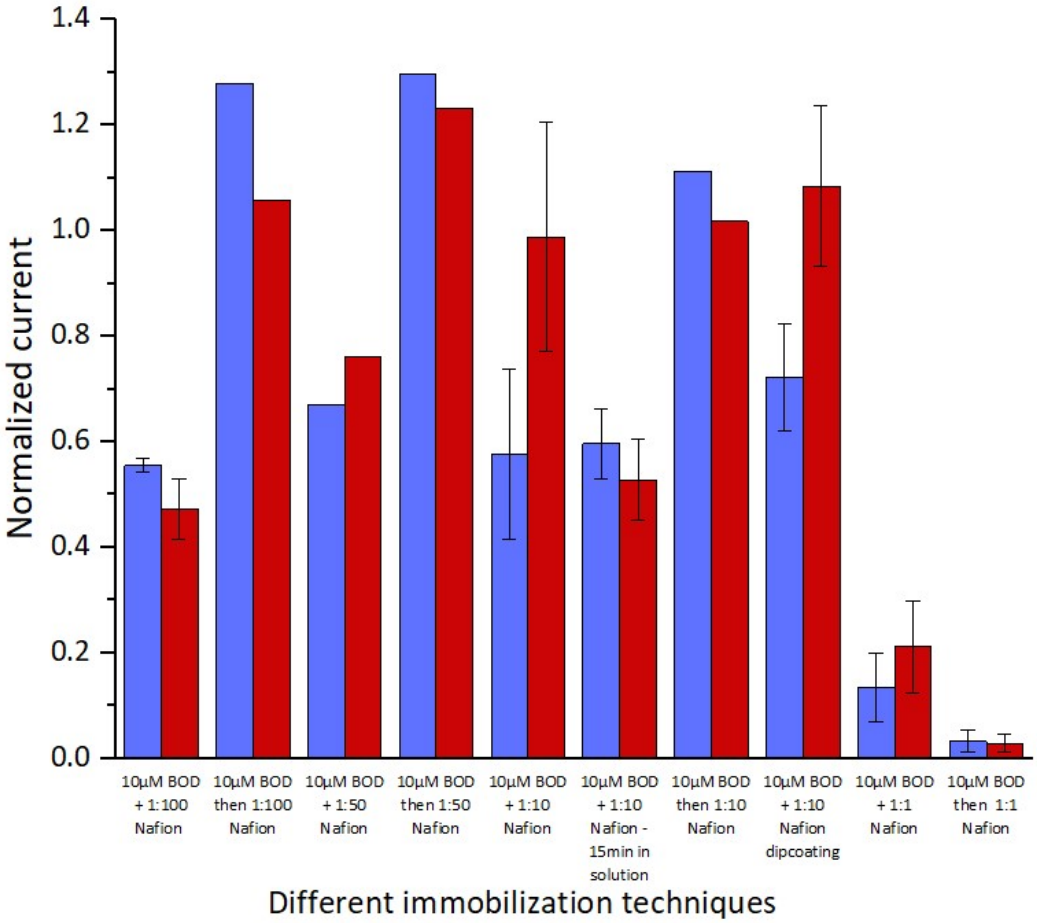

Figure 44: *Comparison of normalized catalytic currents obtained with different immobilization techniques from CVs showing catalytic responses obtained under O_2 before and after the chronoamperometry from BOD + various Nafion (v/v) mixtures after adsorption on a CNTs modified PGE. Scan rate: 5 mV s^{-1} at RT.*

A large increase in current can be observed when the enzyme is immobilized on the electrode surface first and Nafion is only added later to form the protective film (Protocol B). These results correlate well with the assumption that Nafion encapsulates BOD. By immobilizing the BOD first on the surface more enzyme is able to connect to the surface, not hindered by encapsulation. Except for the Nafion 1:1 dilution where the current decreased significantly, the current obtained with this method is twice as high. The decrease of current in the case of Nafion 1:1 deposit might be caused by the low pH. In the

case of Nafion 1:1 deposit on the enzyme layer, it can be supposed that all the enzyme molecules will be affected by the acid pH. On the contrary, when using a mixture of Nafion and enzyme, aggregation occurs in the mixture solution before deposit, leaving more enzyme intact. With the Protocol B, a decrease of the catalytic activity can be observed over time contrary to what was observed with Protocol A.

Concerning the immobilization Protocol C, a similar increase in the current was observed as when using Protocol B. Furthermore, when the enzyme was incubated with Nafion 1:10 in solution for 15 min, before immobilization was performed, no increase in the current was obtained. In this case no increase in current could be observed over the different cycles, as had been the case when Protocol A was employed. The reasons for these last experiments are unclear for the moment. Additional experiments are required such as amount of protein release using the various protocols.

In Figure 45 the stability achieved with the various immobilization techniques is compared.

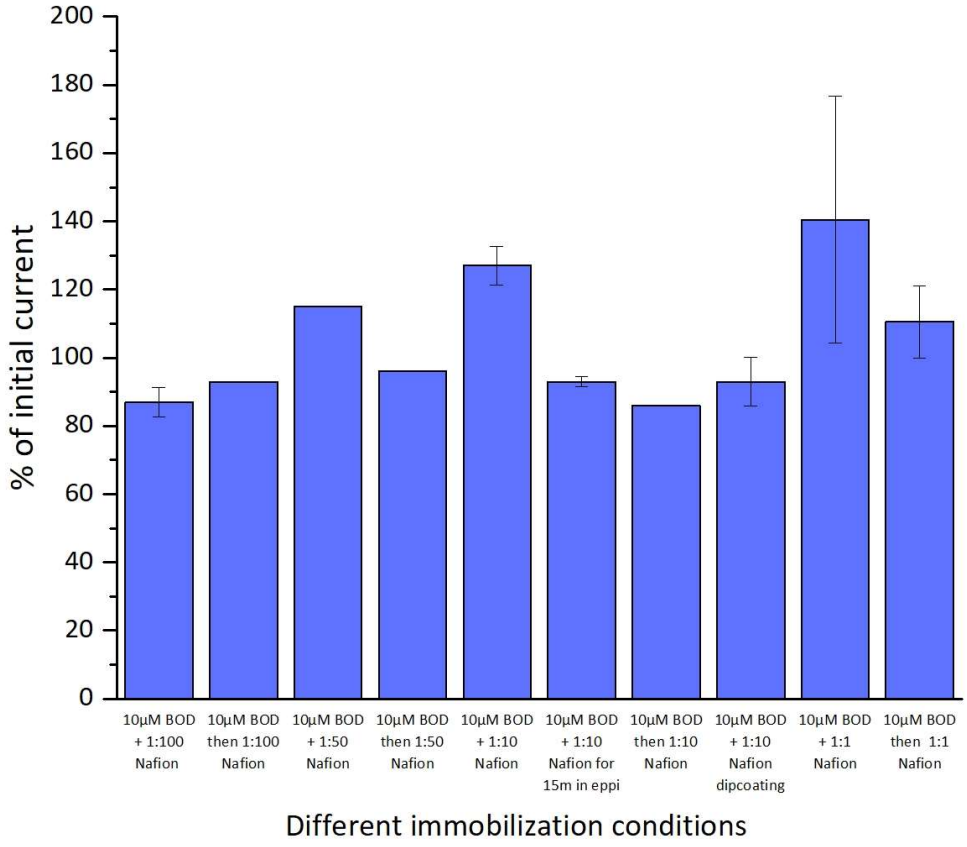

Figure 45: *Comparison of stability of the catalytic signal determined by chronoamperometry for 1 h recorded at -0.12 V under O_2 of BOD + various Nafion (v/v) mixtures with different immobilization techniques after initial CV at RT.*

The stability of the enzyme is not significantly influenced by different immobilization protocols, since still around 90% of the initial current are obtained. These results suggest that the enzyme molecules

that are active after the addition of Nafion remain to the most extent active over 1 h, and that only the amount of enzyme that is active fluctuates depending on the amount of Nafion that is utilized.

Considering all the data that has been discussed so far either dip-coating or successive application seem to be the more promising protocols for Nafion deposition, resulting in a higher enzyme activity, while a high stability is remained throughout. These protocols need now to be validated in future experiments to ensure reproducibility.

4.8.2 SPEEK

Furthermore, the immobilization protocol concerning mixture of SPEEK and enzyme as well as deposition were varied and the results compared and plotted in Figure 46.

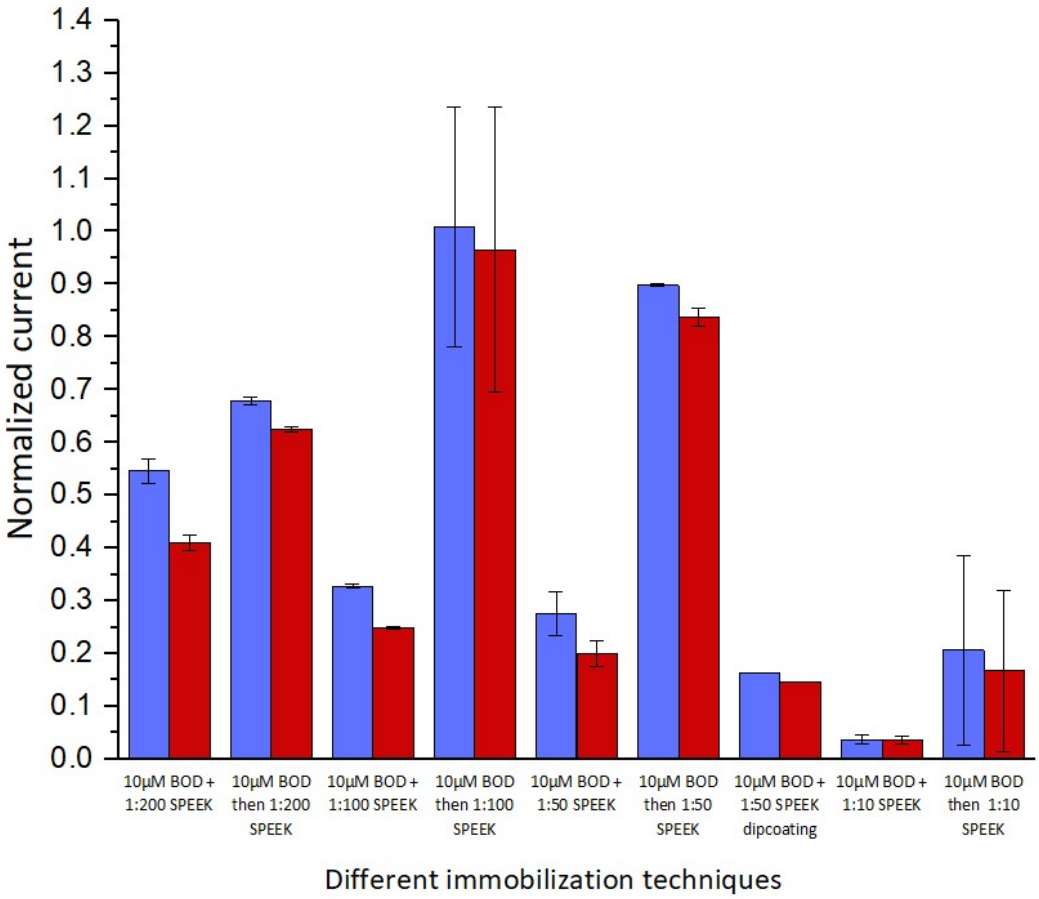

***Figure 46*:** *Comparison of normalized current obtained with different immobilization techniques from CVs showing catalytic response obtained under O_2 before and after the chronoamperometry from BOD + various SPEEK (v/v) mixtures after adsorption on a CNTs modified PGE. Scan rate: 5 mV s^{-1} at RT.*

A significant increase in the current is apparent when first the BOD is immobilized on the PGE and then SPEEK is only applied afterwards (Protocol B), except for the 1:200 and 1:1 dilution. For the 1:1 dilution even with this immobilization method no current was obtained however, thus the data is not given in this graph. Concerning the 1:10 dilution, even though the current increases compared to the data

acquired before, the activity is still very reduced. This reduction can still be linked to the more acidic conditions that prevail. As for the dilutions 1:50 and 1:100, where the activity is not inhibited by the pH the current is three times more than it was when ionomer and enzyme were mixed before immobilization. However, a high standard deviation occurred for the 1:100 dilution. This high current suggests that when SPEEK is only applied after the enzyme, the ionomer changes its polymerization pattern. With this change either BOD is better protected, thus the release is decreased or the enzyme is better electrically connected to the surface, thus more efficiently able to reduce oxygen.

In addition, the stability of the enzyme with the different immobilization protocols is compared.

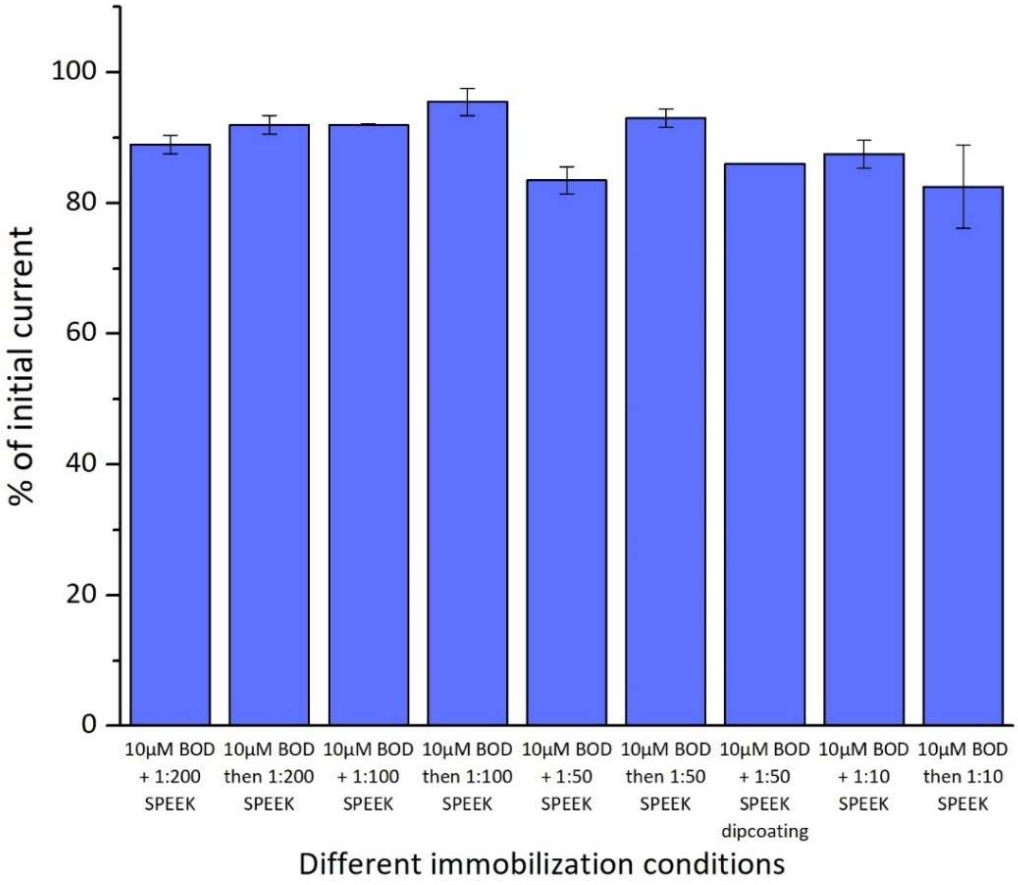

Figure 47: *Comparison of stability of the catalytic signal determined by amperometry for 1 h recorded at -0.12 V under O_2 of BOD + various SPEEK (v/v) mixtures with different immobilization techniques after initial CV at RT.*

The various immobilization protocols show no influence on the stability of the catalytic current, which remains stable at around 90%. These results lead to the conclusion that as with Nafion, the enzyme activity is influenced by the initial encounter with SPEEK, but afterwards remains mostly stable over 1 h. Altogether Protocol C does not seem promising as the current remains low. Only the immobilization Protocol B leads to a considerable improvement of the current, while the stability remains at the same level.

4.9 Enzyme potential aggregation evaluation

As polymerization is likely to occur when the enzyme is immobilized on the electrode surface with the ionomers, their aggregation pattern is examined in order to gain information on the size of the aggregates that might be formed.

4.9.1 Dynamic light scattering

To determine the distribution and the structure of the ionomer in the presence of buffer and enzyme DLS was employed. Necessary parameters as the RI and the viscosity, here the density is essential, were measured in order to perform DLS.

4.9.1.1 Refractive index

The refractive index of Nafion and SPEEK were measured and the values are shown in Table 11 and Table 12.

Table 11: Refractive index results of Nafion dilutions.

Nafion dilution (v/v)	Refractive index [nD]
1:1	1.3596
1:10	1.3415
1:50	1.3354
1:100	1.3344
1:200	1.3338

Table 12: Refractive index results of SPEEK dilutions.

SPEEK dilution (v/v)	Refractive index [nD]
1:1	1.3649
1:10	1.3400
1:50	1.3354
1:100	1.3343
1:200	1.3339

The RI obtained for the various Nafion and SPEEK dilutions is very close to the one of water, which is 1.36622 nD [53]. Thus, the RI for the Nafion dilutions and SPEEK dilutions in combination with the BOD was not measured separately, but a RI of 1.3350 nD was assumed to perform further measurements.

4.9.1.2 Density

Furthermore, the density had to be determined to measure the viscosity. Table 13 and Table 14 show the results for the density obtained for the Nafion dilution and SPEEK dilutions in addition with the same amount of PPB, substituting the BOD.

Table 13: Results for the density measurement of Nafion dilutions.

Nafion dilution (v/v) + PPB	Density [g cm^{-3}]	Specific gravity [-]
1:1	0.9848	0.9877
1:10	0.9963	0.9992
1:50	1.0006	1.0035
1:100	1.0008	1.0037
1:200	1.0015	1.0045

Table 14: Results for the density measurement of SPEEK dilutions.

SPEEK dilution (v/v) + PPB	Density [g cm^{-3}]	Specific gravity [-]
1:1	0.9793	0.9822
1:10	0.9965	0.9994
1:50	1.0009	1.0038
1:100	1.0015	1.0044
1:200	1.0018	1.0047

The density measured for both the ionomers is always around 1 g cm^{-3}, the same as for water. Therefore, a density of 1 g m^{-3} was used to perform the viscosity measurements for all different dilutions.

4.9.1.3 Viscosity

The viscosity of the individual dilutions was measured. The viscosity of PPB alone was determined to be at 0.944 mPas.

In Table 15, Table 16, Table 17 and Table 18 list the data determined by viscosity measurements.

Table 15: Dynamic viscosity results for Nafion dilutions.

Nafion dilution (v/v)	Dynamic viscosity [mPas]
1:1	6.746
1:10	1.801
1:50	1.056
1:100	0.949
1:200	0.945

The viscosity is increased drastically for the 1:1 dilution of Nafion as well as a raised value was obtained for the dilution of 1:10, but the other dilutions are in the same range around 1 mPas.

Table 16: Dynamic viscosity results for Nafion dilutions with PPB.

Nafion dilution (v/v) + PPB	Dynamic viscosity [mPas]
1:1	2.303
1:10	1.169
1:50	0.961
1:100	0.944
1:200	0.926

When the Nafion is further diluted with PPB – or the enzyme – the viscosity is decreased three times for the 1:1 dilution and the 1:10 dilution is closer to 1 mPas.

Table 17: Dynamic viscosity results for SPEEK dilutions.

S-PEEK dilution (v/v)	Dynamic viscosity [mPas]
1:1	5.259
1:10	1.309
1:50	1.018
1:100	0.982
1:200	0.981

For the 1:1 dilution the viscosity is extremely high and also concerning the dilution of 1:10 the viscosity is above 1 mPas, but the other dilutions are in the range of 1 mPas.

Table 18: Dynamic viscosity results for SPEEK dilutions with PPB.

S-PEEK dilution (v/v) + PPB	Dynamic viscosity [mPas]
1:1	1.902
1:10	1.060
1:50	0.945
1:100	0.949
1:200	0.946

Looking at SPEEK with PPB or BOD, when further dilution occurs, the viscosity decreases as well and except for the 1:1 the obtained viscosity values are around 1 mPas.

4.9.1.4 DLS of Nafion

First DLS was measured for only the dilutions of Nafion in order to examine the particle size of Nafion alone to be able to draw a conclusion when Nafion is then measured in combination with the enzyme.

Figure 48 shows the DLS result for Nafion 1:200.

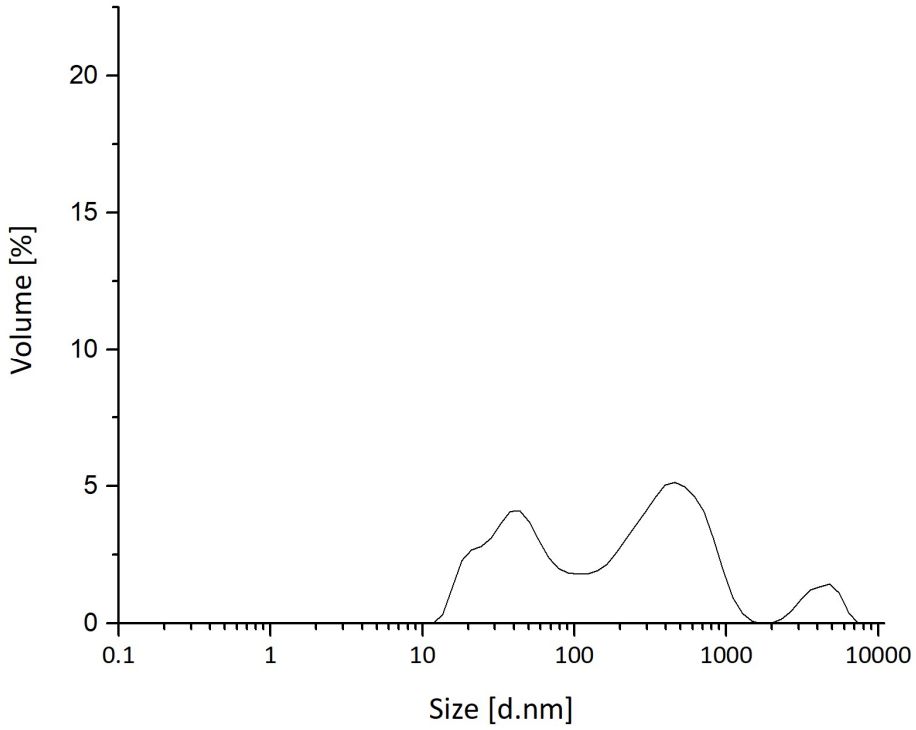

Figure 48: *DLS results* for Nafion *1:200*

Large particles can be observed for Nafion, as well as a high polydispersity as the particle size varies. This is true for all Nafion dilutions, thus the particle sizes that make up the majority of the solution for the individual measurements are shown in Table 19 as the $D(v)_{50}$. The $D(v)_{50}$ gives the size distribution by volume of 50% of the sample. The $D(v)_{50}$ of each individual measurement is shown here, as no mean can be calculated since the standard deviation would be too high.

Table 19: DLS measurement results: Diameter size of the Nafion dilutions.

Nafion diution	$D(v)_{50}$ Size [d.nm]				
1:200	401	37.2	343	70.1	39.6
1:100	219	286	742	211	222
1:50	252	102	351	163	456
1:10	573	53.4	47	172	37.5
1:1	114	156	27.9	135	18.5

DLS shows that aggregates are formed ranging from tens of nm to µm, not following any distribution as the amount of Nafion is changing. As the $D(v)_{50}$ is representing the size majorities of the particles, the values in Table 19 and the peaks in Figure 48 do not match exactly. The peak obtained at a size of

around 4000 is only representing a small amount of particles with this specific size present in the overall solution, while the predominant sizes of particles present in the solution are between 18 and 800 nm, which is shown in Table 19 and represented by the $D(v)_{50}$, since the particles making up most of the solution are more interesting and more representative overall than the 1% of particles larger than 1000 nm.

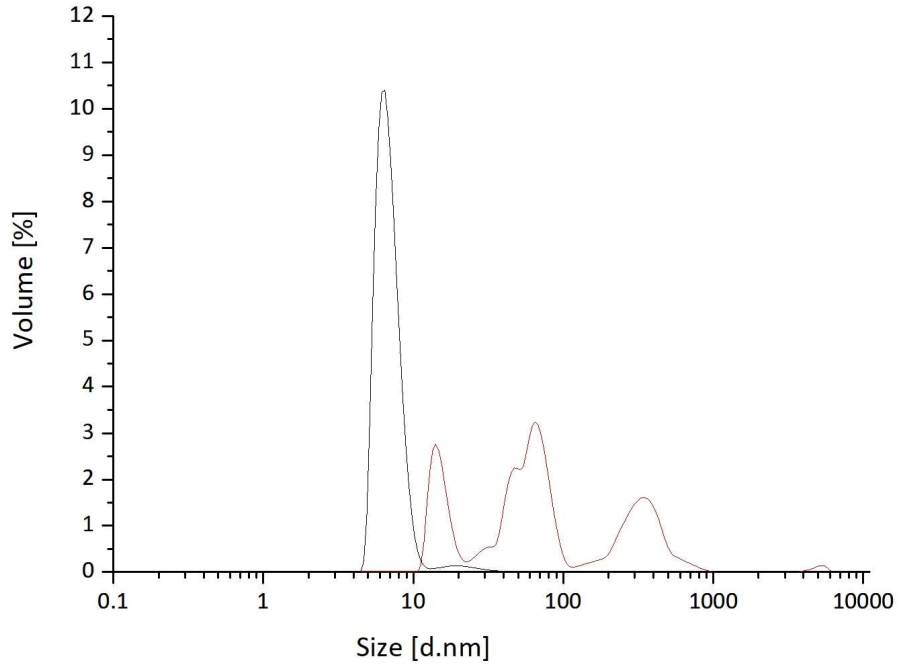

Figure 49: *DLS response signal obtained for BOD alone (black) and BOD + Nafion 1:200 (v/v) dilution (red) at 25°C.*

Figure 49 displays the DLS for BOD alone and mixture of BOD and Nafion 1:200. For BOD, which was measured alone beforehand, an expected size of 6.8 nm diameter for a protein with 60 kDa was obtained [54], verifying that indeed the protein is detected by DLS. This peak of BOD is plotted together with the peaks obtained by BOD together with Nafion. The DLS signal obtained for the mixture also shows that large particles are formed, making it impossible to further identify BOD in the presence of Nafion.

The particle sizes that make up the majority of the solution for the other Nafion dilutions are given in Table 20, as the $D(v)_{50}$, as again no mean could be calculated.

Table 20: DLS measurement results: Diameter size of *Mv*BOD and the Nafion dilutions with *Mv*BOD.

Nafion diution	$D(v)_{50}$ Size [d.nm]		
BOD	6.8 ± 0.3		
BOD + 1:200	61.1	84.3	16.6
BOD + 1:100	228	78.6	203
BOD + 1:50	61.4	154	99.4
BOD + 1:10	417	972	942
BOD + 1:1	848	757	704

These results show that Nafion forms large particles. Thus, when Nafion is added it is not possible to identify BOD anymore. The sizes that are obtained with Nafion and BOD are larger than the ones measured with the enzyme alone, leading to the hypothesis that BOD might be incorporated into these aggregates either by being bound or being encaged by Nafion.

The correlation of diffusion of light by different particle sizes can also be plotted. By the decay of light an observation whether a molecule is small or large can be made.

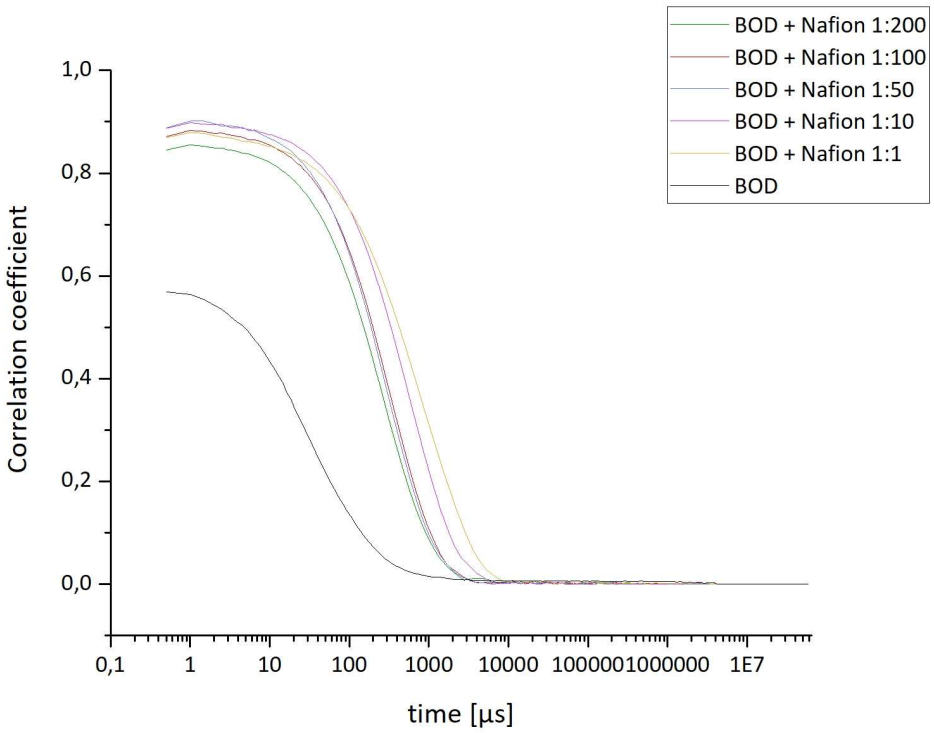

Figure 50: *Correlation coefficient obtained for BOD alone and BOD + various Nafion (v/v) mixtures at 25°C.*

The correlation in Figure 50 shows that there is a large difference in the light that is diffused by the protein and the light being diffused from the mixture of BOD and Nafion, also showing that BOD is not able to be detected by DLS anymore. DLS clearly demonstrates that Nafion has an effect on the BOD and large aggregates are formed, even when only small amounts of Nafion are present.

4.9.1.5 DLS of SPEEK

For SPEEK, the results of the reference measurement of SPEEK, BOD and both together are portrayed in one graph to show the shift that is occurring. Only SPEEK 1:200 is plotted, the values that were obtained for the other dilutions are given in Table 21 and Table 22.

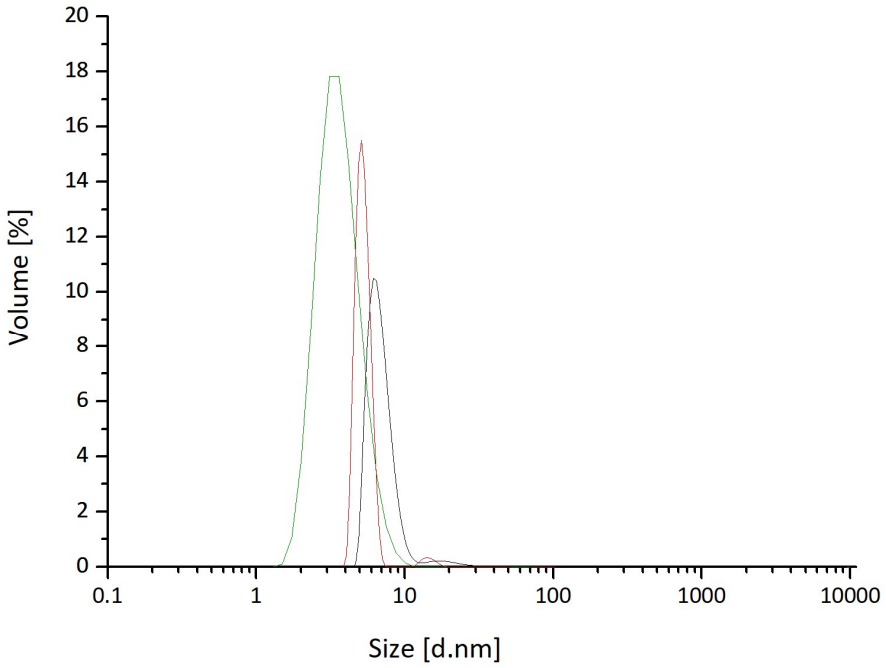

Figure 51: *DLS response signal obtained for BOD alone (black), BOD + SPEEK 1:200 (red) and SPEEK 1:200 (green) mixtures at 25°C.*

A monomeric enzyme with a molecular mass of 60 kDa as BOD [54] has a diameter of around 6.8 (± 0.3) nm. Thus, with the obtained value for BOD, it is verified that indeed the protein is detected by DLS.

In Figure 51 the peak that is observed for SPEEK alone, shows a small particle diameter size of 3.5 (± 0.4) nm. The size that is measured when BOD is in combination with SPEEK 1:200 move to a size comprised between those of BOD and SPEEK. The shift in particle size can be clearly seen.

In Table 21 and Table 22 the diameter size of the particles in the solution plus their deviation is given for the enzyme, the individual SPEEK dilutions as well as in combination with the enzyme.

Table 21: DLS measurement results: Diameter size of the SPEEK dilutions.

	$D(v)_{50}$ Size [d.nm]
SPEEK 1:200	3.5 ± 0.4
SPEEK 1:100	3.2 ± 0.3
SPEEK 1:50	3.1 ± 0.5
SPEEK 1:10	2.6 ± 0.2
SPEEK 1:1	0.9 ± 0.1

Table 22: DLS measurement results: Diameter size of *Mv*BOD and the SPEEK dilutions with *Mv*BOD.

	$D(v)_{50}$ Size [d.nm]
BOD	6.8 ± 0.3
BOD + SPEEK 1:200	5.1 ± 0.3
BOD + SPEEK 1:100	4.2 ± 0.3
BOD + SPEEK 1:50	3.6 ± 0.2
BOD + SPEEK 1:10	3.5 ± 0.2
BOD + SPEEK 1:1	2.5 ± 0.9

A single peak centered at 2.6-3.5 nm can be observed for all the SPEEK dilutions alone, except for SPEEK 1:1 dilution which only gives a size of 0.9 nm. Here the highly acidic pH might be responsible for this divergent result. When comparing those values to the ones obtained when the enzyme is added, an increase in size is detected. Nevertheless, a unique peak can still be observed. In contrast when the size of BOD alone is compared to the size obtained in combination with the SPEEK a trend is going on that as the amount of SPEEK increases, while BOD gets smaller and smaller. One possible explanation for this decrease in diameter of BOD might be that SPEEK induces a conformational change of the enzyme, changing the protein structure by folding the enzyme. Through this refolding of the enzyme the diameter size decreases as the enzyme becomes more and more compact. What is clear is that some kind of interaction between SPEEK and BOD is occurring, resulting is this size shift. The correlation of light that is diffused by the SPEEK particles is also plotted in Figure 52.

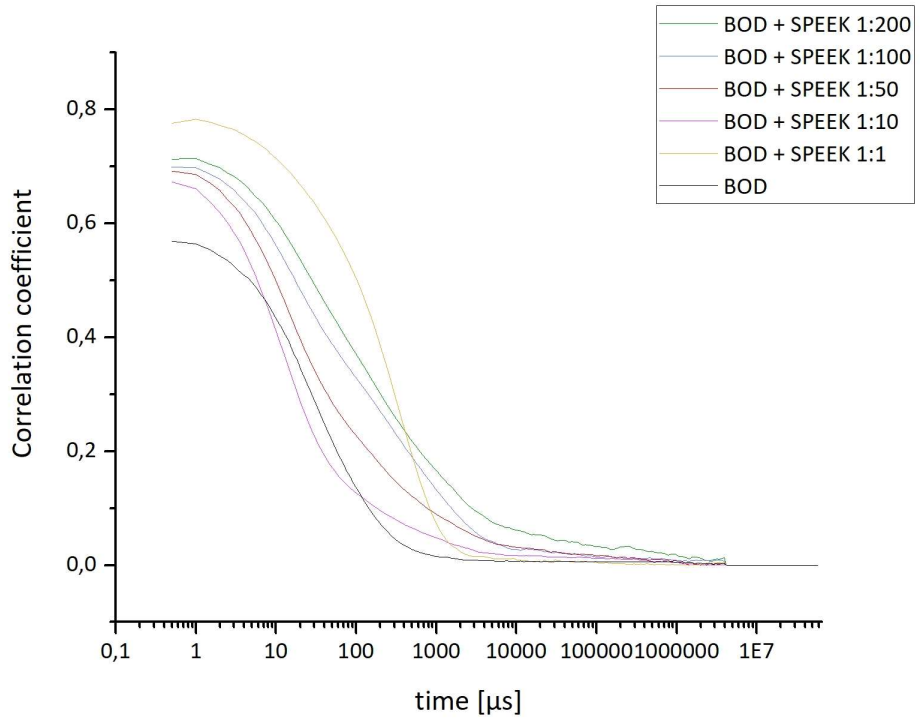

Figure 52: *Correlation coefficient obtained for BOD alone and BOD + various SPEEK (v/v) mixtures at 25°C.*

The correlation obtained for BOD and the various SPEEK dilutions shows that there is not such a big difference in the diffusion of light occurring from BOD alone and the various SPEEK dilutions.

4.9.2 SDS-PAGE

SDS-PAGE gel was further performed to observe the aggregation pattern of the ionomers with BOD.

4.9.2.1 Nafion

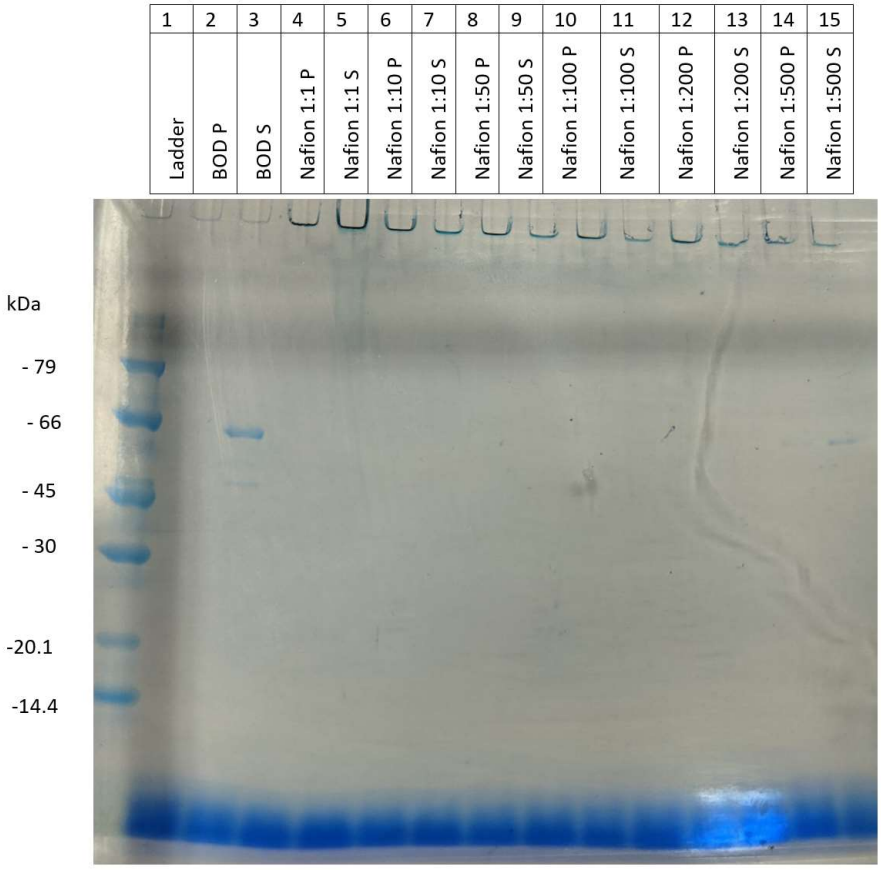

Figure 53: *SDS-PAGE gel of BOD and mixtures of BOD and Nafion dilutions 1:1 – 1:500.*

A band can be seen on the gel below 66 kDa for the *Mv*BOD alone as expected. For the enzyme/Nafion dilution 1:500 a band can be observed in the supernatant, which is marked in red. No other bands can be seen on the gel with the other mixtures, but the loading pockets are still strikingly blue colored. This indicates that Nafion together with BOD polymerizes to big complexes, which are not able to enter the gel.

The supernatant and the pellet were further examined via electrochemistry. 5 µL of each solution were transferred into Eppendorf tubes after centrifugation. 2 µL of each solution were immobilized on the PGE using Protocol A and CV was performed at 5 mV s^{-1} at RT. For the pellet no catalytic current was obtained, while for the supernatant some electrochemical activity of the enzyme was obtained, proving that the enzyme is not fully deactivated by Nafion. This pattern is in agreement with the hypothesis and results obtained so far, that Nafion forms big complexes with the enzyme that irreversibly encapsulate the enzyme, but still some enzyme molecules remain free to perform oxygen reduction.

4.9.2.2 SPEEK

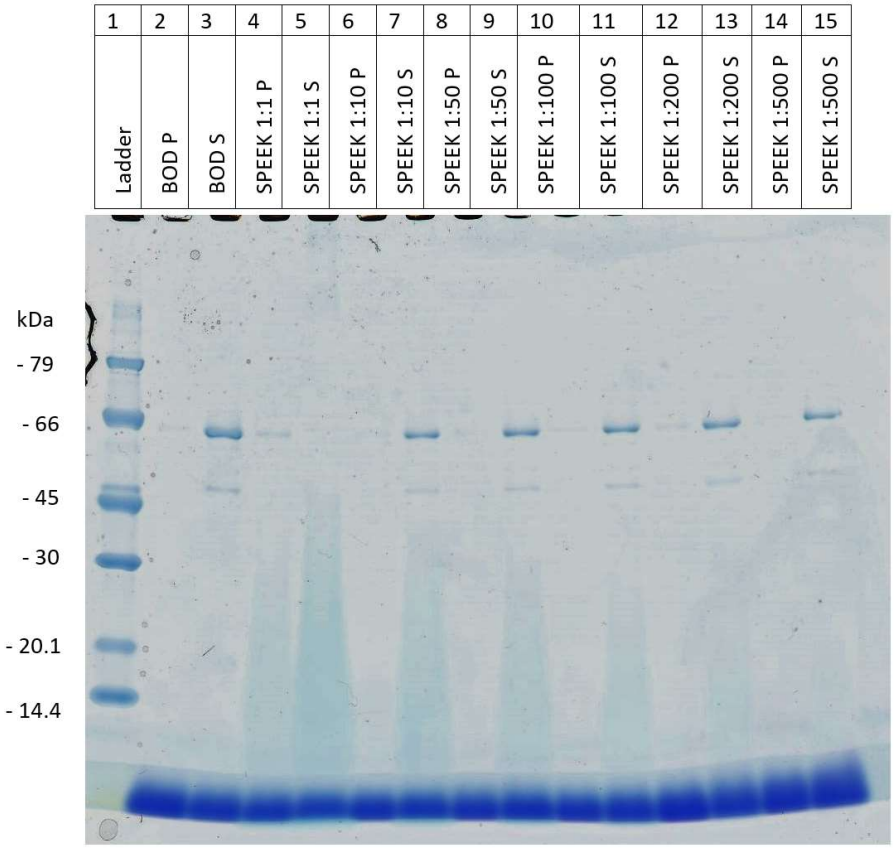

Figure 54: *SDS-PAGE gel of BOD and Nafion dilutions 1:1 – 1:500.*

BOD can be clearly identified at 60 kDa. Thus, this proves that BOD is present in all the lanes that were obtained with the SPEEK dilutions forming the bands that are observed at 60 kDa. Regarding the lanes from SPEEK 1:1 dilution a band is visible in the pellet. This confirms inactivation of BOD by SPEEK through enzyme aggregation caused by the acidic conditions. In all the other lanes, a band below 66 kDa is observed only in the supernatant, thus demonstrating that the enzyme is present and no aggregation occurred. Therefore, the conclusion can be drawn that SPEEK does not form large aggregates with the enzyme nor aggregates the protein itself, which is also in accordance with the results obtained from DLS. Consequently, the decrease in catalytic activity that is obtained with SPEEK in electrochemistry is not linked to protein aggregation.

5 Conclusion and Outlook

This thesis has examined the influence of the ionomers SPEEK and Nafion on the enzymatic activity and stability of BOD and provided some specific knowledge on their main interacting parameters. In the first part, the enzymatic activity of BOD in solution and in the immobilized state is compared and evaluated, establishing a reference activity. Basic parameters as the influence of pH and the enhancement of surface properties by CNTs are shown. One of the main physiological parameters influencing enzyme activity is shown to be pH, as Nafion as well as SPEEK are highly acidic solutions. Thus, for the dilutions containing the highest amount of ionomer only little to none activity is obtained. Here improvement of the catalytic current could be achieved by either an increase of pH or the ionic strength of the buffer solution.

Further the activity and stability of BOD has been measured as a function of ionomer concentration in solution as well as in the immobilized state. It is shown that SPEEK in solution with BOD shows a 50% activity decrease up till the 1:50 dilution. SPEEK is presumably linked through the Cu T1 site, thus the highest dilution of SPEEK possesses less free SO_3^- groups, meaning more and more enzyme is active. This reduction of free SO_3^- groups eventually leads to a neutralization when no free SO_3^- groups are available anymore and at this point the full activity of BOD is recovered as is seen starting with the 1:100 dilution. When SPEEK is immobilized on the electrode surface the same process is occurring with the exception that here SPEEK is polymerizing upon deposit hence preventing some enzyme from electrically connecting to the PGE, but not preventing enzyme release. Here a very low catalytic current is observed with the electroactivity staying in a range of below 40% of the initial activity of BOD for the dilutions 1:50 and 1:100. When the amount of SPEEK is further reduced (1:500) the initial activity can be almost recovered as 90% activity are obtained. These results are contrary to what has been obtained by UV-Vis measurements. In contrast with Nafion not only the free SO_3^- groups are still able to bind to the enzyme but here steric hindrance also seems to be contributing to the limitation of the enzymatic activity. Thus, when Nafion is in solution this steric hindrance is limiting full enzymatic recovery, only 50% of the activity can be recovered even with the highest possible dilution, even when all free SO_3^- groups are neutralized as well. The electroactivity obtained with Nafion in the immobilized state is not corresponding to the UV-Vis measurements, reaching an activity in the range of 60–70%. Here this steric hinderance is then contributing to the protection of BOD and hindering it from leaching after immobilization on the electrode surface.

In the second part additional parameters that could impact the electroactivity of the enzyme are examined. It is shown that the alcohol present in the ionomer dilutions causes no significant impact. Nafion creates no barrier for O_2 diffusion that would limit ET, while in contrast SPEEK decreases the

oxygen reduction at high amounts of ionomer, reducing the ET and limiting BOD activity to some extent.

Additionally, different immobilization patterns are compared and contrasted to further investigate the experimental conditions. Immobilization of BOD on the PGE surface before ionomer deposition leads to an increase in electroactivity of BOD of around 40% for Nafion and 60% for SPEEK in most cases, suggesting that the polymerization process occurring here is favorable. Therefore, to further enhance the catalytic activity, more extensive investigation of the other immobilization protocols is necessary, since they seem promising. These results obtained with the various measurements suggests that for SPEEK the particle size is in the same range as BOD and only binding to free SO_3^- groups, while Nafion consists of particles that in addition entrap BOD, which seems to be true whether this encounter occurs in solution or on the electrode surface.

Thus finally, the aggregation pattern occurring between the individual ionomers and BOD is observed, to examine this hypothesis. DLS results as well as the gels obtained from SDS-PAGE strongly support the conclusion that SPEEK and Nafion have divergent polymerization patterns depended on their size. DLS gives a diameter of SPEEK alone at 2.6-3.5 nm, and a diameter ranging from 2.5-5.1 nm when mixed with BOD. For Nafion alone, DLS shows the formation of aggregates that ranging in size from nm to µm, and even with the addition of BOD DLS only shows peaks for Nafion. The SDS-PAGE gels further show that BOD with SPEEK can be clearly observed at the band where BOD is supposed to appear, but in the presence of Nafion the wells are colored blue, indicating this mixture is in some way aggregated and not able to migrate through the gel. These results suggest that the different polymerization patterns, created by the divergent sizes, are most likely the significant factor influencing the enzymatic activity and stability.

Nevertheless, this thesis only scratches the surface of the investigations of the properties and their influence on the enzymatic activity and stability and further research has to be performed to fully uncover the physio-chemical parameters of the ionomers affecting the enzyme. Further experiments are necessary in order to fully understand the influence of SPEEK and Nafion on enzymatic activity. The release of BOD from the PGE surface with UV-Vis has to be studied in more detail, as well as the release of BOD from the surface when different immobilization protocols are used to establish reliable and reproducible results. Further, examination of the ionomer film on the electrode surface by microscopy might provide some additional insight into the process occurring during polymerization and thus lead to more conclusive explanations on the arrangement happening between ionomer and BOD as well as visualizing how the protons are able to pass through the ionomer layers. In order to examine more closely whether BOD is really protected by the ionomer film and to investigate whether the ionomer has a stabilizing effect on BOD or not, a temperature ramp followed by DLS could lead to more precise

results. Finally, some preliminary electrochemical experiments with ionomer membranes in a half cell would have to be performed in order to see whether it would actually be achievable to use SPEEK as a membrane in an EFC.

Summarizing, the desired goal for an enhancement for the catalytic activity of BOD was not achieved with either ionomer. However, extensive insight and more specific knowledge concerning the interaction of enzyme and the respective ionomer as well as the main physio-chemical parameters were obtained.

6 References

1. Mazurenko, I., Wang, X., de Poulpiquet, A. & Lojou, E. H2/O2 enzymatic fuel cells: from proof-of-concept to powerful devices. *Sustainable Energy and Fuels* **1**, 1475–1501 (2017).
2. Hitaishi, V. P. Enzymatic oxygen electroreduction: from molecular basis of effective enzymes immobilization on planar electrodes to the electrocatalysis on nanostructured electrodes.
3. Kulkarni, A., Siahrostami, S., Patel, A. & Nørskov, J. K. Understanding Catalytic Activity Trends in the Oxygen Reduction Reaction. *Chemical Reviews* vol. 118 2302–2312 (2018).
4. Xiao, X. *et al.* Tackling the Challenges of Enzymatic (Bio)Fuel Cells. *Chemical Reviews* **119**, 9509–9558 (2019).
5. Dai, L., Xue, Y., Qu, L., Choi, H. J. & Baek, J. B. Metal-Free Catalysts for Oxygen Reduction Reaction. *Chemical Reviews* vol. 115 4823–4892 (2015).
6. Solomon, E. I. *et al.* Copper active sites in biology. *Chemical Reviews* vol. 114 3659–3853 (2014).
7. Mano, N., Soukharev, V. & Heller, A. A laccase-wiring redox hydrogel for efficient catalysis of O2 electroreduction. *Journal of Physical Chemistry B* **110**, 11180–11187 (2006).
8. Varfoloneev, -sergey D, YARoPorov, Ndef. I., T, E. R. & Bogdxnovsmyao, V. A. *Bioelectrocatalysis. Hydrogenase as Catalyst of Electrochemkal Hydrogen Ionization*. *Bioeleclrocliemisfry and Bioenergetics* vol. 4 (1977).
9. Vashchenko, G. & MacGillivray, R. T. A. Multi-copper oxidases and human iron metabolism. *Nutrients* vol. 5 2289–2313 (2013).
10. Solomon, E. I., Sundaram, U. M. & Machonkin, T. E. *Multicopper Oxidases and Oxygenases*. https://pubs.acs.org/sharingguidelines.
11. Bento, I., Martins, L. O., Lopes, G. G., Carrondo, M. A. & Lindley, P. F. Dioxygen reduction by multi-copper oxidases; a structural perspective. *Dalton Transactions* 3507–3513 (2005) doi:10.1039/b504806k.
12. Solomon, E. I., Augustine, A. J. & Yoon, J. O2 Reduction to H2O by the multicopper oxidases. *Dalton Transactions* 3921–3932 (2008) doi:10.1039/b800799c.
13. Murao, S. & Tanaka, N. A new enzyme “bilirubin oxidase” produced by myrothecium verrucaria MT-1. *Agricultural and Biological Chemistry* **45**, 2383–2384 (1981).
14. Mano, N., Kim, H. H., Zhang, Y. & Heller, A. An oxygen cathode operating in a physiological solution. *Journal of the American Chemical Society* **124**, 6480–6486 (2002).
15. Mano, N. & de Poulpiquet, A. O2 Reduction in Enzymatic Biofuel Cells. *Chemical Reviews* vol. 118 2392–2468 (2018).
16. Hosein Mohimani, Alexey Gurevich, Alla Mikheenko, Neha Garg, Louis-Felix Nothias, Akihiro Ninomiya, Kentaro Takada, Pieter C. Dorrestein3, and P. A. P. Mechanism of chloride inhibition of bilirubin oxidases and its dependence on potential and pH. *Physiology & behavior* **176**, 139–148 (2017).
17. Mano, N. & Edembe, L. Bilirubin oxidases in bioelectrochemistry: Features and recent findings. *Biosensors and Bioelectronics* vol. 50 478–485 (2013).

18. Antiochia, R., Oyarzun, D., Sánchez, J. & Tasca, F. Comparison of direct and mediated electron transfer for bilirubin oxidase from myrothecium verrucaria. Effects of inhibitors and temperature on the oxygen reduction reaction. *Catalysts* **9**, (2019).

19. Mazurenko, I. *et al.* How the intricate interactions between carbon nanotubes and two bilirubin oxidases control direct and mediated O2 reduction. *ACS Applied Materials and Interfaces* **8**, 23074–23085 (2016).

20. Mazurenko, I., Hitaishi, V. P. & Lojou, E. Recent advances in surface chemistry of electrodes to promote direct enzymatic bioelectrocatalysis. *Current Opinion in Electrochemistry* vol. 19 113–121 (2020).

21. Hitaishi, V. P. *et al.* Controlling redox enzyme orientation at planar electrodes. *Catalysts* vol. 8 (2018).

22. Beaufils, C., Man, H. M., de Poulpiquet, A., Mazurenko, I. & Lojou, E. From enzyme stability to enzymatic bioelectrode stabilization processes. *Catalysts* vol. 11 (2021).

23. Narducci, R., di Vona, M. L. & Knauth, P. Cation-conducting ionomers made by ion exchange of sulfonated poly-ether-ether-ketone: Hydration, mechanical and thermal properties and ionic conductivity. *Journal of Membrane Science* **465**, 185–192 (2014).

24. Wang, R., Liu, S., Wang, L., Li, M. & Gao, C. Understanding of nanophase separation and hydrophilic morphology in Nafion and SPEEK membranes: A combined experimental and theoretical studies. *Nanomaterials* **9**, (2019).

25. Kreuer, K. D. *On the development of proton conducting polymer membranes for hydrogen and methanol fuel cells*. *Journal of Membrane Science* vol. 185 (2001).

26. Narducci, R., di Vona, M. L., Marrocchi, A. & Baldinelli, G. Stabilized SPEEK membranes with a high degree of sulfonation for enthalpy heat exchangers. *Coatings* **8**, (2018).

27. Vijh, A. K. Electrochemical principles involved in a fuel cell. *Journal of Chemical Education* **47**, 680–682 (1970).

28. DePoulpiquet, A. *et al.* Exploring Properties of a Hyperthermophilic Membrane-Bound Hydrogenase at Carbon Nanotube Modified Electrodes for a Powerful H2/O2 Biofuel Cell. *Electroanalysis* **25**, 685–695 (2013).

29. Michałowska-Kaczmarczyk, A. M. & Michałowski, T. Dynamic Buffer Capacity in Acid-Base Systems. *Journal of Solution Chemistry* **44**, 1256–1266 (2015).

30. Quinn, C. F. Buffer Compatibility with Nano DSC. *TA Instruments, Technical Note* 1–9 (2011).

31. Carmody, W. R. An easily prepared wide range buffer series. *Journal of Chemical Education* **38**, 559–560 (1961).

32. Elgrishi, N. *et al.* A Practical Beginner's Guide to Cyclic Voltammetry. *Journal of Chemical Education* **95**, 197–206 (2018).

33. Mabbott, G. A. An introduction to cyclic voltammetry. *Journal of Chemical Education* **60**, 697–702 (1983).

34. Tasca, F., Farias, D., Castro, C., Acuna-Rougier, C. & Antiochia, R. Bilirubin oxidase from myrothecium verrucaria physically absorbed on graphite electrodes. insights into the alternative resting form and the sources of activity loss. *PLoS ONE* **10**, 1–9 (2015).

35. Hitaishi, V. P. *et al.* Interplay between Orientation at Electrodes and Copper Activation of Thermus thermophilus Laccase for O2 Reduction. *Journal of the American Chemical Society* **142**, 1394–1405 (2020).

36. Kissinger, P. T. & Heineman, W. R. Cyclic voltammetry. *Journal of Chemical Education* **60**, 702–706 (1983).

37. Guy, O. J. & Walker, K. A. D. *Graphene Functionalization for Biosensor Applications*. *Silicon Carbide Biotechnology: A Biocompatible Semiconductor for Advanced Biomedical Devices and Applications: Second Edition* (Elsevier Inc., 2016). doi:10.1016/B978-0-12-802993-0.00004-6.

38. Schumm, B. *Encyclopedia of Applied Electrochemistry*. *Encyclopedia of Applied Electrochemistry* (2014). doi:10.1007/978-1-4419-6996-5.

39. Brownson, D. A. C. & Banks, C. E. *The Handbook of Graphene Electrochemistry*. *The Handbook of Graphene Electrochemistry* (2014). doi:10.1007/978-1-4471-6428-9.

40. Yadav, L. D. S. Ultraviolet and Visible. *Organic Spectroscopy* 7–51 (2005).

41. Gohain, N. Studies on the structure and function of phenazine modifying enzymes PhzM and PhzS involved in the biosynthesis of pyocyanin. (2015) doi:10.17877/DE290R-8364.

42. Picollo, M., Aceto, M. & Vitorino, T. UV-Vis spectroscopy. *Physical Sciences Reviews* **4**, 1–14 (2019).

43. Kenzom, T., Srivastava, P. & Mishra, S. Structural insights into 2,2'-azino-bis(3-ethylbenzothiazoline-6-sulfonic acid) (ABTS)-mediated degradation of reactive blue 21 by engineered Cyathus bulleri laccase and characterization of degradation products. *Applied and Environmental Microbiology* **80**, 7484–7495 (2014).

44. Falke, S. & Betzel, C. *Dynamic Light Scattering (DLS)*. (Springer International Publishing, 2019). doi:10.1007/978-3-030-28247-9_6.

45. Stetefeld, J., McKenna, S. A. & Patel, T. R. Dynamic light scattering: a practical guide and applications in biomedical sciences. *Biophysical Reviews* **8**, 409–427 (2016).

46. Tomaszewska, E. *et al.* Detection Limits of DLS and UV-Vis Spectroscopy in Characterization of Polydisperse Nanoparticles Colloids. **2013**, (2013).

47. Dolník, V. Capillary zone electrophoresis of proteins. *Electrophoresis* **18**, 2353–2361 (1997).

48. Pavlova, A. S. *et al.* SDS-PAGE procedure: Application for characterization of new entirely uncharged nucleic acids analogs. *Electrophoresis* **39**, 670–674 (2018).

49. Muharram, M. M. & Abdel-Kader, M. S. Utilization of gel electrophoreses for the quantitative estimation of digestive enzyme papain. *Saudi Pharmaceutical Journal* **25**, 359–364 (2017).

50. GE Healthcare & Booklet, P. Amersham Low Molecular Weight Calibration Kit for SDS Electrophoresis. *Manual* 1–12 (2006).

51. Kreuer, K. D. On the development of proton conducting polymer membranes for hydrogen and methanol fuel cells. *Journal of Membrane Science* **185**, 29–39 (2001).

52. Mazurenko, I., de Poulpiquet, A. & Lojou, E. Recent developments in high surface area bioelectrodes for enzymatic fuel cells. *Current Opinion in Electrochemistry* **5**, 74–84 (2017).

53. Meng, Z., Zhai, X., Wei, J., Wang, Z. & Wu, H. Absolute measurement of the refractive index of water by a mode-locked laser at 518 nm. *Sensors (Switzerland)* **18**, (2018).

54. Mizutani, K. *et al.* X-ray analysis of bilirubin oxidase from Myrothecium verrucaria at 2.3 Å resolution using a twinned crystal. *Acta Crystallographica Section F: Structural Biology and Crystallization Communications* **66**, 765–770 (2010).